

3D MODELING AND GROUND MOTION SCALING FOR THE PREDICTION  
OF SEISMIC DEMANDS ON THE GRAVITY DAMS

A THESIS SUBMITTED TO  
THE GRADUATE SCHOOL OF NATURAL AND APPLIED SCIENCES  
OF  
MIDDLE EAST TECHNICAL UNIVERSITY

BY

MILAD BYBORDIANI

IN PARTIAL FULFILLMENT OF THE REQUIREMENTS  
FOR  
THE DEGREE OF MASTER OF SCIENCE  
IN  
CIVIL ENGINEERING

SEPTEMBER 2016



Approval of the thesis:

**3D MODELING AND GROUND MOTION SCALING FOR THE  
PREDICTION OF SEISMIC DEMANDS ON THE GRAVITY DAMS**

submitted by **MILAD BYBORDIANI** in partial fulfillment of the requirements for  
the degree of **Master of Science in Civil Engineering Department, Middle East  
Technical University** by,

Prof. Dr. Gülbin Dural Ünver  
Dean, Graduate School of **Natural and Applied Sciences**

\_\_\_\_\_

Prof. Dr. İsmail Özgür Yaman  
Head of Department, **Civil Engineering**

\_\_\_\_\_

Assoc. Prof. Dr. Yalın Arıcı  
Supervisor, **Civil Engineering Dept., METU**

\_\_\_\_\_

**Examining Committee Members:**

Prof. Dr. Barış Binici  
Civil Engineering Dept., METU

\_\_\_\_\_

Assoc. Prof. Dr. Yalın Arıcı  
Civil Engineering Dept., METU

\_\_\_\_\_

Assoc. Prof. Dr. Ayşegül Askan Gündoğan  
Civil Engineering Dept., METU

\_\_\_\_\_

Asst. Prof. Dr. Bekir Özer Ay  
Department of Architecture, METU

\_\_\_\_\_

Asst. Prof. Dr. Burcu Güldür Erkal  
Civil Engineering Dept., Hacettepe University

\_\_\_\_\_

Date: 01.09.2016

**I hereby declare that all information in this document has been obtained and presented in accordance with academic rules and ethical conduct. I also declare that, as required by these rules and conduct, I have fully cited and referenced all material and results that are not original to this work.**

Name, Last Name: Milad Bybordiani

Signature:

## **ABSTRACT**

### **3D MODELING AND GROUND MOTION SCALING FOR THE PREDICTION OF SEISMIC DEMANDS ON THE GRAVITY DAMS**

Milad Bybordiani

M.Sc., Department of Civil Engineering

Supervisor: Assoc. Prof. Dr. Yalın Arıcı

September 2016, 104 pages

Seismic behavior of gravity dams has long been evaluated using the classical two dimensional modeling approach and time history analyses the assumptions for which have been rarely challenged. Formulated for the gravity dams built in wide-canyons, 2D modeling is utilized extensively for almost all concrete dams due to the established procedures as well as the expected computational costs of a three dimensional model. However, a significant number of roller compacted concrete (RCC) dams, characterized as such systems, do not conform to the basic assumptions of these methods by violating the conditions on canyon dimensions and joint-spacing/details. Based on the premise that the 2D modeling assumption is overstretched for practical purposes in a variety of settings, the first purpose of this study is to critically evaluate the use of 2D modeling for the prediction of the seismic demands on these systems. Using a rigorous dam-foundation-reservoir interaction (DFRI) approach, the difference between the 2 and 3D response for gravity dams were investigated in the frequency and time domain for a range of canyon widths and foundation to dam moduli ratios. The results of the analyses show the significant

variance in the dam response for different ground motions. In the light of this data, the second purpose of this study is to investigate the selection and the scaling of the ground motions usually required for the reduction of this variance in the determination of the seismic demands on gravity dams. In this regard, the existing ground motion scaling techniques are evaluated for determining the efficiency and accuracy of the scaling technique for predicting the target demands for concrete gravity dams. A large ensemble of near fault ground motions were used in order to consider the effect of the soil-structure interaction (SSI) on the motion selection for concrete gravity dams. The required number of ground motions for the consistent and efficient analyses of such systems was investigated. The results of the study show that the conventional approach for the modeling of gravity dams, including 2D modeling and common scaling procedures optimized for buildings, can significantly mislead the designers on the demands on these systems.

**Keywords:** Gravity Dam, Seismic Design, Soil-Structure Interaction, 2D vs. 3D Analyses, Frequency domain, Ground Motion Scaling

## ÖZ

### **AĞIRLIK BARAJLARININ DEPREM İSTEMLERİNİN BELİRLENMESİ İÇİN 3 BOYUTLU MODELLEME VE YER HAREKETİ ÖLÇEKLENMESİ**

Bybordiani, Milad

Yüksek Lisans, İnşaat Mühendisliği Bölümü

Tez Yöneticisi: Doç. Dr. Yalın Arıcı

Eylül 2016, 104 sayfa

Barajların sismik davranışları uzun zaman geleneksel iki boyutlu modeller ve zaman tanım alanında analizler ile incelenmiştir. Geniş vadilerde yapılmış ağırlık barajları için geliştirilmiş 2 boyut formülasyonu bu kaide ihmal edilerek gerek alışılmış prosedürler gerek de üç boyutlu analizlerin zorlukları nedeni ile bütün barajlar için kullanılmaktadır. Yine son zamanlarda yapılan Silindirle Sıkıştırılmış Barajların (SSB) çoğunluğu bu formülasyonla karakterize edilse de vadi genişliği ve derz aralıkları/detayları ile bu kaideye uymamaktadır. İki boyutlu analizlerin bu şekilde maksadının ötesinde kullanıldığı öngörüsü ile bu çalışmanın ilk amacı iki boyutlu analizlerin sismik davranış tahmininde kullanılmasının incelenmesidir. Bu çalışmada detaylı bir yapı-zemin-rezervuar etkileşimi formülasyonu kullanarak beton ağırlık barajlarının iki ve üç boyutlu davranışları arasındaki farklar değişik vadi genişlikleri ve zemin / yapı modülü farkları için frekans ve zaman alanında incelenmiştir. Bu analiz sonuçları yer hareketine bağlı olarak elde edilen sonuçlarda ciddi varyans oluştuğunu göstermiştir. Bu bilgiler ışığında, bu çalışmanın ikinci amacı ağırlık barajlarının sismik istemlerini değerlendirmek için yapılan analizlerde yer hareketine bağlı olan varyansın azaltılması için yer hareketleri üzerinde kullanılan seçme ve

ölçekleme yöntemlerinin etkinliğinin ve hatasızlığının araştırılmasıdır. Bu bağlamda mevcut yer hareketi ölçekleme yöntemleri ağırlık barajlarındaki hedef istemleri göstermedeki başarı ve etkinlikleri açısından değerlendirilmiştir. Yapı-zemin-rezervuar etkileşiminin bu anlamda ağırlık barajlarına olan etkisini de ele almak için bir çok yakın fay yer hareketinden oluşan geniş bir yer hareketi seti kullanılmıştır. Bu yapıların etkili ve tutarlı analizi için analizlerinde kullanılması gereken yer hareketi sayısı incelenmiştir. Bu çalışmanın sonuçları 2 boyutlu modelleme ve binalar için kullanılan ölçekleme yöntemleri içeren ağırlık barajlarına geleneksel tasarım yaklaşımının tasarımcıyı ciddi anlamda yanıltabileceğini göstermektedir.

**Anahtar Kelimeler:** Beton Ağırlık Barajı, Sismik Tasarım, Yapı-Zemin Etkileşimi, 2 ve 3 Boyutlu Analizler, Frekans Düzlemi, Yer Hareketi Ölçeklemesi

*To my parents...*

## ACKNOWLEDGMENTS

I would like to express my deepest gratitude toward my advisor, Associate Professor Yalın Arıcı for his guidance, advice, encouragement, and help throughout this research.

I am grateful to my family for their support and encouragement. To my mother, Sima Shoarian Sattari, my father Siavash Bybordiani, and my brother Elyad Bybordiani. They were always the never ending source of motivation under all circumstances.

I should also express my sincere appreciation to my friends Hamid Rajebi, Parham Pooyanfar, Golnesa Nassouhi, Assistant Professor Saeid Kazemzadeh, Moein Moeinzadeh, and Elshan Mirzazadeh. I am also honored to express my respect to Mehdi Babaei and Sina Kazemzadeh; the friends and colleagues whose work and research capacity were more of multiplicative factors rather than additive ones to those of mine.

I am also thankful to Professor Barış Binici and Associate Professor Ayşegül Askan Gündoğan. They not only introduced their corresponding extensive research area but also encouraged me to peruse novel research topics as a graduate student.

Finally, I am greatly thankful to Ceren Atakay, for her continuous support, patience, and presence.

This study has been conducted with the funding provided by The Scientific and Technological Research Council of Turkey (TUBITAK) under the grant number 5130011.

## TABLE OF CONTENTS

ABSTRACT .....	v
ÖZ .....	vii
ACKNOWLEDGMENTS.....	x
TABLE OF CONTENTS .....	xi
LIST OF TABLES .....	xiii
LIST OF FIGURES.....	xiv
CHAPTERS	
1. INTRODUCTION.....	1
1.1 General .....	1
1.2 Literature Survey .....	3
1.3 Scope and Objective .....	8
2. COMPARISON OF 3D AND 2D MODELING APPROACHES.....	13
2.1 General .....	13
2.2 Dam-Foundation-Reservoir Interaction.....	15
2.3 3D Dam-Foundation-Reservoir Interaction Modeling.....	17
2.3.1 EAGD-84, Finite Element Modeling of Concrete Dams in 2D including Soil-Structure-Reservoir Interaction Effects.....	17
2.3.2 EACD-3D-08, Finite Element Modeling of Concrete Dams in 3D including Soil-Structure-Reservoir Interaction Effects.....	18
2.3.3 Foundation Boundary Elements .....	20
2.3.4 Impounded Water.....	21
2.3.5 EACD-3D-08 Modifications .....	22
2.4 Numerical Modeling 2 and 3D Response.....	24
2.4.1 2D vs. 3D, SSI Modeling for Gravity Dams.....	24
2.4.2 Eigen Analysis and Mode Shapes .....	25
2.4.3 Frequency Response of the Dam Systems .....	26
2.4.4 Sensitivity Study .....	28
2.5 2D/3D Response of Gravity Dams .....	31
2.5.1 Frequency Response Functions.....	31

2.5.2	The Difference in the Natural Frequencies, 2D vs. 3D Models .....	38
2.5.3	Difference in the Damping Ratio for the First Mode, 2D vs. 3D Models .....	40
2.5.4	Time Domain Effects .....	43
3.	GROUND MOTION SELECTION AND SCALING .....	57
3.1	General.....	57
3.2	Numerical Models .....	59
3.3	Ground Motion Selection and Scaling Procedures .....	61
3.4	Ground Motion Scaling Methods .....	62
3.4.2	Ground Motion Scaling .....	65
3.4.3	Ground Motion Suite.....	65
3.5	Results .....	67
3.5.1	Statistical Investigation of the Scaling Techniques' Effectiveness....	67
3.5.2	Selection of the Records.....	71
3.6	Investigation of the Required Number of Ground Motions.....	75
4.	CONCLUSIONS AND FUTURE STUDIES .....	85
4.1	Conclusions .....	85
4.2	Future Studies .....	89
	REFERENCES .....	91
	APPENDIX A .....	97
	APPENDIX B.....	103

## LIST OF TABLES

### TABLES

Table 2-1 Required Run Time Using Single Core and Parallelized EACD-3D-08	23
Table 2-2 Fundamental Frequency and Damping Ratios for the Fundamental Mode of 2D Models.....	39
Table 2-3 Fundamental Frequency and Damping Ratios for the Fundamental Mode of 3D Systems Along with Corresponding Differences, 3D vs. 2D Models (Without Reservoir).....	41
Table 2-4 Fundamental Frequency and Damping Ratios for the Fundamental Mode of 3D Systems Along with Corresponding Differences, 3D vs. 2D Models (With Reservoir).....	42
Table 2-5 Selected Ground Motions .....	45

## LIST OF FIGURES

### FIGURES

Figure 2-1 RCC Dams in Narrow Valleys .....	14
Figure 2-2 DFRI Solution Procedure .....	17
Figure 2-3 2D Dam Body Finite Elements (Fenves & Chopra, 1984a) .....	18
Figure 2-4 3D Dam Body Finite Elements (Wang & Chopra, 2008b) .....	20
Figure 2-5 Idealized Dam-Foundation-Rock System in an Infinitely Long Uniform Canyon (Wang & Chopra, 2008b) .....	20
Figure 2-6 Surface boundary elements for foundation rock (Wang & Chopra, 2008b).....	21
Figure 2-7 Finite Element Model of Fluid Domain Substructure (Wang & Chopra, 2008b).....	22
Figure 2-8 Parallelization of Foundation Impedances' Calculation in EACD-3D-08 .....	23
Figure 2-9 Analysis Models .....	25
Figure 2-10 Eigen Modes for a Gravity Dam, Monolithic System, and System Comprised of Independent Monoliths and the 2D Model .....	26
Figure 2-11 Determination of the Representative Frequency Response Functions .	27
Figure 2-12 Effect of the Mesh Size on the Frequency Response Functions.....	29
Figure 2-13 Effect of the Number of Frequency Points on Frequency Response Functions .....	30
Figure 2-14 First Mode Shape of a System Idealized Using Independent Monoliths .....	31
Figure 2-15 The Generic 3D Dam and Canyon Setting .....	32
Figure 2-16 Frequency Response Functions, Monolithic Models vs. Plane Strain Models.....	34
Figure 2-17 Frequency Response Functions, Independent Monolith Idealization vs. Plane Stress Models.....	35
Figure 2-18 Frequency Response Functions, Monolithic Models vs. Plane Strain Models.....	36
Figure 2-19 Frequency Response Functions, Independent Monolith Idealization vs. Plane Stress Models.....	37
Figure 2-20 Ground Motion Definition.....	44
Figure 2-21 Difference in the Crest Displacements, 2D vs. 3D Models.....	49
Figure 2-22 Maximum Principal Stress Location .....	50
Figure 2-23 Flowchart of the MATLAB Code for Calculation of Maximum Principal Stress .....	52
Figure 2-24 Difference in the Principal Stress at the Upstream Face, 2D vs. 3D Models.....	53

Figure 2-26 The Distribution of the Maximum Principal Stress on the Foundation	56
Figure 3-1 Response Quantities for the Comparison of Time History Responses ..	60
Figure 3-2 Simple Scaling Procedure (United States Army Corps of Engineers, 2003) .....	62
Figure 3-3 Ground Motion Definition.....	66
Figure 3-4 The Accuracy and Dispersion of the Scaled Suites, Max. Crest Disp. ..	69
Figure 3-5 The Accuracy and Dispersion of the Scaled Suites for the Maximum Principal Stress.....	70
Figure 3-6 The Accuracy and Dispersion of the Scaled Suites for the Cumulative Inelastic Duration .....	70
Figure 3-7 The Accuracy and Dispersion of the Scaled Suite for the Cumulative Stress-Time Area.....	71
Figure 3-8 Error in the Stress Prediction vs. Ground Motion Intensity Measures...	73
Figure 3-9 Error in the CID vs. Ground Motion Intensity Measures.....	74
Figure 3-10 Maximum Principal Stress .....	78
Figure 3-11 Cumulative Inelastic Duration.....	79
Figure 3-12 Comparison of the Accuracy and Efficiency for Different DFRI Systems .....	80
Figure 3-13 Probability of Obtaining Accurate Results.....	83
Figure 3-14 Required Number of Ground Motions to Obtain Accurate Results .....	84



# CHAPTER 1

## INTRODUCTION

### 1.1 General

With the use of roller-compacted concrete, gravity dams are once again popular for the hydroelectric power generation in the emerging economies. Majority of the old dam stock in the developed world are gravity dams built using conventionally vibrated concrete (CVC). Given the need for the design of new systems in the developing world and the evaluation of the seismic performance of the existing dam stock in the developed countries, the analysis technique for these structures becomes an important issue for the designers, owners and the regulators. For the engineers, the foremost issue for the seismic assessment of these systems is the question of using 2 or 3 dimensional analyses for determining the demands on these structures. While the 2D analyses are relatively easy to repeat and less time consuming for a generic monolith in a dam, 3D analyses provide information regarding the demands for the whole of the system at a significant computational cost. After the selection of the analysis approach, the engineer is usually challenged with the ground motions to utilize for assessing the behavior of the dam. The ground motions used should be selected in accordance with the hazard at the site as well as site conditions. However, even for motions similar in this regard, there is a large dispersion in the required demand quantities due to the stochastic nature of the applied earthquake records. The use of a large number of ground motions requires significant resources and time, both of which are always critically limited in a design project. In conclusion, engineers need guidelines on both questions in order to efficiently conduct the seismic design and evaluation of the gravity dams. The primary goal of this thesis is to provide these guidelines in two separate sections.

The analyses of the gravity dams has been traditionally conducted in a 2D setting with the proponents usually pointing out the computational difficulties in solving the problem in 3D, such as the large model sizes. However, this choice is more of a convenience than a rigorous consideration and is likely established because the soil-structure interaction models have been theorized and quantified in this setting. The equivalent damping ratio representing the effect of the radiation damping on the performance of a gravity dam is based on such a solution. However, with the use of RCC in the building of the gravity dams, the assumptions regarding the 2D analysis of these systems are excessively violated. Narrow valleys are increasingly the norm rather than special cases along with the disappearance of the expansion joints. In this regard, the primary goal of the first section is to investigate the limitations of the 2D assumptions for these systems, in other words: What is the minimum width to height ratio of the gravity dams which can satisfy the assumptions of 2D idealizations (plane stress or plane strain) in a practical sense? In order to address the aforementioned question, the effects of soil-structure interaction with and without the impounded reservoir were investigated using the state of the art SSI modelling approaches. The results were compared with the 2D counterparts defining the variable parameters as the ratios of dam width to height and the material stiffness of the foundation to structure. A total number 80 systems with different properties were modelled in both 2 and 3D setting. First, the effects of 2/3D modelling were studied for the major dynamic properties of these systems, namely the fundamental mode period and the corresponding equivalent damping ratio. Subsequently, these differences were further evaluated using time domain quantities such as the heel stress and crest displacement for a suite of 35 ground motion pairs.

The variability in the time domain analyses, hence the motion selection problem, has traditionally been addressed by specifying variability on the response spectrum defining the variability on the demands on a structure. However, for much of the time domain quantities, the variability is due to the frequency content of the motions. Naturally, for dam-reservoir-foundation systems in which DFRI effects are very important, the concern for the frequency content of the motions as well as the frequency response of the systems are much more prevalent. These concerns for the

variability in the demand quantities based on the frequency content of the motions as well as the frequency response of these systems necessitate an investigation on the selection and scaling of ground motions to be used for the design and evaluation of concrete gravity dams, similar to the investigations conducted for multi-story moment frames and bridges. In this regard, the second part of the present study is assigned to the study of common ground motion scaling procedures to be used in the transient analysis of the dam systems. Models including the dam-foundation-reservoir interaction investigated in the first part of the study were subjected to 20 near fault ground motions in order to define the variability in EDPs. The crest displacement and cumulative inelastic duration were chosen as EDPs for the investigation of the accuracy and efficiency of the employed scaling procedures. Benchmark quantities were obtained as the mean EDPs resulting from unscaled motions. Four different scaling procedures, namely, the simple scaling procedure (ASCE 7-10), non-stationary spectral matching, scaling to the maximum incremental velocity and scaling to the response spectrum at fundamental frequency using realistic damping ratios were chosen and the accuracy of each method were studied. In addition, the correlation between the error in EDP predictions and the ground motion intensity measures were investigated. Finally, the minimum required number of ground motions that can provide accurate results compared to those of the benchmark was determined.

## **1.2 Literature Survey**

The seismic analysis and design of concrete gravity dams were studied since the pioneering work of Westergaard (1933) in determining the hydrodynamic pressure on rigid dams during earthquakes, for the case of a dam having vertical upstream face subjected to horizontal seismic forces acting parallel to the stream direction. Dam-reservoir interaction was modeled by means of the simplified added mass approach. Including the hydrodynamic forces in transient analysis of dams had a great impact on the design of these structures as the hydrodynamic forces were shown to be larger by up to 67% compared to the hydrostatic forces due to the reservoir.

Intensive research has been conducted in the past four decades, notably by Chopra and his colleagues toward improved analytical procedures for determining the seismic behavior of these systems. The reservoir interaction effects due to the horizontal earthquake excitation of concrete gravity dams were studied in (Chopra, 1970) and the frequency response functions based on deformations of fundamental mode were derived. Following these studies, a comprehensive investigation of the fluid-dam interaction including the compressibility of the reservoir was carried out by Hall and Chopra (1980) utilizing the substructure method in frequency domain. Later on, Fenves and Chopra (1984b) investigated the effects of sedimentary material deposited on the reservoir bottom and the dam-foundation-reservoir interaction on the seismic response of concrete gravity dams.

The dam-foundation interaction was taken into account based on the plane strain and plane stress formulations of the foundation dynamic stiffness matrices. Subsequently, a computer program named EAGD-84 was developed by Fenves and Chopra (1984a) implementing the rigorous two dimensional DFRI for analysis of concrete gravity dams. In addition, a method for the elastic design and safety evaluation of concrete gravity dams was proposed comprised of a simplified analysis procedure based on the fundamental vibration mode response. The contribution of higher modes was considered using the static correction method and a refined response history analysis method for the FEM idealization of a dam monolith was proposed by Fenves and Chopra (1987).

Modeling the sediment as a linearly viscoelastic, nearly incompressible solid with a very low shear-wave velocity was proposed by Lotfi et al. (1987). The method was based on two dimensional finite element analysis wherein using hyper-elements all the interactions including the water-sediment-foundation interaction were taken into account rigorously. The proposed technique also permitted the treatment of layered foundations. Furthermore, Medina et al. (1990) using the boundary element method obtained results in agreement with those of Lotfi et al. (1987). Bougacha and Tassoulas (1991) improved on the hyper-elements by developing a water-sediment-foundation hyperelement in which the sediment was recognized as a fluid-filled

poroelastic solid, permitting the convenient discretization of the upstream region. It was indicated in (Bougacha & Tassoulas, 1991; Medina et al., 1990) that sediment effects may be important, but not nearly to the extent suggested by Fenves and Chopra (1984b).

The studies given above had focused on the rigorous assessment of the dam-reservoir-foundation interaction in 2D setting. With the recognition of the 3D effects for dams, and the development of computational power, the dam-reservoir-foundation interaction problem was started to be investigated in three dimensions. In this respect, Rashed and Iwan (1984) studied the effects of length to height ratio of gravity dams on generated hydrodynamic pressures. They showed a considerable difference in the results of 2D modeling approach for gravity dams built on narrow canyons compared to 3D counterparts. For 3D SSI modelling, Zhang and Chopra (1991) developed a frequency domain boundary element procedure for uniform cross section canyons extending to infinity in a homogeneous viscoelastic half space. Including inertia and radiation damping effects of the foundation in the complete DFRI problem could be considered as the most prominent asset of such formulation. Tan and Chopra (1995) developed a rigorous three dimensional solution for DFRI problem under seismic effects to analyze the arch dams. Following their work, state of the art analysis tool named EACD-3D-08 was developed by Wang and Chopra (2008b) taking into account the effects of spatially varying ground motions. The frequency dependent foundation approach was determined to yield a decrease in fundamental resonant frequency of the dam; ignoring the inertia effects of foundation model overestimated the stresses on the arch dam.

As presented above, the major part of the literature on the seismic analysis of dams includes the assumption of a representative 2D behavior of a monolith governing the design of the dam system. Provisions of seismic design and evaluation (U.S. Bureau of Reclamation, 1976; United States Army Corps of Engineers, 1995) are mostly based on these works and effective two dimensional analyses of the dam systems discussed above. The effect of the contraction joint behavior was only treated in the context of arch dams (Lotfi & Espandar, 2004). Despite the early evaluations of

(Rashed & Iwan, 1984), who pointed out the need of three dimensional analyses for the seismic design of dams in narrow canyons, such analysis methodologies were rarely employed in the design of concrete gravity dams, but only been used for RCC dams remarkably lacking any expansion joints (Akpinar et al., 2011). In addition, two dimensional DFRI analysis results were significantly different than the results obtained with 3D approaches in prediction of engineering demands in a case study conducted by Yilmazturk et al. (2015) on the seismic performance of Andiraz dam (tallest RCC gravity dam constructed in a narrow valley in Turkey).

The nonlinear response of dams, due to the material nonlinearity, contraction joint and the dam-foundation interaction is generally modeled by using the massless foundation approach (Arici et al., 2014; Lotfi & Espandar, 2004). Hybrid time-frequency domain analysis including the effects of nonlinearity was implemented by Fenves and Chavez (1996) in order to investigate the effect of base sliding on a monolith. However, this approach did not get widespread as the formulation prohibits the implementation for large systems in which massless foundation approach is usually preferred. The effect of the radiation damping is taken into account using an equivalent damping ratio for models with massless foundations. This procedure and the corresponding damping ratios were effectively developed for 2D systems (Fenves & Chopra, 1987). Nonetheless, the recommended damping ratios are used in three dimensional massless idealizations, as well.

The studies on the rigorous formulation of the DFRI enable the realistic estimation of the demand quantities on the concrete gravity dams. However, the rigorous development period as well as the computational demands on such analyses led to a delay in the undertaking of detailed studies on estimating the demands on the dams compared to such problems like multi-story buildings. Both the linear (A. Aldemir et al., 2015; Yilmazturk, 2013) and nonlinear transient analyses (A Aldemir et al., 2012; Soysal, 2014) of 2 and 3D dam systems display the large dependence of the analysis results on the choice of ground motion, similar to building structures. Often methods imported from the moment frames are used in the processing of the ground motions for use in the transient analyses of dams. In the context of time history analysis of

buildings, the proper use of the earthquake records, i.e. the selection and scaling of ground motions for reliable time domain analyses, has been a major challenge for decades. The selection of the records is most often conducted by choosing from the recorded events with the magnitude, source-to-site distance and the fault types complying with the maximum earthquake considered at the site. The ground motions are usually scaled after the selection (Reyes & Kalkan, 2012). Since the demand on the structures is traditionally represented by a response spectrum at the site, the selected ground motions are generally subjected to a scaling or matching procedure in order to conform to the target demand levels defined by the response spectrum. Scaling of the ground motions to a target response spectrum level is traditionally used in practice and included in majority of the provisions (American Society of Civil Engineers, 2010; United States Army Corps of Engineers, 2003).

The scaling approaches can further be divided into two distinctive categories, i.e. 1) scaling of the earthquake records using a single multiplier and 2) spectral matching methods. By means of the scaling the records by a single multiplier, the frequency content of the ground motion remains untouched. The changes are merely applied to the amplitude of the records. In this regard, a wide range of approaches based on different target quantities have been proposed (American Society of Civil Engineers, 2010; Kurama & Farrow, 2003; O'Donnell et al., 2013; United States Army Corps of Engineers, 2003). Scaling of the motions by spectral matching changes the frequency content of the motions as well, in order to obtain a response spectrum that is closely imitating the target spectrum level (Abrahamson, 1992).

Numerous investigations have been conducted on scaling procedures in order to assess the efficiency and the success of the methods in determining the seismic demands on systems such as buildings and bridges. Reyes and Kalkan (2012) showed that scaling earthquake records to the design spectrum level would lead to overestimated engineering demand parameters (EDP) prediction in nonlinear time history analyses of frame structures. Kalkan and Chopra (2012) showed the modal pushover scaling technique, as developed by the first author, is successful in representing the seismic demand with less effort compared to the other techniques.

The poor consideration of the pulse-like characteristics of the ground motions prevalent of near fault motions was recognized early in the literature (Bertero et al., 1978; Hall et al., 1995) leading to development of procedures to include the effects of the velocity pulses in scaling procedure. Kurama and Farrow (2003) investigated the accuracy and efficiency the incremental velocity as the target quantity for scaling on nonlinear response prediction of a wide range of single degree of freedom (SDOF) and multi degree of freedom (MDOF) structures having different fundamental periods and R factors. It was shown that scaling the records to the mean value of maximum incremental velocity would led to considerable decrease in the mean EDP prediction as well as the dispersion of the results specifically in case of structures with high levels of nonlinearity ( $R > 4$ ) built on soft soil profiles (Kurama & Farrow, 2003; O'Donnell et al., 2013).

Spectral matching methods are rarely used for buildings given the target damage states leading the engineers to question the response spectrum based on linear analysis methodology. While amplitude scaling methods just change the intensity of the record, the spectral matching procedures (Lilhanand & Tseng, 1988) modify both the amplitude of the record and the frequency content to comply with the target spectrum over the range of interest. In this approach, the possibility of introducing non-realistic amplitudes to specific frequencies associated with the frequency domain modifications was eliminated. With an effort to preserve the non-stationary nature of the earthquake records, the aforementioned procedure was modified and implemented in the computer program RSPM (Abrahamson, 1992).

### **1.3 Scope and Objective**

The practice of the design of the new gravity dams as well as evaluation of the old dam stock has been a challenging task given the complex nature of the problem and the associated risk of such structures. In this realm, the linear and nonlinear time history analysis methodologies are getting to be normative analysis procedures. Yet, the common modeling techniques in practice are not fully capable of representing the interacting effects of foundation, structure, and reservoir medium on the overall

response of the structure. In addition, with the increasing demand toward construction of RCC and gravity dams on narrow canyons, the convention of two dimensional analysis for these basically three dimensional structures becomes questionable and the feasibility of using such procedures for these systems has to be investigated. Moreover, even with the use of more advanced numerical approaches, the problem of selection and scaling of the input ground motion still valid: unlike the analyses schemes of yester years based on the response spectrum, time history analyses introduces much more variability into the analyses results. However, in contrast to the case of building and bridges, the recommendations for scaling of ground motions to be used in seismic analysis of such infrastructure are scarce.

In this context, the primary goals of this study are:

- ❖ *Comparison of the 2 and 3D modeling approaches in order to recommend the limitations for the use of 2D models:* The results of the 2 and 3D models in a frequency domain DFRI setting were compared in this study with the goal of establishing the limitations of 2D modeling.
- ❖ *Examination of the applicability of the damping ratio propositions based on 2D models on the 3D systems:* The damping ratios for 3D systems were determined using the frequency domain responses such as the displacements and the values were compared for the 2 and 3D settings.
- ❖ *Investigation of the scaling techniques' efficiency for the seismic demand assessment of gravity dams in three dimensions:* The accuracy, efficiency and the robustness of the scaling techniques in the prediction of the seismic demand parameters were compared.
- ❖ *Determination of the number of ground motions to use in the seismic assessment of concrete gravity dams:* The minimum required number of motions to accurately predict the displacement or stress quantities in gravity dams was studied. In addition, using a damage indicator from these analyses as a proxy for the nonlinear behavior, the effect of the scaling methods on the possible nonlinear behavior of these systems was investigated.

The study is comprised of two main chapters on the study of the 2 vs 3D effects and the ground motion scaling procedures. In chapter 2, first, the theoretical background

of the rigorous SSI modeling of the concrete gravity dams are presented. Next a set of Eigen analyses are presented showing the dominant effect of the foundation / structure moduli ratio and the width of the canyon on the 3D SSI response. Covering a wide range of these parameters (for the structure/foundation moduli ratios of 2, 1, 0.5 and infinity and for the canyon widths of 2, 4, 6 to 12 times the dam height), the frequency domain responses are presented. The differences between the 2 and 3D modeling approaches in the prediction of the fundamental mode frequency and equivalent damping ratio are compared. The comparison of this frequency domain parameters are followed by the comparison of the time domain responses of the models for the selected engineering demand parameters. Statistical investigation of the time domain displacement and stress results are conducted incorporating 70 earthquake records; the results are compared to their counterparts from the 2D analysis in order to establish the limits for 2D modeling of these systems.

In chapter 3, first a brief introduction on the scaling procedures are presented. Afterwards, the utilized ground motion suite comprised of 20 motions, whose results are treated as the benchmark results determining the target EDPs, is presented. The accuracy and efficiency of the scaling procedures in the prediction of the target EDPs are investigated next by comparing the mean and variance values for the displacement, stress and the stress exceedance quantities predicted by the scaling of the motions in this suite. Next, the possibility of selection among these ground motions by using seismic intensity measures (IM) is investigated with the goal of reducing the variance in a given set. The number of motions that should be used for the effective demand prediction for the gravity dam systems are investigated in the final part of this section.

The conclusions of the study and the future directions of follow-up research are presented in the final chapter.

This study is subject to some limitations. For both the 2 and 3D models, the ground motion effect was only assumed to be in the direction perpendicular to the dam axis: the multidirectional effect was not considered. The contact forces and the possible pounding between the monoliths in the cross-stream direction were not considered.

The spatial asynchronous nature of the ground motion for the 3D models was also not included within the scope of the analyses. The effect of the vertical ground motion at a dam site was not considered.

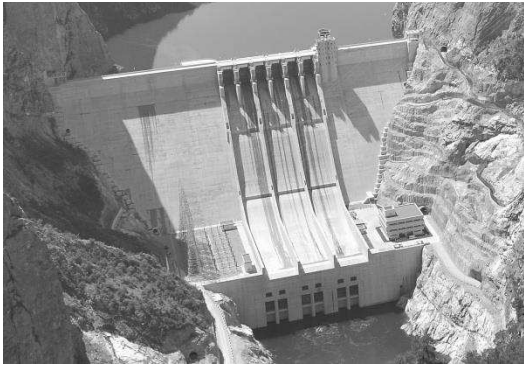


## CHAPTER 2

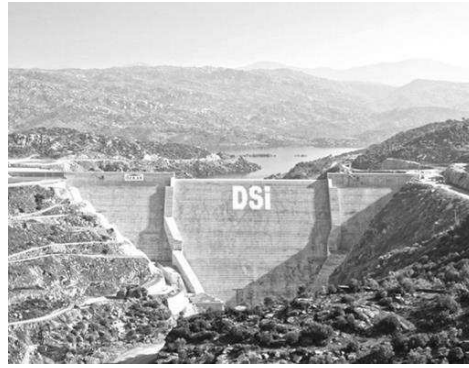
### COMPARISON OF 3D AND 2D MODELING APPROACHES

#### 2.1 General

Two dimensional analyses have been the prevalent approach to the prediction of the performance of dams (almost regardless of the geometry of the problem) mostly due to the absence of the computational capacity required to conduct rigorous 3D simulations as well as the historical background of the development of the analysis methods for these systems. These analyses are extensively used for the design of gravity dams assuming the following conditions are valid, i.e. 1) A plane stress condition permitted by the use of traditional intermittent expansion joints separating monoliths or 2) A plane strain condition for a system constructed in a wide canyon. With the extensive use of the RCC material, both of these assumptions are questionable due to the construction technique. Construction joints are hardly built in the former fashion. The expansion joints are prepared usually by rotary saws in RCC dams, partial slicing at the upstream or downstream facades or often alternating the cutting at different lifts in order to expedite the construction. The joint spacing is also considerably larger in new dams owing to the low heat of hydration of RCC. With the speed advantage provided by RCC construction, gravity dams are also being built in narrow valley locations otherwise suitable for arch dams such as the examples shown in Figure 2-1.



a) Boyabat Dam



b) Cine Dam

Figure 2-1 RCC Dams in Narrow Valleys

In the context of the discussion above, the main purpose of this chapter is to investigate the engineering demand parameters of the 2D modeling approach in lieu of the 3D analyses for the seismic assessment of the gravity dams, specifically for the RCC systems. For this purpose, the frequency response functions of a range of generic dam systems were obtained and compared for the 2 and 3D settings. Rigorous frequency domain solutions for both cases were used in order to compare the frequency response functions for the crest response quantities. In the 3D configuration, monolithic models with no construction joints as well as models composed of independent monoliths were used as the two ideal cases in order to investigate the behavior of the 3D model. The corresponding cases in the 2D configuration were chosen as the plane strain and plane stress solutions, respectively. The effect of the narrowness of the canyon on the frequency response functions were evaluated by assuming the generic system to be built in a canyon with the width varying between two to twelve times the dam height. The first mode frequency and the damping ratio were estimated for these systems and the differences between the 2 and 3D solutions were presented. Given the need for the comparison of engineering response parameters in the time domain as well as the frequency domain, a set of 70 ground motions were then used to compare the peak time history response values between 2 and 3D models (Bybordiani & Arici, 2016).

## 2.2 Dam-Foundation-Reservoir Interaction

The general analytical approach to evaluate the response of concrete gravity dams subjected to strong ground motions were developed by using the substructure method in (Fenves & Chopra, 1984b) for 2D systems. The response of the dam-reservoir-foundation rock system is formulated by discretizing the system into the dam, foundation and fluid domain substructure. The general equation of motion of a two-dimensional finite element system characterized in this fashion is given in the frequency domain by:

$$\begin{aligned} & \left[ -\omega^2 \begin{bmatrix} \underline{\mathbf{m}} & \underline{\mathbf{0}} \\ \underline{\mathbf{0}} & \underline{\mathbf{m}}_b \end{bmatrix} + (1 + i\eta_s) \begin{bmatrix} \underline{\mathbf{k}} & \underline{\mathbf{k}}_b \\ \underline{\mathbf{k}}_b^T & \underline{\mathbf{k}}_{bb} \end{bmatrix} \right] \begin{Bmatrix} \bar{\mathbf{r}}^l(\omega) \\ \bar{\mathbf{r}}_b^l(\omega) \end{Bmatrix} \\ & = - \begin{Bmatrix} \underline{\mathbf{m}} \underline{\mathbf{1}}^l \\ \underline{\mathbf{m}}_b \underline{\mathbf{1}}_b^l \end{Bmatrix} + \begin{Bmatrix} \bar{\mathbf{R}}_h^l(\omega) \\ \bar{\mathbf{R}}_b^l(\omega) \end{Bmatrix} \end{aligned} \quad (2-1)$$

In Equation 2-1,  $\bar{\mathbf{r}}^l$  and  $\bar{\mathbf{r}}_b^l$  represent the relative displacements of the nodal points above the base and the nodal points on the base,  $\bar{\mathbf{R}}_h^l$  and  $\bar{\mathbf{R}}_b^l$  represent the hydrodynamic forces on the upstream face and the dam-foundation interaction forces on the base. The term  $\eta_s$  represents the constant hysteretic factor for the dam body. The abovementioned formulation is implemented in computer program EAGD-84 and used in the present study in modeling and analysis of DFRI systems in two dimensional setting.

Building on these studies, a similar formulation was proposed for the 3D domain by Wang and Chopra (2008a). The treatment of dam-reservoir interaction is based on (Fenves & Chopra, 1984b; K.-L. Fok & Chopra, 1986; Hall & Chopra, 1980) whereas the dam-foundation interaction is considered by using the boundary element approach of Zhang and Chopra (1991). The complete formulation of the DFRI problem can be found in (Wang & Chopra, 2008a), therefore only a brief summary is given below. The equation of motion in the frequency domain including DFRI for spatially varying ground motion is presented in Equation 2-2.

$$\begin{aligned}
& \left[ -\omega^2 \begin{bmatrix} \mathbf{m} & \mathbf{0} \\ \mathbf{0} & \mathbf{m}_b \end{bmatrix} + (1 + i\eta_s) \begin{bmatrix} \mathbf{k} & \mathbf{k}_b \\ \mathbf{k}_b^T & \mathbf{k}_{bb} \end{bmatrix} + \begin{bmatrix} \mathbf{0} & \mathbf{0} \\ \mathbf{0} & \mathbf{S}_f(\omega) \end{bmatrix} \right] \begin{Bmatrix} \hat{\mathbf{r}}(\omega) \\ \hat{\mathbf{r}}_b(\omega) \end{Bmatrix} \\
& = \begin{Bmatrix} \hat{\mathbf{R}}_h(\omega) \\ \mathbf{0} \end{Bmatrix} \\
& + \left[ \omega^2 \begin{bmatrix} \mathbf{m} & \mathbf{0} \\ \mathbf{0} & \mathbf{m}_b \end{bmatrix} - (1 + i\eta_s) \begin{bmatrix} \mathbf{0} & \mathbf{0} \\ \mathbf{k}_b^T & \mathbf{k}_{bb} \end{bmatrix} \right] \begin{Bmatrix} \hat{\mathbf{r}}^s(\omega) \\ \hat{\mathbf{r}}_f^f(\omega) \end{Bmatrix}
\end{aligned} \tag{2-2}$$

In Equation 2-2, the subscript  $b$  refers to the dam foundation interface and the  $\hat{\phantom{x}}$  symbol refers to the Fourier transformed quantities. The equation of motion, transformed into the frequency domain, is partitioned above for the nodes of the dam finite element model at the dam-foundation interface ( $\hat{\mathbf{r}}_b(\omega)$ ) and for those not located at the dam-foundation interface ( $\hat{\mathbf{r}}(\omega)$ ). The vector  $\hat{\mathbf{R}}_h(\omega)$ , the Fourier transforms of the hydrodynamic forces, contains non-zero terms only at the nodal points on the upstream face of the dam and they are calculated from the solution of the Helmholtz equation (Wang & Chopra, 2008a). The radiation condition due to infinite reservoir is satisfied along with the compatibility condition at the upstream face of the dam (Fenves & Chopra, 1984b; K.-L. Fok & Chopra, 1986; Hall & Chopra, 1980) during the solution of the Helmholtz equation. The vector  $\hat{\mathbf{r}}^s(\omega)$  is the structural displacements due to the static application of the earthquake induced free field displacements  $\hat{\mathbf{r}}_f^f(\omega)$  i.e.  $\hat{\mathbf{r}}^s(\omega) = -\mathbf{k}^{-1}\mathbf{k}_b\hat{\mathbf{r}}_f^f(\omega)$ . The complex valued impedance matrix of the foundation  $\mathbf{S}_f(\omega)$ , is used to set the relation between the interaction forces and displacements relative to the free-field ground motion on the dam-foundation interface. It should be noted that the reservoir-foundation interaction effects are neglected as they were determined to be negligible by Fenves and Chopra (1984b).

For a computationally efficient solution of Equation 2-2, the degrees of freedom of this system are reduced by expressing the displacement vector  $\hat{\mathbf{r}}_c(\omega) = [\hat{\mathbf{r}}(\omega) \ \hat{\mathbf{r}}_b(\omega)]^T$  as a linear combination of Ritz vectors (Equation 2-3).

$$\hat{\mathbf{r}}_c(\omega) = \sum_{j=1}^J \hat{Z}_j(\omega) \boldsymbol{\Psi}_j \tag{2-3}$$

The following eigenvalue problem is then solved and the first  $J$  eigenvalues,  $\lambda_j^2$ , and the eigenvectors  $\Psi_j$  are calculated.

$$\begin{bmatrix} \mathbf{k} & \mathbf{k}_b \\ \mathbf{k}_b^T & \mathbf{k}_{bb} + \mathbf{S}_f(\omega) \end{bmatrix} \Psi_j = \lambda_j^2 \begin{bmatrix} \mathbf{m} & 0 \\ 0 & \mathbf{m}_b \end{bmatrix} \Psi_j \quad (2-4)$$

Introducing Equation 2-3 into Equation 2-2, premultiplying with  $\Psi_j^T$  and using the orthogonality property of eigenvectors, the system of equations are reduced to  $J$  equations which can be solved for generalized coordinates' displacements,  $\hat{Z}_j(\omega)$ , at the desired frequencies,  $\omega$ . The inverse Fourier transform  $\hat{Z}_j(\omega)$  gives the displacement of the generalized coordinates in the time domain as  $Z_j(t)$ , which in turn provides the displacements and stresses by using the standard stress-displacement relations in the finite element method. The flowchart of the solution is summarized in Figure 2-2.

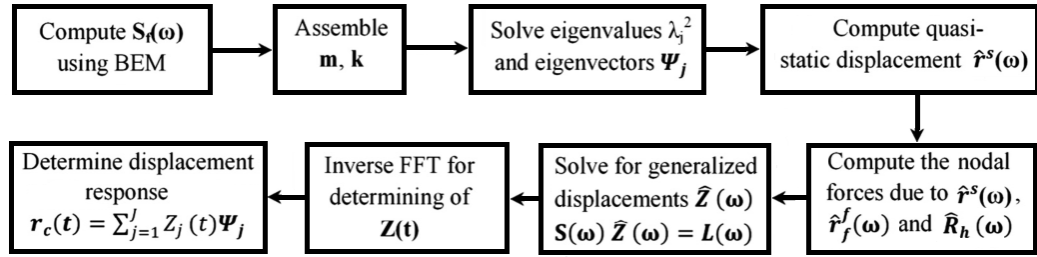


Figure 2-2 DFRI Solution Procedure

## 2.3 3D Dam-Foundation-Reservoir Interaction Modeling

### 2.3.1 EAGD-84, Finite Element Modeling of Concrete Dams in 2D including Soil-Structure-Reservoir Interaction Effects

EAGD-84 is a computer program particularly developed for the analysis of concrete gravity dams considering the effects of dam-foundation as well as dam-reservoir interaction in a 2D setting (Fenves & Chopra, 1984a). In the present research, plane stress and plane strain modeling of the DFRI systems was conducted using the above

mentioned program. Computation of the foundation impedance matrices in EAGD-84 is merely the two-dimensional form of the formulation presented in Section 2.2. Linear shape functions are the only available element type for discretization of the structure (Figure 2-3). Four point Gauss quadrature integration scheme is implemented in the program for the calculation of stiffness and mass matrices. However, stress results are just reported at the center of the finite elements, averaging the primary results at the integration locations.

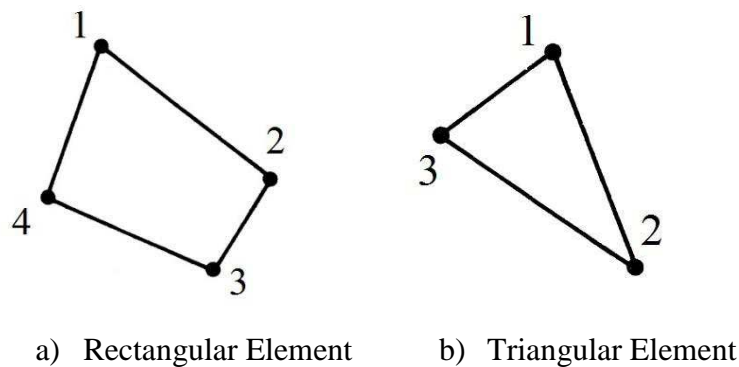


Figure 2-3 2D Dam Body Finite Elements (Fenves & Chopra, 1984a)

### 2.3.2 EACD-3D-08, Finite Element Modeling of Concrete Dams in 3D including Soil-Structure-Reservoir Interaction Effects

Three dimensional modeling of the DFRI systems was conducted using EACD-3D-08. The aforementioned state of the art modeling tool for dynamic analysis of concrete arch and gravity dams including the effects of structure-foundation and structure-reservoir interaction was developed in three decades by K. Fok et al. (1986), Tan and Chopra (1996), and Wang and Chopra (2008b). Input data for the engine is similar to any conventional FEM modeling software. Solution of the problem requires completion of the seven subprograms. The primary functions of each subprogram is listed below:

- Subprogram 1: The complex-valued frequency-dependent foundation impedance matrix of the flexible foundation rock for DOFs along the dam-foundation rock interface is computed.
- Subprogram 2: The element stiffness, mass, and stress matrices of the dam are computed.
- Subprogram 3: In dynamic analysis, the natural frequencies and mode shapes of the dam-foundation rock are computed. In static analysis, the self-weight load vector of the dam is computed.
- Subprogram 4: The five fluid meshes are defined, and in dynamic analysis, the element “stiffness”, “mass”, and “damping” matrices of the meshes are computed. In static analysis, the hydrostatic pressure load vector on the dam is computed.
- Subprogram 5: It is left for future developments.
- Subprogram 6: The complex-valued frequency responses of the dam modal coordinates are computed in dynamic analysis. In static analysis, the static displacements and stresses of the dam are computed.
- Subprogram 7: The earthquake time-history responses of the dam are computed

3D continuum of the dam body is discretized using quadratic solid elements. The Hexahedral element shown in Figure 2-4 is comprised of a total number of 20 nodes in 3D Cartesian coordinates leading to elements with 60 degrees of freedom (DOF). Prismatic and tetrahedral elements on the other hand, are constructed by collapsing the redundant nodes onto a common coordinate having respectively 15 and 10 nodes. Gauss quadrature integration scheme is implemented with 8 locations for all solid elements. It should be noted that the numbering of the nodes are in the counter-clockwise direction from the upstream side as shown in Figure 2-4. Although other types of solid and shell finite elements are available in the EACD-3D-2008 element library, in order to preclude any numerical error associated with finite element approach such as hourglassing or shear lock, only quadratic solid elements were used for 3D modeling.

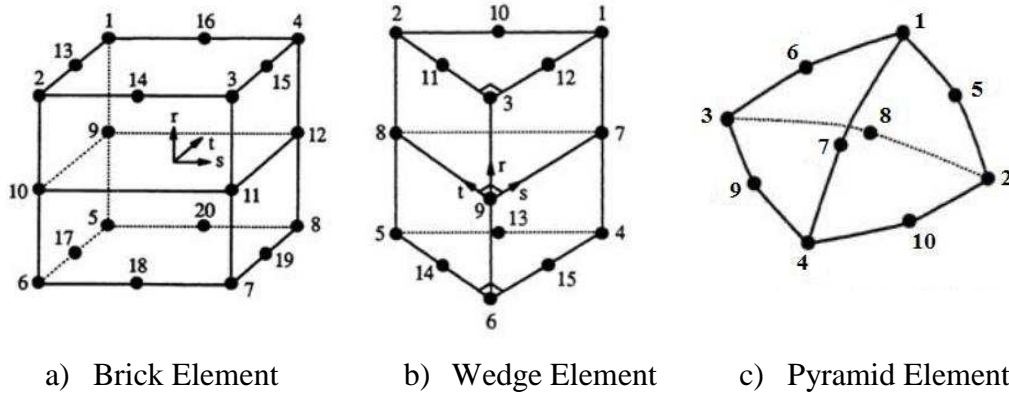


Figure 2-4 3D Dam Body Finite Elements (Wang & Chopra, 2008b)

### 2.3.3 Foundation Boundary Elements

The rigorous solution of the DFRI problem in a 3D setting was obtained in the homogeneous viscoelastic half space (K.-L. Fok & Chopra, 1986) using a frequency domain boundary element procedure for canyons extending to infinity (Figure 2-5).

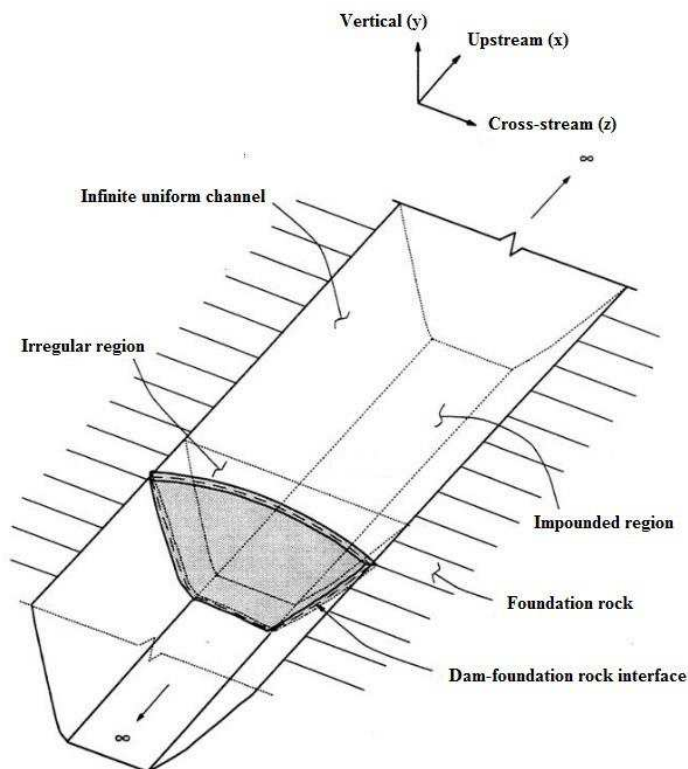


Figure 2-5 Idealized Dam-Foundation-Rock System in an Infinitely Long Uniform Canyon (Wang & Chopra, 2008b)

Using direct boundary element procedure for dam-foundation interaction, dynamic stiffness matrices of the soil media are constructed at discrete frequency values. In order to model the interface between the dam and foundation, rectangular and triangular surface elements were employed. Similar to the case of dam structure finite elements, quadratic surface elements with 8 and 6 nodes were used (Figure 2-6). It is worth noting that, node numbering of these elements follows no specific rule.



a) Rectangular Surface Elements      b) Triangular Surface Elements

Figure 2-6 Surface boundary elements for foundation rock (Wang & Chopra, 2008b)

### 2.3.4 Impounded Water

The impounded water is limited by the upstream side of the dam on the x direction and defined by the natural topography of the valley on the z direction (Figure 2-5). 3D quadratic elements interpolating the pressure field in the fluid medium were used to model the reservoir. The assumption of zero permeability at the dam upstream face required the equilibrium of nodal pressure and displacement of respectively fluid and structure media. In the finite element model for an infinite reservoir consisting of possible irregular geometry right next to the upstream face of the dam and an infinite channel of uniform cross section, it is useful to introduce five types of meshes (Figure 2-7): Mesh 1 discretizes the entire irregular region; Mesh 2 spans the transmitting plane (the interface between the irregular region and the infinite uniform channel); Mesh 3 discretizes the dam-water interface of the reservoir; Mesh 4 spans the reservoir bottom and sides of the irregular region; and Mesh 5 discretizes the bottom and sides of the transmitting plane.

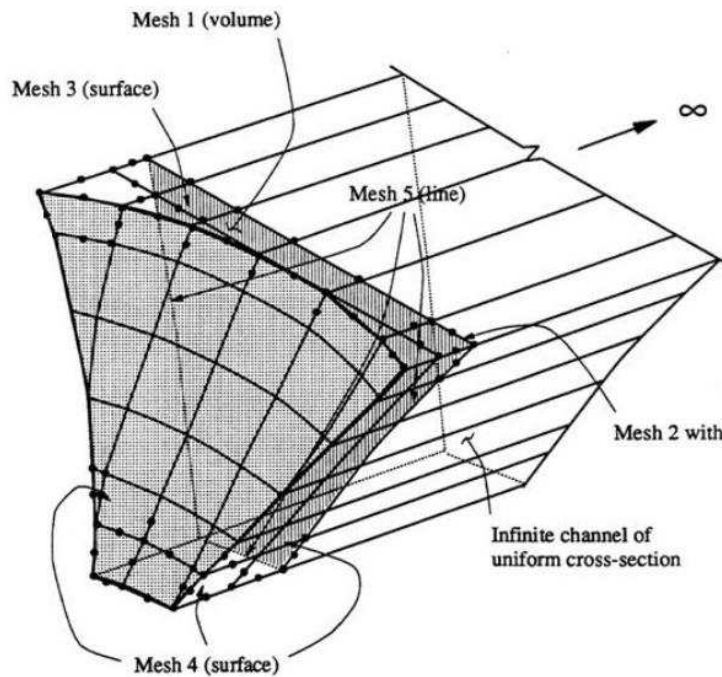


Figure 2-7 Finite Element Model of Fluid Domain Substructure (Wang & Chopra, 2008b)

Effects of reservoir bottom absorption is included using the wave reflection coefficient defined as the ratio of the reflected hydrodynamic pressure waves to the amplitude of perpendicular pressure wave on the reservoir. The radiation of the pressure waves was considered using the semi-infinite 1D channel in the discretization of the fluid domain.

### 2.3.5 EACD-3D-08 Modifications

Throughout this research, the EACD-3D-08 analysis engine was subjected to some modifications. Improvements regarding the numerical errors and the output format as well as the efficient use of computing potential for practical purposes were implemented. A pre- and post-processing GUI platform using MATLAB was developed as a part of this research project (Appendix A). In the meantime, in order to address the problems regarding the immense amount of runtime and memory needed for the computation of foundation impedance matrices, additional modifications in the source code were made. Parallelization of source code using an

automated Bash file (Appendix B) on Linux operating system (OS) lead to considerable decreases of runtime (Figure 2-8). For instance, the total amount of required analysis time decreased from an expected 75 day to 10 days for one of the largest DFRI models. The prepared Bash file has the maximum capacity of using 32 CPU cores simultaneously for 32 different frequency values in computation of the foundation impedance matrices. Working on the Linux OS also eased the use of larger amounts of memory needed during the calculation of Ritz vectors.

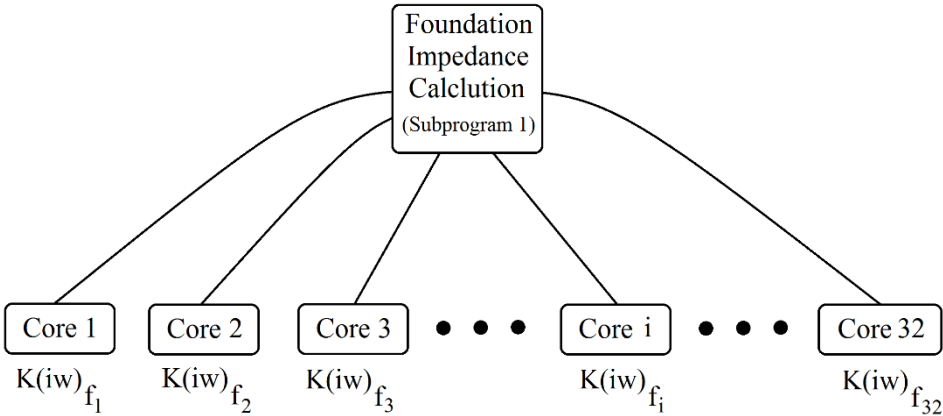


Figure 2-8 Parallelization of Foundation Impedances' Calculation in EACD-3D-08

With the additional available memory of the source codes compiled in Linux OS, the run time of Ritz vectors' computation was also significantly reduced. The actual run time for models enabling parallel computation is shown in Table 2-1 for a series of models having the identical foundation and structure moduli with different canyon widths. It is clearly seen that the use of parallel calculation of the impedance matrices along with large amounts of memory can lead to 90% decrease in the run time. It is worth noting that the decrease in the computational effort is more pronounced for models with higher number of frequency points.

Table 2-1 Required Run Time Using Single Core and Parallelized EACD-3D-08

<b>Model</b>	<b>4H</b>	<b>6H</b>	<b>12H</b>
Single core, run time (days)	0.1	3	100
Parallelized, run time (days)	0.01	0.3	11

## 2.4 Numerical Modeling 2 and 3D Response

### 2.4.1 2D vs. 3D, SSI Modeling for Gravity Dams

Two different 3D model idealizations were used in order to assess the behavior of dam systems (Figure 2-9). The first idealization was fully monolithic, representing the RCC dams built with interlocking expansion joints and/or partial expansion joints. The second, named as the “independent” case from hereon, represented the typical gravity dam construction, (applicable to some RCC dams with fully sawed expansion joints), with independent monoliths only to be connected at the foundation level. In this case, it was assumed that the construction joints in the system were large enough to preclude an interaction between the neighboring monoliths in both the cross-stream and stream directions. 20 node brick elements and 15 node wedge elements were used to model the dam body in this study while 8 node quadrilateral boundary elements were used at the dam body-foundation interface. In two dimensions, the plane stress and the plane strain model idealizations were used to represent the independent and monolithic cases for the 3D system, respectively. linear elements were used in the 2D models (Yucel, 2013).

For the sake of simplicity, all the systems considered within the study were assumed to be of a generic 3D geometry built in canyons with 45 degree sloping shoulders as shown in Figure 2-9. The upstream face of the dam was assumed flat while the downstream was modeled with a slope of 1V/1H. The modulus of elasticity of the dam body was assumed as 20 GPa. The width of the valley and the foundation modulus were treated as the variables effective in determining the response of the system. The hysteretic damping constant for the foundation was assumed as 0.1 while the damping ratio for the dam body was assumed as 5%.

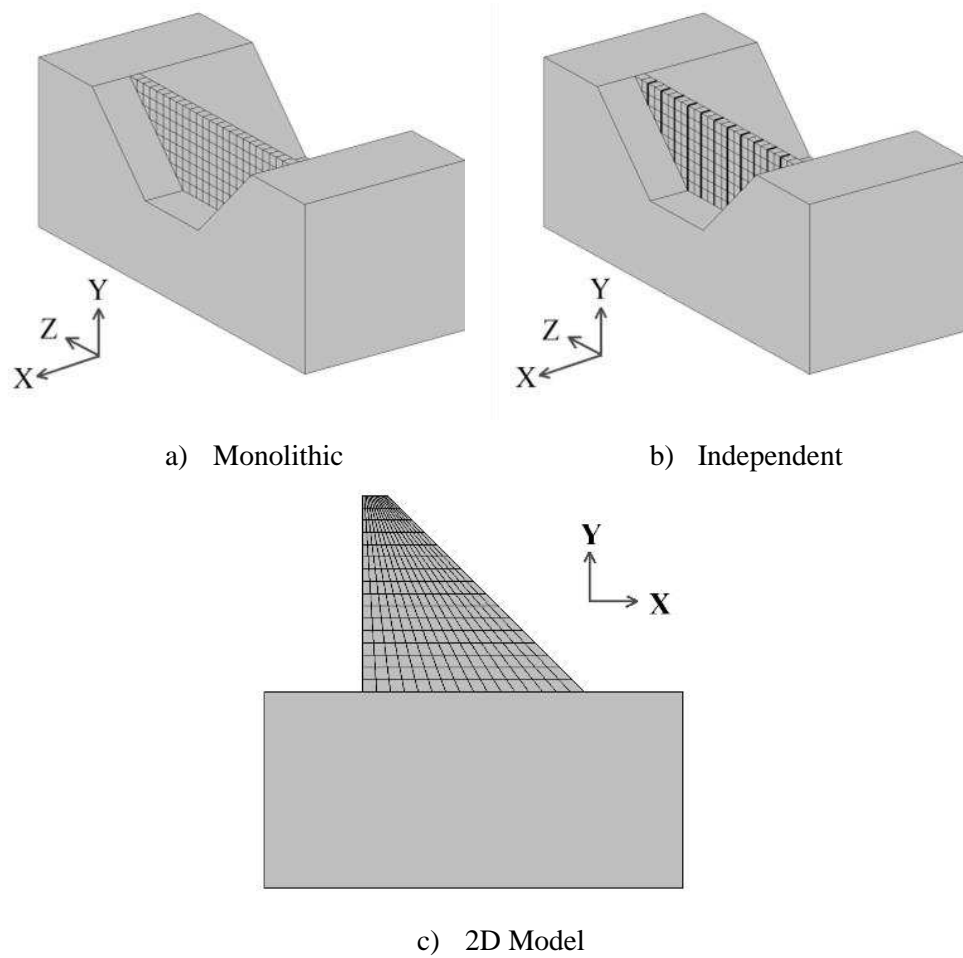


Figure 2-9 Analysis Models

### 2.4.2 Eigen Analysis and Mode Shapes

Eigen value analysis is a valuable tool to evaluate the dynamic behavior of the dam system as the interaction modes between the monoliths can perhaps best be compared by the simple visualization of the mode shapes. Such a sample analysis was conducted for a generic 80m tall dam located in a narrow valley of 240m width. The first three natural modes of the system are presented in Figure 2-10 for the monolithic and independent cases and the representative 2D model. For this case, the dam and the foundation modulus were assumed identical as 20 GPa. As given in Figure 2-10, the monolithic system was significantly stiffer compared to the system comprised of independent monoliths. However, the dam system with independent monoliths also

displays a significant coupling between the monoliths due to the shared rock foundation. In other words, the neighboring monoliths cannot easily exhibit independent behavior as expected given the strong coupling at the base due to the foundation. The motions in all the given modes were in phase with the other monoliths which could only be avoided for a perfectly ideal rigid base condition. The 2D model was the most flexible among these models with a substantially reduced fundamental frequency value. Naturally, the 2D model could not predict the deformation in the higher order 3D modes of either monolithic or independent monoliths.

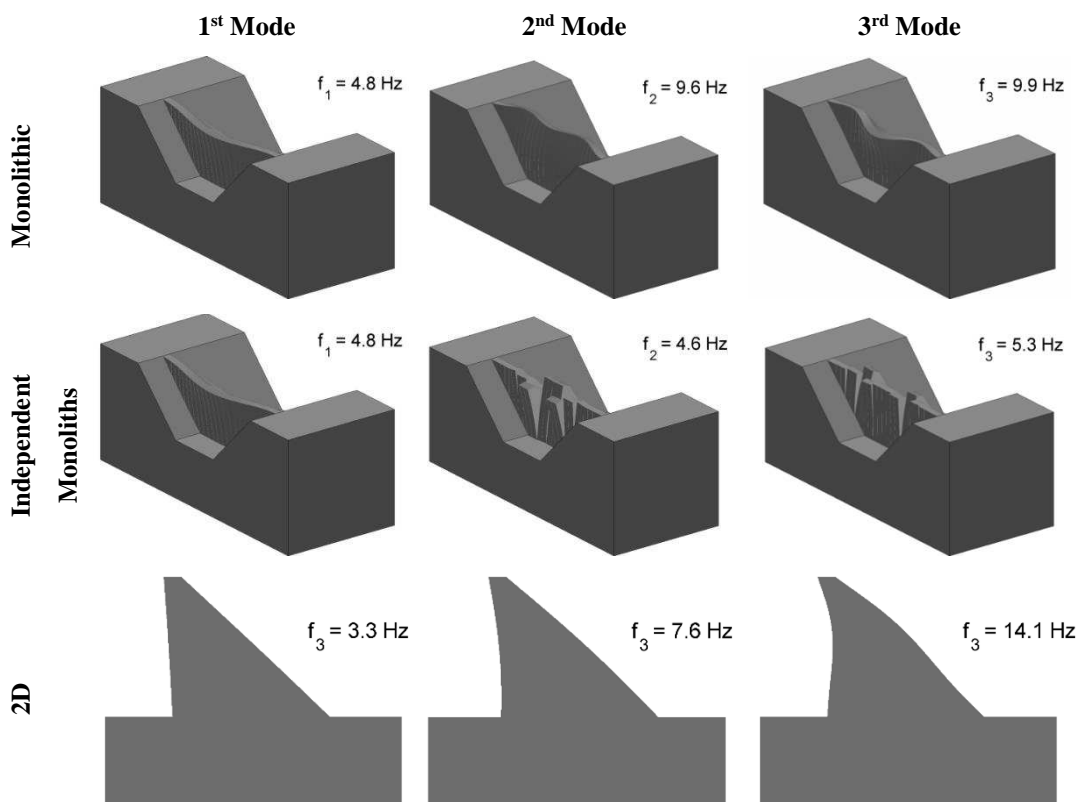


Figure 2-10 Eigen Modes for a Gravity Dam, Monolithic System, and System Comprised of Independent Monoliths and the 2D Model

### 2.4.3 Frequency Response of the Dam Systems

Soil-structure interaction is the primary factor determining the seismic behavior of the concrete dams. Given the prevalence of this issue on the problem, as well as the

requirement of a frequency domain solution, frequency response functions have been used as the common assessment tool for determining the behavior of dams while using the robust analyses techniques. In order to compare the behavior of 3D models (comprised of the monolithic dam and independent monoliths) to 2D models, a simple analysis methodology to obtain frequency domain functions was utilized herein.

Given the full frequency response matrix is impossible to obtain and even harder to present, the frequency response function for the crest acceleration at the center of the dam system was used as a representative tool. The frequency response functions for the systems were obtained by applying a pulse with a very short duration as the base excitation of the system (Figure 2-11). The transfer function between the base and the crest acceleration (i.e. the impulse response function) was obtained for this pulse excitation (Bybordiani & Arici, 2015).

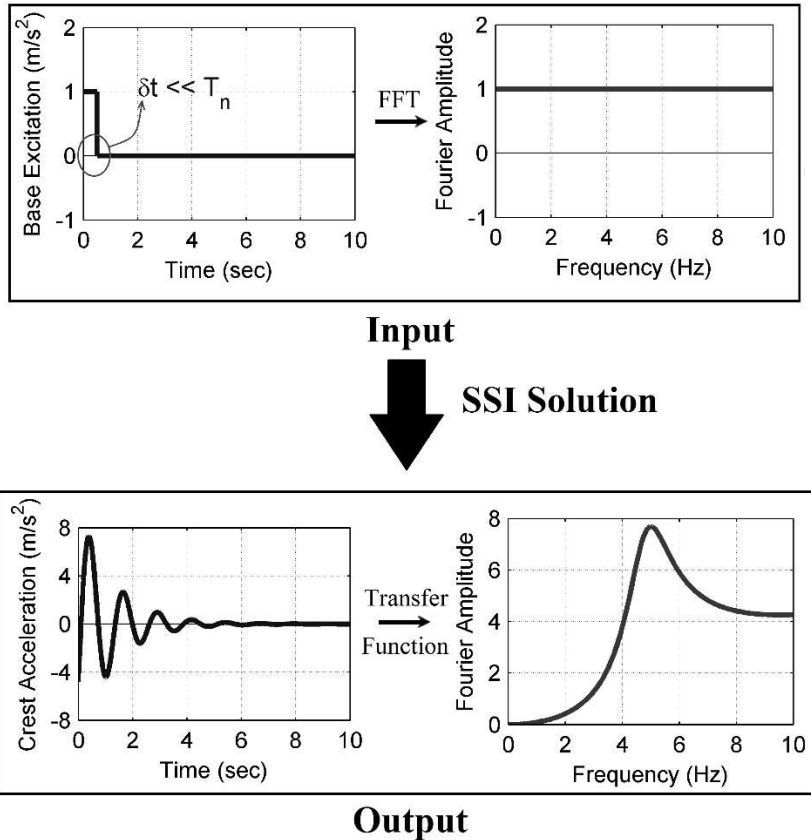


Figure 2-11 Determination of the Representative Frequency Response Functions

The frequency response function, as given above, offers an effective tool of for the comparison of the effect of the soil-structure-reservoir interaction effect on the response of dam systems. It also provides a rapid method of obtaining the output response for any given input time signal as the time consuming step wise integration method in the time domain (corresponding to the convolution integral) in the conventional finite element codes is avoided. Once one obtains the response function estimate for a system, the output time history response for any given motion can be obtained without a repetition of the analysis by multiplying the frequency response function by the Fourier transform of the input motion. The aforementioned procedure provides a convenient tool for comparing the response of the system for many different ground motions. The frequency response functions for the 2 and 3D systems are compared in the next section in order to demonstrate the differences between the approaches in the frequency domain. However, the solutions to engineering problems are generally based on the time domain quantities, such as the stresses, strains or the displacements, which can formally be treated as limiting or target quantities in a design process. In the proceeding section, the time domain effects of the differences between the FRFs of the 2 and 3D models are compared.

#### **2.4.4 Sensitivity Study**

##### **2.4.4.1 Mesh Size**

Effect of the mesh size were studied on two dam-foundation systems with different Young's modulus for the foundation material. Chosen model was the monolithic dam as shown in Figure 2-9 with two different foundation elasticity moduli ( $E_f$ ) of 10 and 20 GPa. Both of the models were discretized using four different mesh sizes. The required size of the elements for obtaining accurate results was not largely affected by finite elements but was determined by the effect on the impedance matrices of the foundation. On the other hand, even with the help of parallelized EACD-3D-08 engine (Sec. 1.3.5) the use of quadratic boundary elements seemed completely impractical for element sizes less than 5 meters.

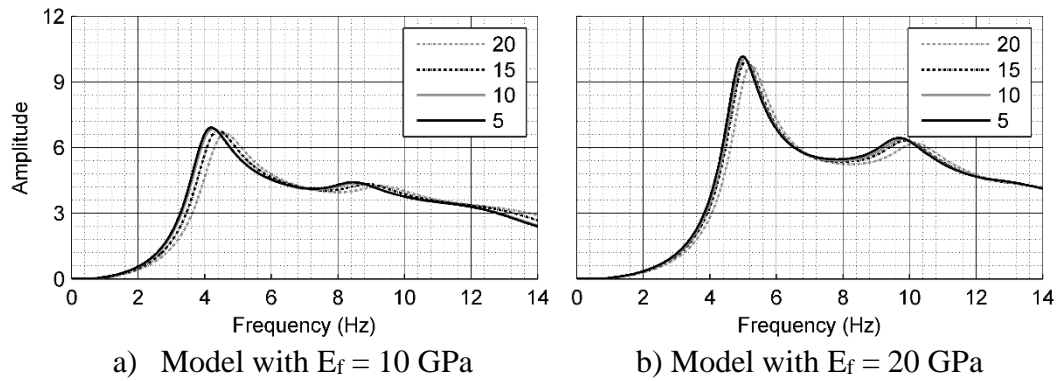


Figure 2-12 Effect of the Mesh Size on the Frequency Response Functions

Wang and Chopra (2008b) recommended limiting the element length to half and one fourth of the shear wavelength, respectively, for the quadratic and linear dam-foundation interface elements for accurate results. The aforementioned suggestions lead to a maximum interface element size of 12.5 meters for models built on canyon with  $E_f$  of 10 GPa. Using stiffer foundation materials, the maximum element size increases due to an increase in shear wavelength for the same maximum frequency of interest. The results of the aforementioned mesh are depicted in Figure 2-12. It is evident that the frequency response functions of crest acceleration converges for element sizes equal to or less than 10 meters. Consequently, the final element size of 10 meters was chosen for quadratic elements except for the case of models on foundation with  $E_f$  of 40 GPa. This was due to the numerical issues related to EACD-3D-08 analysis engine. In order to overcome this issue, a more conservative element size (20/3 meters) was used for this case.

#### 2.4.4.2 Number of Frequency Points

Foundation complex-valued impedance matrices can be computed at every frequency value using the analytical procedure implemented in EACD-3D-08. However, it requires an enormous amount of computational effort. In addition, it has been shown that the corresponding elements of the impedance matrix can be interpolated using a third degree polynomial function over the frequency range of interest (Tan & Chopra, 1996). The computations of impedance matrices are conducted at discrete frequency values with equal step sizes starting from zero frequency representing the static case

to maximum frequency value defined as the Nyquist frequency. Similar to the mesh size sensitivity study, two models with a foundation moduli  $E_f$  of 10 and 20 GPa were chosen in this section in order to assess the effect of the number of frequency points on the analysis results. Four different frequency intervals, i.e. with 5, 10, 20, and 40 frequency points were selected. The frequency response functions of the crest acceleration are presented in Figure 2-13 for each case. It is evident that for the models having 20 or more frequency points, the results converge: the use of more than 20 frequency points appears unnecessarily excessive.

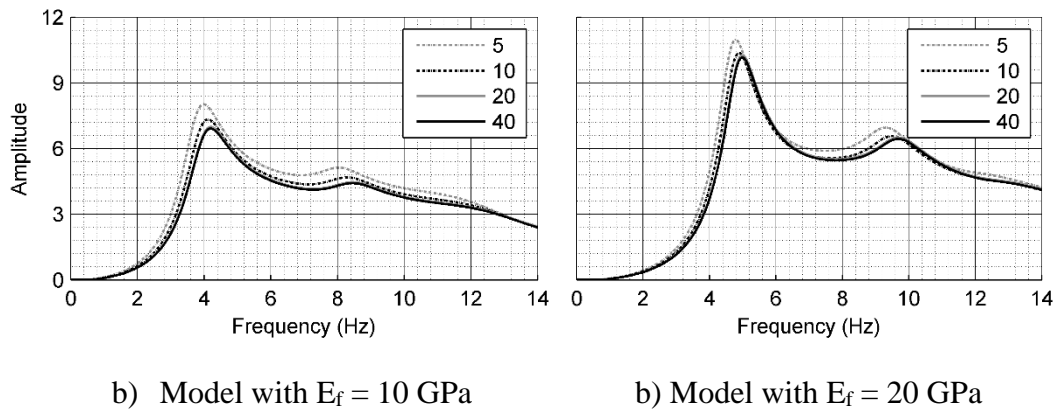


Figure 2-13 Effect of the Number of Frequency Points on Frequency Response Functions

### 2.4.4.3 Number of Modes

The minimum number of modes required in the modal analysis was also investigated for the case of dams with monolithic as well as independent monolith idealizations. The dominant effect determining the sensitivity of the analysis results in the previous sections was largely the foundation material properties. For the case of mode numbers, however, it was seen that the most prominent factor is the idealization type. As mentioned earlier, the main objective of the present research is the investigation of the seismic response of the DFRI systems in the upstream-downstream direction. The frequency response functions of the crest acceleration were obtained for the systems in this direction. The systems idealized with the independent monoliths tend to have numerous modes in both directions. For example, the first mode in the

upstream-downstream direction appeared as the 14<sup>th</sup> mode for a dam system comprised of independent monoliths. Figure 2-14 shows the first mode shape of a model with foundation moduli  $E_f$  of 20 GPa built in a 3H wide canyon. The lateral modes as observed in this figure shows that a much larger mode number have to be included in the dam's analysis in order to accurately obtain the response in the fundamental direction. Inclusion of higher modes in this direction was even more challenging: a preliminary investigation for the widest of the 3D models revealed 150 modes were needed to be included in the analysis in order to obtain the 10<sup>th</sup> mode in the upstream-downstream direction.

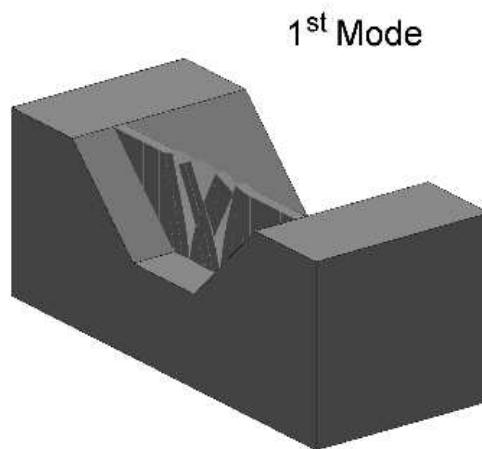


Figure 2-14 First Mode Shape of a System Idealized Using Independent Monoliths

## 2.5 2D/3D Response of Gravity Dams

### 2.5.1 Frequency Response Functions

The comparison of the 2 and 3D responses of the gravity dams are conducted in this section using the frequency response functions for the crest acceleration at the mid-section of the dam. In order to investigate the effect of canyon width on the 3D response of a given system, an identically shaped gravity dam section was assumed to be built in five different canyon settings. A V-shaped canyon with 45 degree shoulders were assumed in the analyses (Figure 2-15). The width of the canyon (V) was chosen as 180m, 240m, 320m, 480m and 960m (designated as 2H, 3H, 4H, 6H and 12H in terms of the dam height, respectively). The base excitation was assumed

in the direction of the stream; the response of the dam was only evaluated in this direction as well (perpendicular to the axis of the dam).

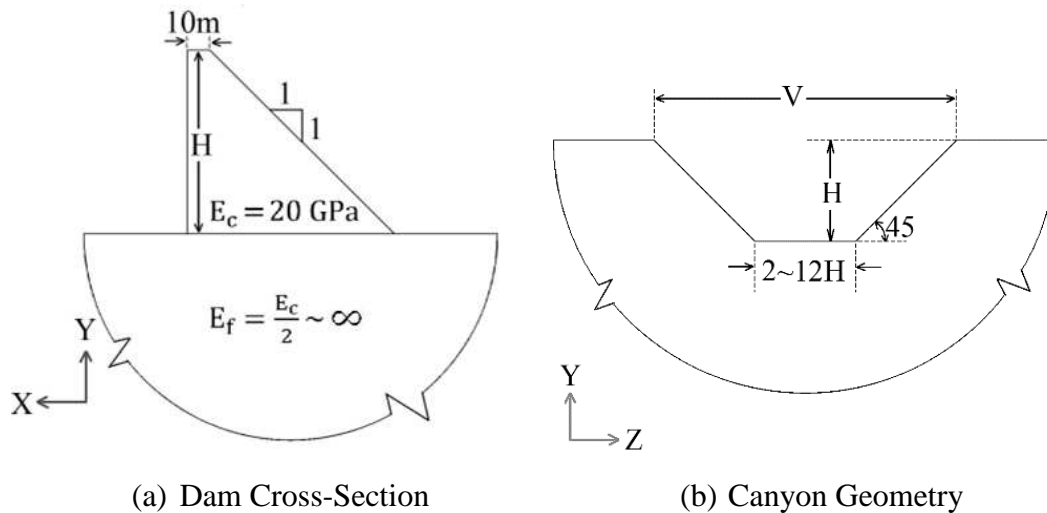


Figure 2-15 The Generic 3D Dam and Canyon Setting

### 2.5.1.1 Dam without Reservoir

The frequency response functions for the 2D plane strain and the monolithic idealizations of a 3D system in absence of reservoir are compared in Figure 2-16. The counterparts of these results for the 3D model, with independent monoliths, are compared to the results from a 2D plane stress model in Figure 2-17. The frequency response was evaluated at four different moduli ratios. The foundation was first treated as rigid, then assigned Young's Moduli ( $E_f$ ) of 40, 20 and 10 GPa in order to obtain  $E_f/E_c$  ratios of  $\infty$ , 2, 1 and 0.5, respectively. The elastic modulus of the dam body ( $E_c$ ) was kept constant at 20 GPa. Investigation of the frequency response functions given in these figures show:

- 1) There was a significant difference in the natural frequency between the 2D and the 3D models for the monolithic systems. This trend was valid even for a canyon width of six times the dam height. The difference in the fundamental frequency was valid for all ranges of the foundation to dam moduli ratios.

- 2) There was a surprising difference in the natural frequency estimate between the 2D models and the 3D models even for the cases of the independent monolith idealization. However, as expected, this disparity was reduced for increasing foundation stiffness and canyon width.
- 3) The maximum amplitudes for the 2D models (for the fundamental mode) appeared to be significantly different than the 3D models. For the monolithic dam case, this difference was valid for a wide range of  $V/H$  and  $E_f/E_c$  values.

### **2.5.1.2 Dam with Reservoir**

In order to study the coupling effects of dam-reservoir interaction, reservoir contribution was considered in the analysis for the same 2 and 3D models described in the preceding section. The unit mass and the p-wave velocity of the reservoir fluid were defined as 1000 kg/m<sup>3</sup> and 1439 m/s, respectively. The radiation of the pressure waves was considered using the semi-infinite 1D channel in the discretization of the fluid domain. The wave reflection coefficient, defining the bottom absorption at the base of the reservoir due to the accumulation of the reservoir sediment, was assumed as 0.9. Investigation of the frequency response functions given in Figure 2-18 and Figure 2-19 for this case shows:

- 1) Fundamental frequencies of all models were significantly reduced compared to their counterparts without the reservoir. In addition, the resonant amplitude of systems with reservoir was increased as a result of the added hydrodynamic forces.
- 2) Similar to the results obtained for the models without reservoir, the natural frequencies of the 2D and the 3D models for the monolithic systems were obtained significantly different.
- 3) The maximum amplitudes for the 2D models (for the fundamental mode) were significantly different than the 3D models as before.

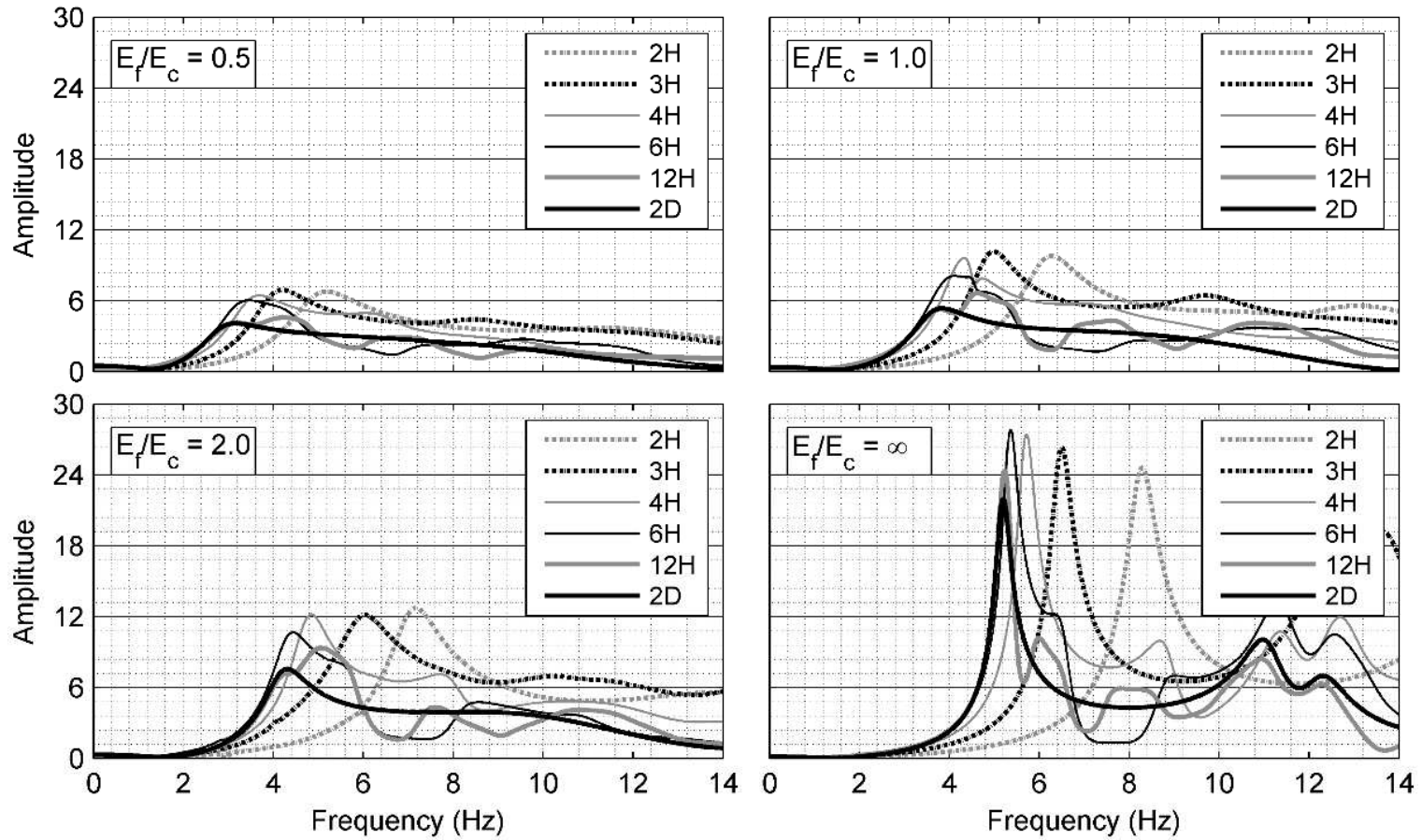


Figure 2-16 Frequency Response Functions, Monolithic Models vs. Plane Strain Models

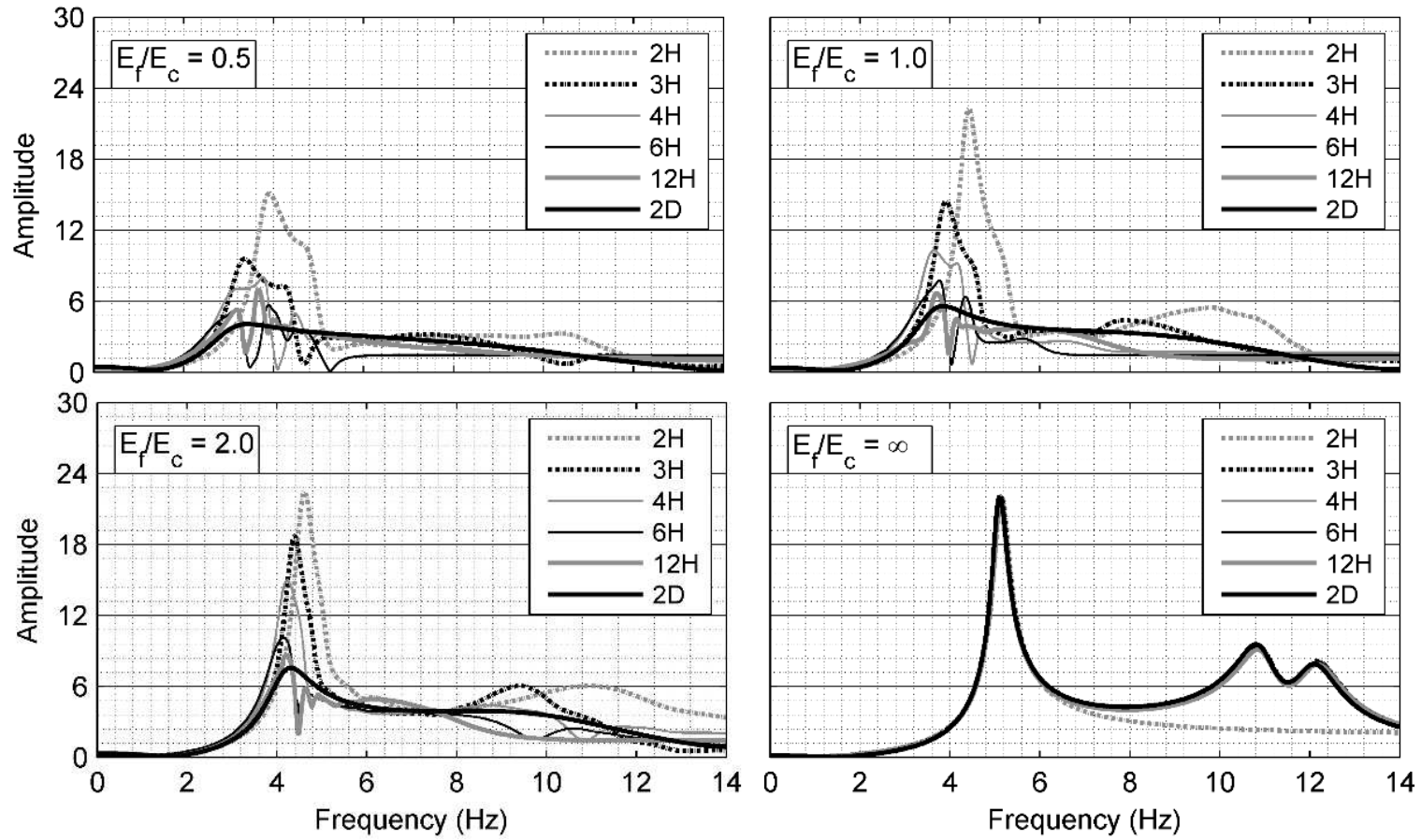


Figure 2-17 Frequency Response Functions, Independent Monolith Idealization vs. Plane Stress Models

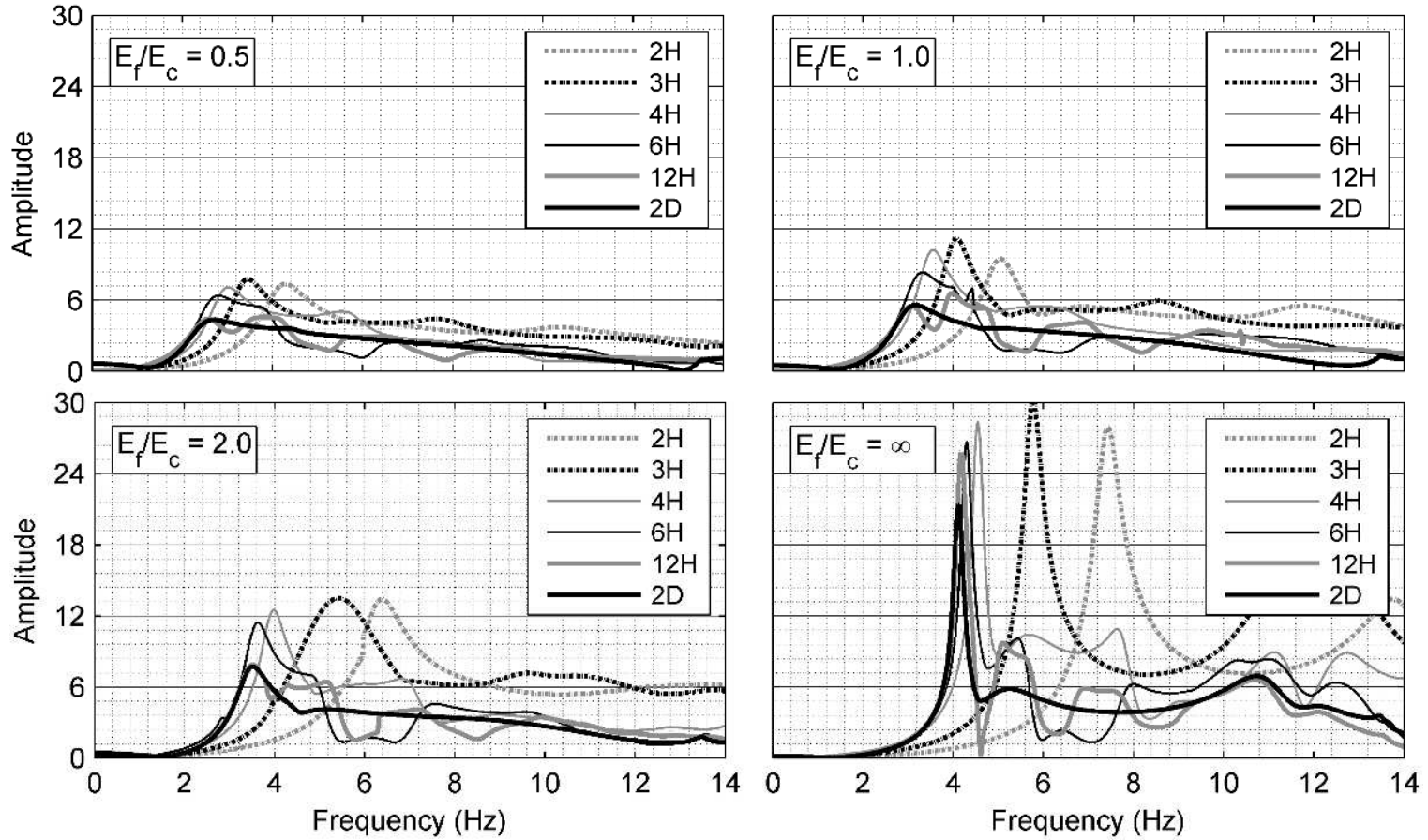


Figure 2-18 Frequency Response Functions, Monolithic Models vs. Plane Strain Models

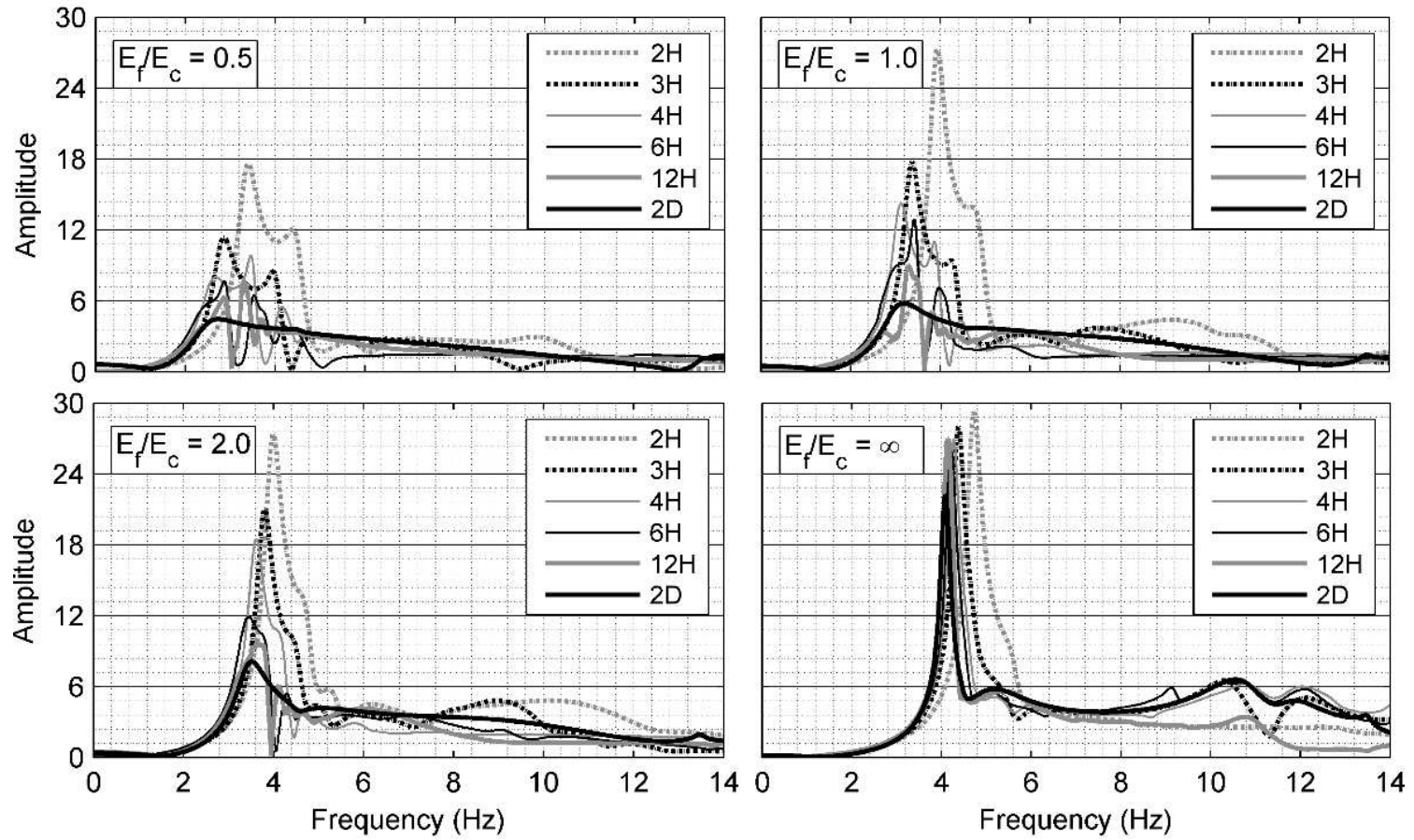


Figure 2-19 Frequency Response Functions, Independent Monolith Idealization vs. Plane Stress Models

The qualitative comparison for the frequency response functions of the 2 and 3D models showed that there was a significant difference in the frequency response for the 2 idealizations. For the quantitative comparison of the response, the differences in the fundamental frequency values and the first mode damping ratios were determined as given in the next section.

### 2.5.2 The Difference in the Natural Frequencies, 2D vs. 3D Models

The natural frequency and damping ratio in the natural frequency are commonly utilized analytical parameters for the prediction of the demand on the gravity dam systems (United States Army Corps of Engineers, 1995). The differences in the natural frequencies for the 2 and 3D idealizations of the same system were calculated in this section using the 1<sup>st</sup> mode frequency response (Section 2.4). The damping ratio is a function of the frequency response curve determining the amplitude of the response for the mode considered. Consequently, the damping ratio for the first mode was obtained using the half-power bandwidth method on the first mode frequency response function. In contrast to the conventional application for systems with low damping ratios, the full functional form of the aforementioned method was used so as to avoid the introduction of approximations (chopra, 2012). For  $f_{1,1}, f_{1,2}$  as the bounding frequency values corresponding to  $1/\sqrt{2}$  times the first mode resonant amplitude at either sides of the fundamental frequency ( $f_1$ ) peak, Equation 2-5 was solved to determine the equivalent damping ratio for the first mode. The natural frequency and the damping ratio values for the 2D models are presented in Table 2-2.

$$\left(\frac{f_{1,2}}{f_1}\right)^2 - \left(\frac{f_{1,1}}{f_1}\right)^2 = 4\xi_1\sqrt{1 - \xi_1^2} \quad (2-5)$$

The frequency response functions for the monolithic idealization of the dam system showed a significant difference in the fundamental frequency compared to the 2D models for the narrower canyons (Table 2-3 and Table 2-4). The fundamental frequency of the 3D rigorous solution agreed well with the 2D prediction at the 12H

canyon width, however, the difference was greater than 10% for canyon widths less than 6H. For a monolithic system in a narrow canyon, 3D models yielded fundamental frequencies higher by as much as 50 and 45%, respectively, for models with the moduli ratios  $E_f/E_c$  of 0.5 and 1. The difference in the fundamental frequency between the 2 and 3D models was amplified by the decrease in the ratio of the foundation/structure moduli: i.e. softer foundation medium caused 3D models to yield higher fundamental frequency values compared to 2D models. In terms of the fundamental frequency, the difference between the 2 and 3D modeling appears to be significant for the monolithic systems. The difference in the fundamental frequency between the 2 and 3D modeling was affected only to a small extent by the reservoir.

Table 2-2 Fundamental Frequency and Damping Ratios for the Fundamental Mode of 2D Models

Material $E_f/E_c$	Without Reservoir				With Reservoir			
	Plane Strain		Plane Stress		Plane Strain		Plane Stress	
	$f_1$ (Hz)	$\xi_1$ (%)	$f_1$ (Hz)	$\xi_1$ (%)	$f_1$ (Hz)	$\xi_1$ (%)	$f_1$ (Hz)	$\xi_1$ (%)
0.5	2.7	30.8	2.7	29.7	2.3	28.4	2.4	27.3
1.0	3.5	21	3.5	19.7	2.9	19.7	3.0	18.7
2.0	4.1	14.1	4.1	13.3	3.4	12.8	3.4	12.3
$\infty$	5.2	5	5.1	5	4.1	4.3	4.1	4.3

For the idealization with the independent monoliths, the difference between the fundamental frequency of the 2D and the 3D models decreased to some extent regardless of presence of reservoir. For a V/H ratio of 12, the fundamental frequency obtained from the 3D models corresponded to the 2D counterparts, with the disparity only visible at the low end of  $E_f/E_c$  ratios. For systems in narrow canyons, the difference in the fundamental frequencies was still significant. At the  $E_f/E_c$  ratio of 0.5, the natural frequency of a 3D model with independent monoliths in a canyon 2H wide was 30% higher than a 2D counterpart, showing the significant coupling occurring between the monoliths due to the foundation. Monoliths cannot move independently from each other, even separated at the joints, as their motion was

constrained at the base by the common boundary. The coupling at the base, hence the difference in the fundamental frequency between the 2 and 3D models, was significantly reduced by an increase in the foundation modulus rendering each monolith independent of each other. In conclusion, even with the assumption of perfectly separated monoliths, the coupling between the monoliths due to the common foundation boundary condition was significant. The difference in the fundamental frequency between the 2 and 3D modeling approaches was still large provided that the dam was built on a flexible foundation.

### **2.5.3 Difference in the Damping Ratio for the First Mode, 2D vs. 3D Models**

Damping ratio is usually the most recognized effect of the soil-structure interaction on the response prediction of gravity dams given the consideration allows for significant reductions in the demand quantities. Comparison of the 1<sup>st</sup> mode damping ratios for the 2 and 3D models shows there were significant differences in the damping ratios between the two idealizations. For a monolithic system, the damping ratio estimate for a 2D model appears to be generally significantly larger than the 3D counterpart (Table 2-3). The 3D solution agrees better with the 2D counterpart only for higher  $E_f/E_c$  and  $V/H$  values. The difference was as much as 102%, 99% and 38%, respectively, for  $E_f/E_c$  ratios of 0.5, 1.0 and 2, decreasing as the canyon width increased. The damping ratios agreed well only for  $V/H$  ratios of 12, i.e. for the case when the 2 and 3D solutions converged.

Considering the reservoir, the damping ratios were obtained lower for both cases. The difference in the damping ratios between the 2 and 3D models followed the same trend with the no reservoir case. For the case with the independent monoliths, much larger differences between the response peaks of the 2 and 3D solutions were observed. The highest peaks compared to the 2D results were observed especially at lower  $E_f/E_c$  ratios corresponding to large differences in the damping ratio estimates between the models.

Table 2-3 Fundamental Frequency and Damping Ratios for the Fundamental Mode of 3D Systems Along with Corresponding Differences, 3D vs. 2D Models (Without Reservoir)

Material $E_f/E_c$	Width	Monolithic				Independent Monoliths			
		$f_1$ (Hz)	$\Delta f_1$ (%)	$\xi_1$ (%)	$\Delta \xi_1$ (%)	$f_1$ (Hz)	$\Delta f_1$ (%)	$\xi_1$ (%)	$\Delta \xi_1$ (%)
0.5	2H	5.2	-48.1	15.1	104.0	3.9	-30.8	9.1	226.4
	3H	4.1	-34.1	16.7	84.4	3.3	-18.2	12.2	143.4
	4H	3.4	-20.6	20.2	52.5	3.0	-10.0	17.1	73.7
	6H	2.9	-6.9	26.1	18.0	2.8	-3.6	22.4	32.6
	12H	2.6	3.8	41.7	-26.1	2.6	3.8	39.8	-25.4
1.0	2H	6.1	-42.6	12.4	69.4	4.4	-20.5	6.3	212.7
	3H	4.8	-27.1	12.7	65.4	3.9	-10.3	8.5	131.8
	4H	4.0	-12.5	13.9	51.1	3.6	-2.8	10.7	84.1
	6H	3.6	-2.8	20.2	4.0	3.4	2.9	17.3	13.9
	12H	3.3	6.1	35.0	-40.0	3.3	6.1	33.9	-41.9
2.0	2H	7.0	-41.4	9.4	50.0	4.7	-13.0	5.1	160.3
	3H	5.3	-22.6	9.6	46.4	4.3	-4.7	6.7	98.5
	4H	4.7	-12.8	10.8	30.6	4.1	0.0	8.2	62.2
	6H	4.2	-2.4	12.7	11.0	4.0	2.5	12.5	6.4
	12H	3.9	5.1	18.7	-24.6	3.9	5.1	22.4	-40.6
$\infty$	2H	8.3	-37.3	6.4	-21.9	6.1	-16.4	5.0	0.0
	3H	6.5	-20.0	6.3	-20.6	6.1	-16.4	5.0	0.0
	4H	5.7	-8.8	6.3	-20.6	6.1	-16.4	5.0	0.0
	6H	5.4	-3.7	6.3	-20.6	6.1	-16.4	5.0	0.0
	12H	5.3	-1.9	6.3	-20.6	6.1	-16.4	5.0	0.0

Table 2-4 Fundamental Frequency and Damping Ratios for the Fundamental Mode of 3D Systems Along with Corresponding Differences, 3D vs. 2D Models (With Reservoir)

Material $E_f/E_c$	Width	Monolithic				Independent Monoliths			
		$f_1$ (Hz)	$\Delta f_1$ (%)	$\xi_1$ (%)	$\Delta \xi_1$ (%)	$f_1$ (Hz)	$\Delta f_1$ (%)	$\xi_1$ (%)	$\Delta \xi_1$ (%)
0.5	2H	4.1	-44.0	14.0	102.3	3.4	-28.6	8.9	206.4
	3H	3.4	-31.5	14.4	97.2	2.8	-14.0	11.1	145.1
	4H	2.9	-19.9	17.1	66.1	2.5	-5.5	15.7	74.0
	6H	2.5	-9.1	21.7	31.1	2.3	5.3	21.2	28.5
	12H	2.4	-3.4	30.1	-5.7	2.4	1.7	28.9	-5.4
1.0	2H	5.0	-41.8	9.9	99.0	3.9	-23.1	6.4	192.2
	3H	4.0	-27.3	10.3	92.2	3.3	-9.4	7.9	136.7
	4H	3.5	-16.4	12.4	58.5	3.1	-2.6	8.9	110.1
	6H	3.1	-6.8	16.6	19.0	2.9	4.5	14.0	33.9
	12H	3.0	-3.0	24.6	2.8	2.8	7.5	25.3	-26.1
2.0	2H	6.3	-45.8	9.3	37.6	4.4	-22.7	6.1	101.6
	3H	4.8	-29.2	9.8	30.6	3.8	-9.6	6.7	84.1
	4H	3.9	-13.0	9.6	33.8	3.6	-5.0	7.1	72.5
	6H	3.6	-4.2	10.5	21.7	3.4	1.2	10.2	20.1
	12H	3.5	-2.8	12.1	5.8	3.3	3	16.3	-24.5
$\infty$	2H	7.5	-45.2	5.2	-17.3	5.3	-22.9	5.2	-17.3
	3H	5.8	-29.1	5.0	-14.0	4.4	-6.0	4.8	-10.4
	4H	4.5	-9.7	4.3	0.0	4.3	-5.3	4.8	-10.4
	6H	4.3	-4.4	4.3	0.0	4.3	-5.3	4.3	0.0
	12H	4.1	-1.0	4.3	0.0	4.2	-1.2	4.5	-4.4

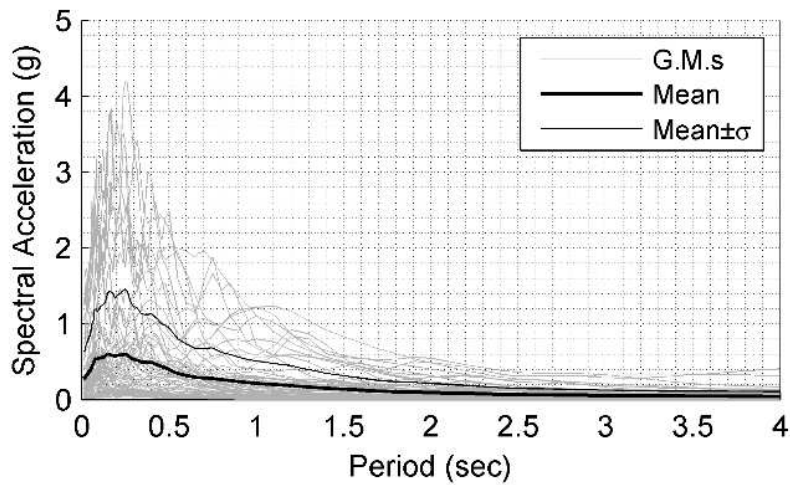
For the canyon with the lowest width, the difference in the damping ratio was obtained as much as 226%, 213% and 160%, respectively, for  $E_f/E_c$  ratios of 0.5, 1.0 and 2. The difference reduced as the canyon width increased. The 2D models appeared to yield significantly higher damping ratios compared to their 3D counterparts. The results follow a similar trend when the reservoir contribution was considered in the analyses. In conclusion, for the foundation modulus equal or lower than the structure modulus, 2D rigorous solution appeared to significantly flatten the response peak even for systems in very wide canyons such as those with width to height ratios of 6.

#### **2.5.4 Time Domain Effects**

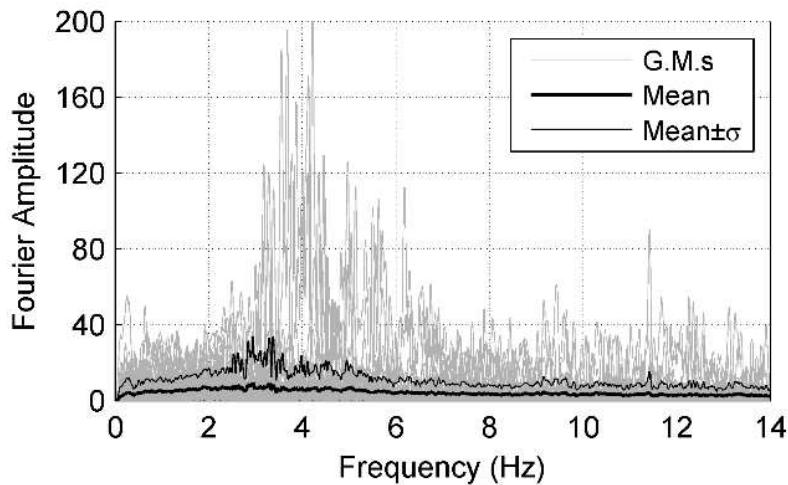
The comparison of the frequency response parameters is effective only to an extent in identifying the different behavior of the chosen models. While comparing the peak response values (or the equivalent damping), the location of the frequency and the corresponding interaction with the ground motion is inadvertently ignored. The effects of both discrepancies can only be simplified to a comparative basis in the time domain results. The consideration of the response in the time domain is also essential as almost all of our engineering decision parameters (except the fundamental frequency) are based on time domain results. Naturally, the uncertainty due to variation in the ground motions is introduced to the analysis results in order to quantify the effect of the different frequency responses on the engineering demand parameters (addressed further in Chapter 3).

A ground motion suite chosen from the Pacific Earthquake Engineering Research strong motion database (PEER, 2015) was used in order to compare the response of the 2 and 3D models in the time domain. The suite, comprised of 37 pairs of time histories, was chosen so as to reflect the different characteristics of the ground motions on the chosen demand parameter. The recordings, from 20 different earthquakes in a magnitude range of 6.2 to 7.6, were selected from sites designated as rock/hard rock (NEHRP site conditions A and B) with epicentral distances of 0 to

57 km. The response spectra and the Fourier spectra of the motions are presented in Figure 2-20.



a) Response Spectra of the Ground Motions



b) Fourier Spectra of the Ground Motions

Figure 2-20 Ground Motion Definition

The crest displacement of the dam and maximum principal stress at the upstream face (both located at the central monolith for the 3D models) were chosen as the response quantities of interest for comparison purposes. Using these demand parameters, the difference statistics between the 2 and 3D modeling approaches were obtained for the chosen ground motions which can help the designers predict the expected difference of their own 2D solution from the 3D counterparts.

Table 2-5 Selected Ground Motions

#	Event	Date	PGA (g)	PGV (cm/sec)	M <sub>w</sub>	R <sub>jb</sub> (km)	V <sub>s30</sub> (m/sec)	Fault Mech.
1	San Fernando	1971	1.23	114.41	6.6	0.00	2016.1	Rev.
2	San Fernando	1971	0.20	12.83	6.6	21.5	969.1	Rev.
3	Tabas, Iran	1978	0.86	123.34	7.4	1.79	766.8	Rev.
4	Morgan Hill	1984	0.09	2.89	6.2	14.9	1428.1	Str. S.
5	Loma Prieta	1989	0.48	33.62	6.9	8.84	1428.1	Rev.O
6	Landers	1992	0.78	133.33	7.3	2.19	1369.0	Str. S.
7	Northridge-01	1994	0.15	14.63	6.7	15.1	1222.5	Rev.
8	Northridge-01	1994	0.43	44.26	6.7	4.92	2016.1	Rev.
9	Northridge-01	1994	1.58	103.33	6.7	4.92	2016.1	Rev.
10	Northridge-01	1994	0.15	18.37	6.7	23.1	996.4	Rev.
11	Kobe, Japan	1995	0.31	55.27	6.9	0.90	1043.0	Str. S.
12	Kocaeli,Turkey	1999	0.26	44.60	7.5	7.57	792.0	Str. S.
13	Kocaeli,Turkey	1999	0.23	38.27	7.5	3.62	811.0	Str. S.
14	Chi-Chi,Taiwan	1999	0.05	6.97	7.6	36.0	804.4	Rev.O
15	Chi-Chi,Taiwan	1999	0.09	10.86	7.6	53.3	789.2	Rev.O
16	Chi-Chi,Taiwan	1999	0.14	19.12	7.6	52.4	1525.9	Rev.O
17	Chi-Chi,Taiwan	1999	0.06	7.42	7.6	55.1	999.7	Rev.O
18	Duzce- Turkey	1999	0.05	9.98	7.1	25.8	782.0	Str. S.
19	Chi-Chi,Taiwan 04	1999	0.06	3.38	6.2	39.3	804.4	Str. S.
20	Chi-Chi,Taiwan-05	1999	0.04	3.44	6.2	44.3	789.2	Rev.
21	Chi-Chi,Taiwan-05	1999	0.03	5.91	6.2	49.8	1525.9	Rev.
22	Chi-Chi,Taiwan-06	1999	0.02	3.76	6.3	47.8	789.2	Rev.
23	Chi-Chi,Taiwan-06	1999	0.04	8.79	6.3	52.3	1525.9	Rev.
24	Loma Prieta	1989	0.44	95.73	6.9	3.2	1070.3	Rev.O
25	Tottori, Japan	2000	0.18	12.63	6.6	15.2	940.2	Str. S.
26	Tottori, Japan	2000	0.23	21.45	6.6	15.6	967.3	Str. S.
27	Parkfield-02	2004	0.24	14.60	6.0	4.66	907.0	Str. S.
28	Niigata, Japan	2004	0.14	2.64	6.6	52.1	829.0	Rev.
29	Iwate, Japan	2008	0.08	5.04	6.9	37.4	829.5	Rev.
30	Iwate, Japan	2008	0.29	26.24	6.9	16.3	825.8	Rev.
31	Iwate, Japan	2008	0.09	2.68	6.9	56.7	934.0	Rev.
32	Iwate, Japan	2008	0.23	5.42	6.9	40.4	849.8	Rev.
33	Iwate, Japan	2008	0.18	4.29	6.9	57.1	859.2	Rev.
34	Duzce, Turkey	1999	1.03	40.20	7.1	4.21	760.0	Str. S.
35	San Simeon	2003	0.05	8.76	6.5	37.9	1100.0	Rev.

The relative difference between the maximum of the time history response for the 2 and 3D models are computed using Equation 2-6 separately for each ground motion.

$$\varepsilon_{disp}(\%) = \frac{d_{top}^{2D} - d_{top}^{3D}}{d_{top}^{3D}} \times 100 \quad \& \quad \varepsilon_{stress}(\%) = \frac{S_1^{2D} - S_1^{3D}}{S_1^{3D}} \times 100 \quad (2-6)$$

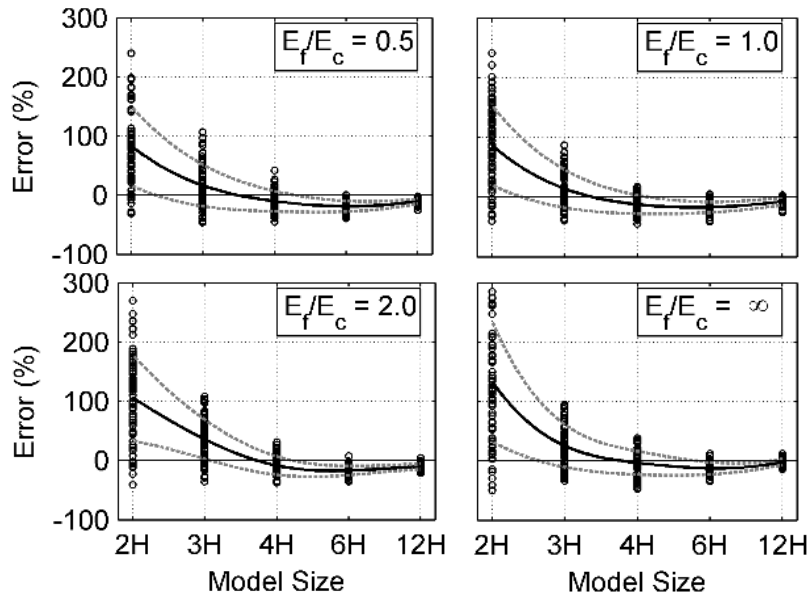
### 2.5.4.1 Crest Displacement

The mean values as well as the  $\pm$  standard deviation of the difference between the 2 and 3D crest displacement predictions for each model are presented in Figure 2-21 in order to show the common range of errors one can obtain by using a 2D analysis tool for predicting the performance of this essentially 3D system. Each point for a given V/H ratio represents the difference between the 2 and 3D models for a particular ground motion irrespective of the scale of the motion. The results for the 2D plane strain and plane stress models were compared to their counterparts, the monolithic and the independent monolith case, respectively, in the 3D setting. The statistics of the particular V/H ratio were calculated considering the results for the 70 different ground motions utilized.

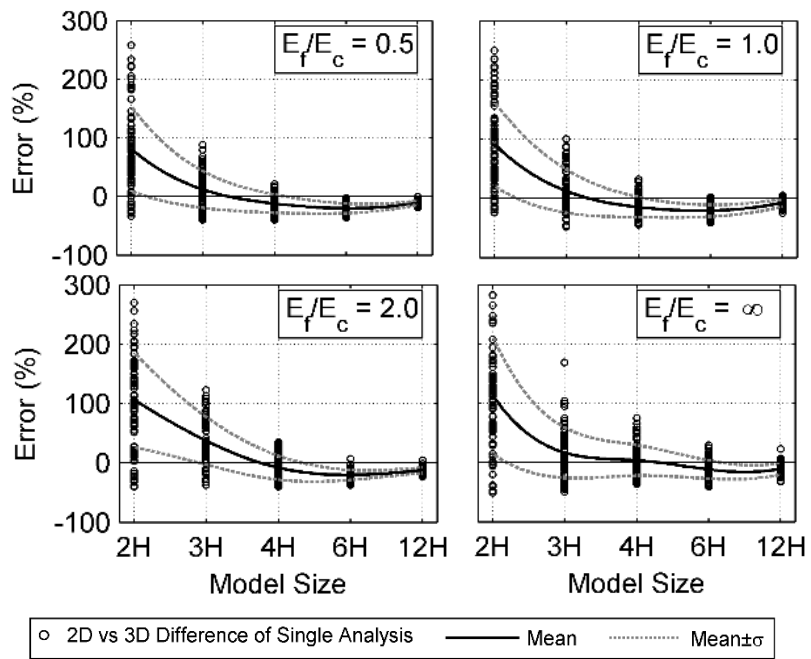
For the monolithic systems, the results show a large variation in the displacement predictions corresponding to the difference in the 2 and 3D frequency response functions as well as the frequency contents of the utilized motions. As given in Figure 2-21, a 2D model can predict the top displacement by as much as 250% over the 3D counterpart for a narrow canyon. The error in the estimate was reduced with the increasing canyon width. For a canyon width of 4 times the dam height, the mean error for the 2D estimate was reduced to zero for all moduli ratios. However, the variance was still significant. The maximum displacement predicted by a 2D model could be as much as 40% lower and higher than the 3D estimate, underlining the importance of the differences in the frequency response functions between the 2 and 3D models over the whole frequency range. The difference in the frequency content of the motions, coupled with the difference in the FRFs in the 0-10 Hz range, yielded considerably large differences between the 2 and 3D results for some motions. Similar to the mean value, the variance of the difference between the 2/3D results reduced with increasing canyon width as expected.

The results for the differences between the plane stress 2D models and the 3D independent monolith idealization was considerably different compared to the aforementioned case for a monolithic dam. The 2D displacement response was lower than the 3D counterpart. The significantly reduced peaks of the FRFs for this case were not matched by the 3D counterparts, especially for narrow canyons. Coupled with the frequency content of the motions, the 2D prediction underestimated the displacement response by around 25% (in the mean sense) for canyon widths of 2 to 6H for all moduli ratios. The demand predictions for independent monoliths from 2D analyses were significantly closer to 3D counterparts compared to the monolithic systems. Yet, for a given ground motion the maximum displacement predicted from a 2D analysis can be as low as 50% of the 3D analysis. The variance on the estimate followed the same pattern with the previous case, reducing with increasing canyon width.

The differences of the maximum response quantities of interest were also investigated for the dam-reservoir-foundation system. Comparison of the results shown in Figure 2-21 with their counterparts (models with empty reservoir) reveals a similar pattern in the difference between the 2 and 3D approaches for the prediction of displacements in the presence of the reservoir. The predictions for the 2D model can be as high as 200% of the 3D solution for a monolithic system constructed in a narrow canyon. For the corresponding canyon, the maximum displacement for the 2D solution can be as low as 50% of the 3D prediction with independent monoliths.

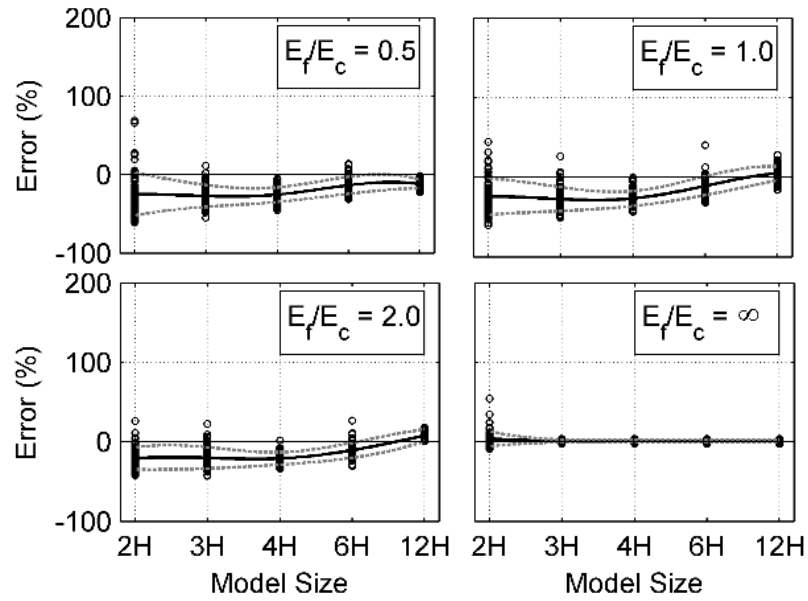


a) Monolithic Models vs. Plane Strain Models (without Reservoir)

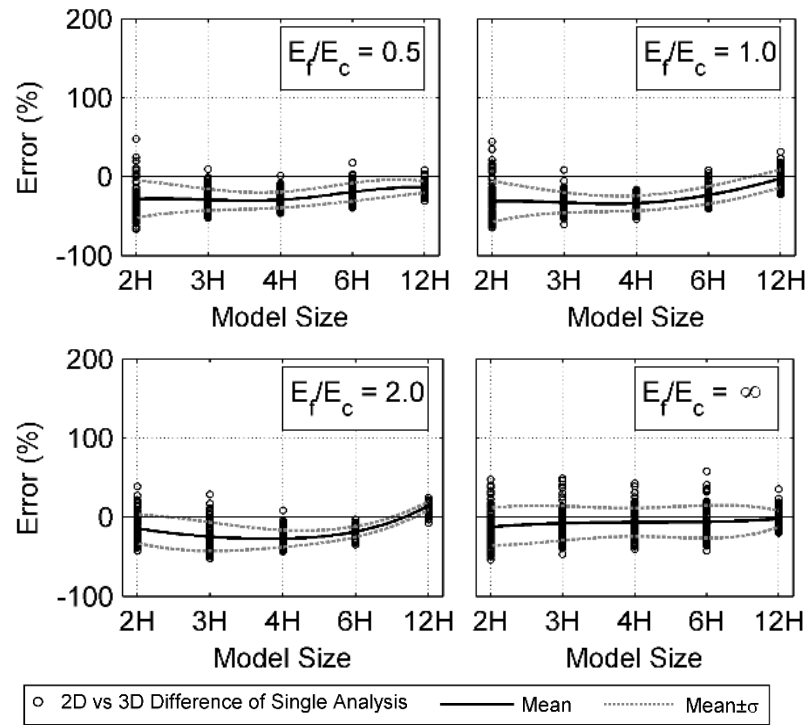


b) Monolithic Models vs. Plane Strain Models (with Reservoir)

Figure 2-21 Difference in the Crest Displacements, 2D vs. 3D Models



c) Independent Monolith Idealization vs. Plane Stress Models (without Reservoir)



d) Independent Monolith Idealization vs. Plane Stress Models (with Reservoir)

Figure 2-21 (Continued) Difference in the Crest Displacements, 2D vs. 3D Models

### 2.5.4.2 Maximum Principal Stress

The stress demand at the base of the dam is often critically important in order to decide on the possible damage expected on the dam system. The stress demands for the 2 and 3D models were computed at the heel of the dam. It is worth noting that the locations of the stress quantities reported by EACD-3D-08 and EAGD-84 were slightly different due to the different element type, mesh size, and the number of Gauss quadrature points employed in these programs. Thus, in order to compare consistent results, a procedure calculating the maximum principal stress at the corner node (on the upstream face of the dam at the center of the valley) was developed and implemented in MATLAB (Figure 2-22).

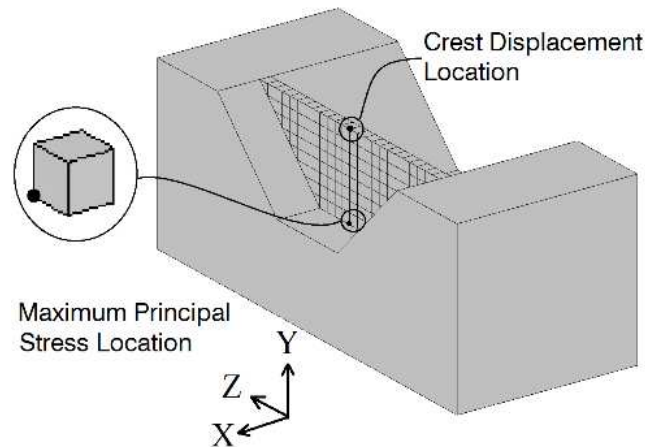


Figure 2-22 Maximum Principal Stress Location

In this procedure, the transfer functions of the six local stress quantities were obtained first using the displacement results of the dam structure subjected to a white noise input. Then the Fourier transform of the ground motion was multiplied with the aforementioned transfer functions and the time histories of the stress states were obtained using the inverse Fourier transform. The time history of the maximum principal stress was then determined using these local stress time history responses and the maximum value was obtained (Figure 2-23). This process enables the retrieval of the stresses at consistent locations and consequently reliable comparisons of the 2D and 3D results. The computational resources are more efficiently used in

this approach compared to the local routines in the software. Moreover, EACD-3D-08 assumes a simplified formulation for the calculation of the principal stresses based on a 2D state of stress including the so called arch and cantilever stresses. The incorrect results that would be obtained from this formulation is avoided using this calculation procedure.

The stress demands at the toe of the dam for the 2 and 3D models, compared using the same approach employed for the displacement demand, are presented in Figure 2-24. separately for the monolithic and independent systems. For the sake of brevity, the  $\text{mean} \pm \sigma$  of the differences of the maximum principal stress between the 2 and 3D models are presented in the same chart for all the moduli ( $E_f/E_c$ ) and canyon width ratios ( $V/H$ ). Following the same trend as the displacements, the 2D analysis of monolithic dams in a narrow canyon resulted in significant overestimation of the stress demands for the whole range of moduli ratios.

The mean error in the stress estimate for a monolithic system in a canyon width of  $2H$  was as high as 350% for the rigid base condition, reducing to 180% for the foundation/dam moduli ratio of 0.5. This error can be considered to be acceptably small only when the canyon width increased to  $6H$ , six times the dam height. It is also observed that the mean error of stress predictions are almost two times the corresponding quantity for the crest displacement and can be as much as 3 times of the displacement error for the case of models on rigid foundations.

The analyses for the independent monolith case displayed a completely opposite trend as given in Figure 2-24. The 2D analyses markedly underestimated the stress. For a moduli ratio of  $E_f/E_c=0.5$ , the 2D analysis underestimated the stresses consistently by around 40% for all canyon widths. Similar to the displacement predictions, the variance on the difference between the 2 and 3D analyses results was also substantially reduced, indicating the differences were obtained consistently with the same trend for the whole range of ground motions.

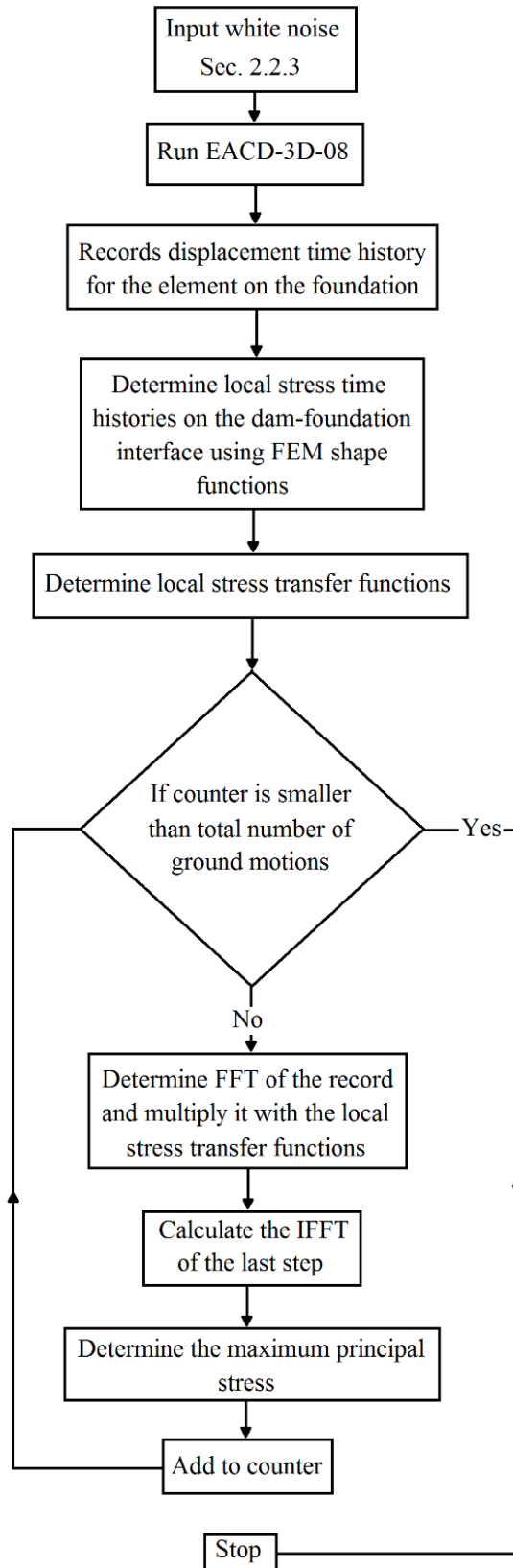
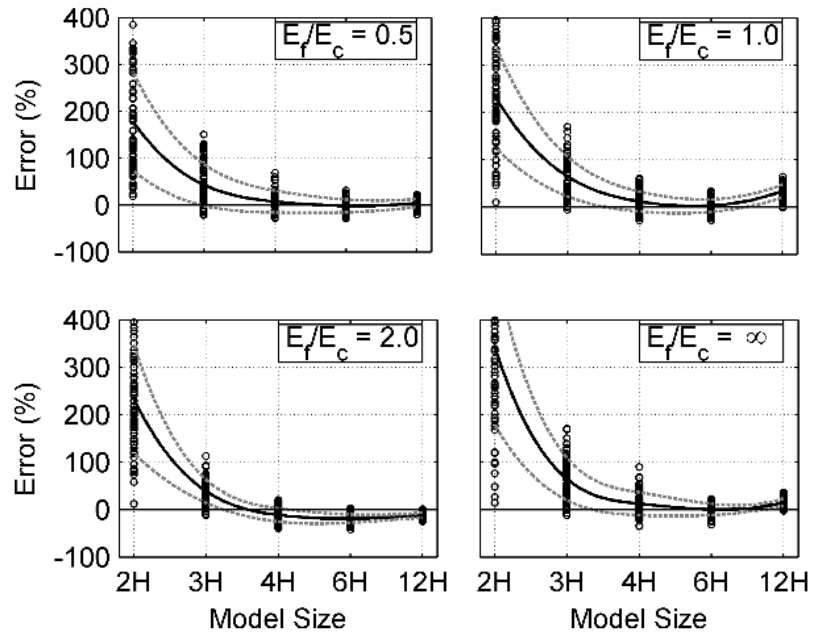
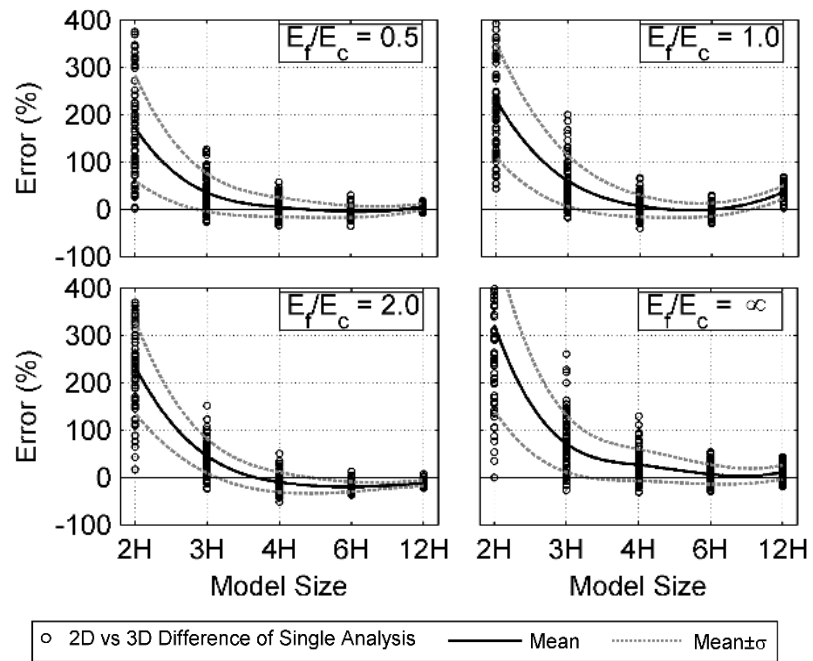


Figure 2-23 Flowchart of the MATLAB Code for Calculation of Maximum Principal Stress

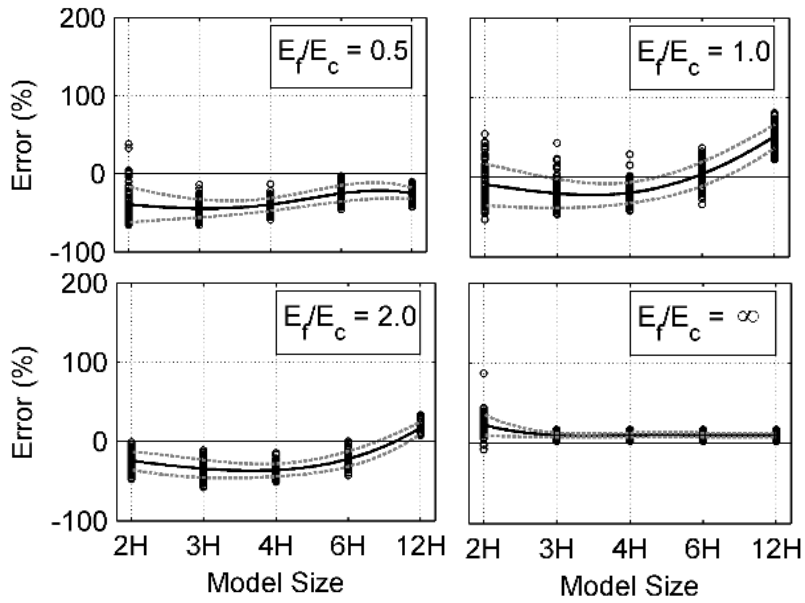


a) Monolithic Models vs. Plane Strain Models (without Reservoir)

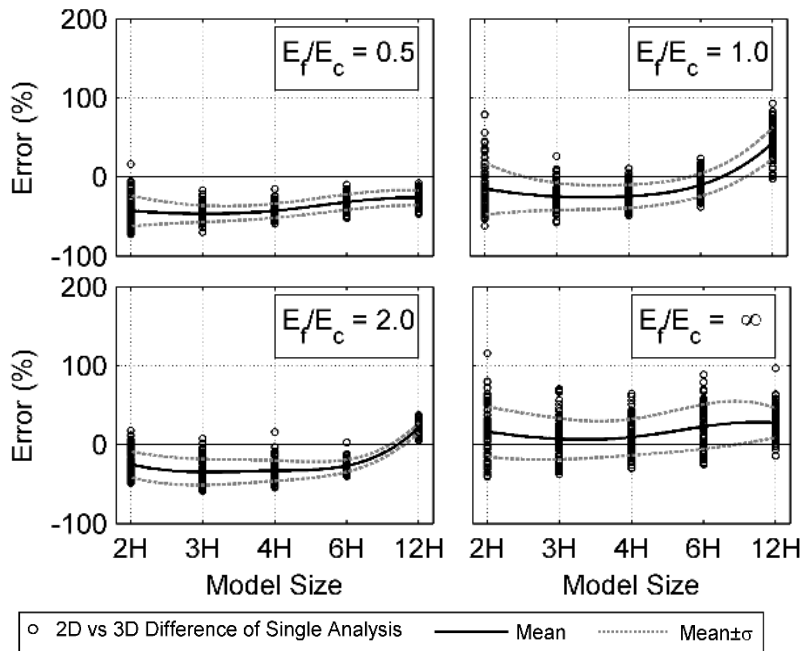


b) Monolithic Models vs. Plane Strain Models (with Reservoir)

Figure 2-24 Difference in the Principal Stress at the Upstream Face, 2D vs. 3D Models



c) Independent Monolith Idealization vs. Plane Stress Models (without Reservoir)



d) Independent Monolith Idealization vs. Plane Stress Models (with Reservoir)

Figure 2-24 (Continued) Difference in the Principal Stress at the Upstream Face, 2D vs. 3D Models

The stress predictions for the 2D models with reservoir can be as high as 500% of the 3D solution for a monolithic system built in a narrow canyon. 2D stress predictions of models with independent monoliths can be lower, significantly on the unconservative side. As in the case of monolithic systems, the standard deviations of the differences, showing the effect of the motion properties coupled with the frequency response function of the systems, tended to decrease as the canyon width increased.

#### **2.5.4.3 The Distribution of the Stresses at the Base**

The stress distribution at the base of the dam, obtained from the 2 and 3D models, were similar (Figure 2-25), albeit the differences in the maximum values at the toe and heel of the dam. The results are presented for both the monolithic system and the system comprised of independent monoliths for a foundation-structure moduli ratio ( $E_f/E_c$ ) of 1.0. For the sake of brevity, the results are presented for a single ground motion for which the difference in the stress between the 2 and 3D models were obtained at the mean level of the analysis, i.e. the stress obtained for the 2D model was approximately 200% higher than 3D result at the upstream face of the dam (+88m). For the monolithic system, the stress distribution for the 2D and the 3D system with 12H canyon width agree well: however, for lower canyon widths, the differences between the stress distributions were more pronounced. For the more narrow valleys, the 3D stresses were clearly below the 2D distribution along the whole length of the base, following the pattern for the difference at the upstream face.

For the case with the independent monoliths, the stress distribution between the 2D model and the 3D model in the largest valley were different, although agreeing well at the downstream face (+5m). The 3D stress distribution for the model in the widest canyon was lower than the 2D counterpart along the whole length of the base. For narrower canyons, however, the stress distributions for the 3D models were clearly above the 2D values. The results obtained were in parallel with Figure 2-24, showing that the comparison of the maximum stresses given in this figure can be applied to the distribution of the stresses as well. It should again be noted that these results were

obtained for a single ground motion, therefore, the difference between the distributions can be obtained much higher or lower as demonstrated by the differences in the maximum principal stresses presented in Figure 2-25.

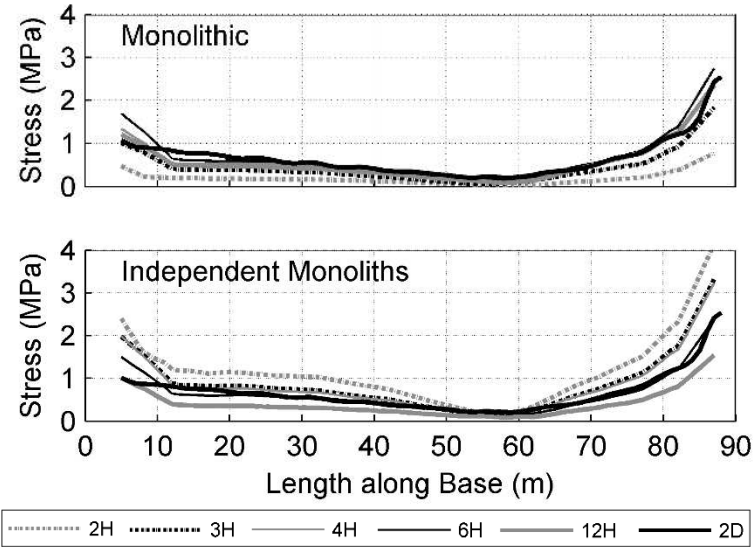


Figure 2-25 The Distribution of the Maximum Principal Stress on the Foundation

## CHAPTER 3

### GROUND MOTION SELECTION AND SCALING

#### 3.1 General

The requirement to accurately simulate the dam-foundation-reservoir interaction for the determination of the seismic response of concrete gravity dams necessitates rigorous frequency domain analyses in 3D setting in order to obtain the seismic demands on these systems. In this regard, there is a large dispersion in the required demand quantities in such analyses due to the stochastic nature of the applied earthquake records. The variability in the time domain analyses, hence a seismic analysis problem, has traditionally been addressed by specifying dispersion on the response spectrum defining the variability on the demands on a structure. However, for much of the time domain quantities, the variability is due to the frequency content of the motions. Naturally, for dam-reservoir-foundation systems in which DFRI effects are very important, the concern for the frequency content of the motions as well as the frequency response of the systems are much more prevalent. These concerns for the variability in the demand quantities based on the frequency content of the motions as well as the frequency response of these systems necessitate an investigation on the selection and scaling of ground motions to be used for the design and evaluation of concrete gravity dams, similar to the investigations conducted for multi-story moment frames (Alavi & Krawinkler, 2004) and bridges (Somerville, 2002).

The goal of the selection and scaling of the ground motions is to obtain a robust, efficient and accurate time domain analysis framework for the evaluation of the seismic demand on the structures. In this framework, robustness implies the

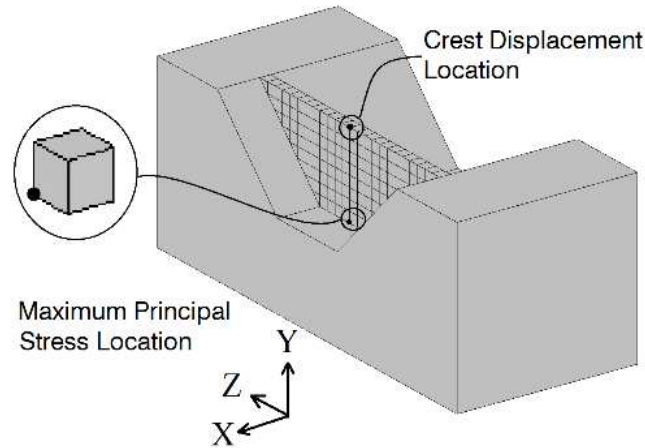
expectation of reduced variability in the analysis results among possible different choices while efficiency implies reaching the analysis goals with the minimal consumption of time/resources. Accuracy, as the primary goal, represents reaching the design or the evaluation goals and the targets on the time domain analysis results within a certain precision.

The selection and the scaling of the ground motions for the determination of the seismic demands on gravity dams is an important task that determines the end result of the seismic assessment. However, most of the recommendations given regarding the selection and scaling of the ground motions are proposed for moment frame structures and the guidance on these procedures for seismic assessment of the gravity dams is scarce. In this context, the primary goal of this study was to evaluate the existing ground motion scaling techniques in a robust soil-structure interaction (SSI) setting for determining the efficiency and accuracy for predicting the target demands for the concrete gravity dams. The prediction bias in the results following the selection and scaling of the motions was investigated in order to provide guidelines on the use of ground motions in the seismic analysis of gravity dams. For this purpose, a large ensemble of ground motions were used on a range of systems with different canyon geometries and moduli ratios in order to consider the effect of the SSI on the motion selection. As well as displacement demands, the variability in the stress demand quantities were investigated so as to provide suggestions on the use of ground motions for the nonlinear analysis for concrete gravity dams. The duration of the critical loading on the system, which is considered to be very important in determining the crack propagation on these systems, was also considered as a demand parameter in the study. Considering a set of target demand quantities, a range of ground motion selection techniques were utilized and tested for accuracy, robustness and efficiency. The required number of ground motions for the consistent and efficient analyses of such systems was investigated.

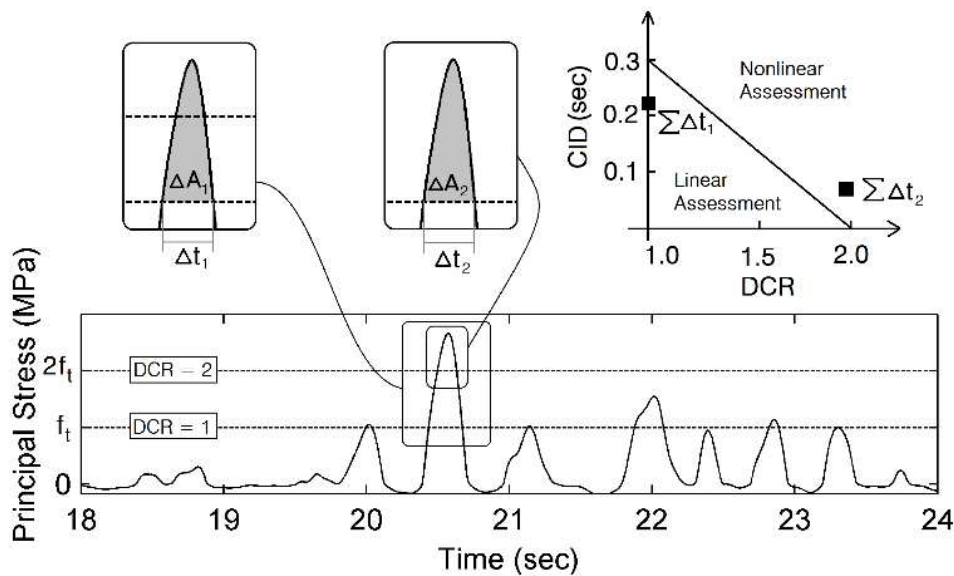
### 3.2 Numerical Models

Frequency domain quantities, or the response functions as given in Section 2.4.3, can hardly be used for engineering purposes as all of our design parameters are based on time domain responses which can be tied to the specific design goals. For the dam structures, the crest displacement or the acceleration is a regularly reported quantity; however, this is mostly based on the tradition of using these as the engineering demand parameters for dams in the absence of other quantities. In contrast to the use of drift ratio as a damage indicator for buildings (American Society of Civil Engineers, 2010), utilizing the displacement for dam structures is merely a visual means of validation the results, providing a qualitative measure for the overall stability of the dam (United States Army Corps of Engineers, 2003). As an indicator of the possible damage on the system, the use of the principal stress and the duration of exceedance quantities were proposed in (Ghanaat, 2004). The exceedance of the tensile strength and the corresponding cumulative duration (in which the tensile strength was exceeded) was associated with the expected damage level on the system in order to determine the effects of the ground motions on dam systems. Given the need to cover the damage inducing potential of the ground motions, the aforementioned four different demand parameters, as summarized below, were used as the response quantities, i.e. EDPs, on the 3D DFRI systems (presented in chapter 2) in this study:

- 1) Crest displacement: Crest displacement at the top of the middle monolith (Figure 3-1a),
- 2) Maximum Principal Stress: Maximum principal stress at the bottom of the middle monolith (Figure 3-1a),
- 3) Cumulative Inelastic Duration (CID): Cumulative duration over a selected strength limit in seconds for the middle monolith (Figure 3-1b),
- 4) Cumulative Stress-Time Area: The total area of the principal stress vs. time curve over a given strength limit for the middle monolith (Figure 3-1b).



a) Crest Displacement and Maximum Principal Stress



b) Duration and Stress-Time Area as Demand Quantities

Figure 3-1 Response Quantities for the Comparison of Time History Responses

Considering the required computational effort, the cumulative inelastic duration and stress-time area EDPs were calculated only at the most critical location for the overstressed regions at the heel of the central monolith of the dam systems. The DCR was also calculated above a single tensile strength at this location. In addition to the use of the crest displacement and maximum principal stress values, the above mentioned time domain response quantities are also going to be used as the EDPs for which the efficiency and effectiveness of the ground motion scaling techniques will be evaluated in the following sections. In other words, the selection and manipulation of the ground motion records should yield an effective prediction of these demand quantities for use in the design or evaluation of these systems.

### **3.3 Ground Motion Selection and Scaling Procedures**

The selection of the records is generally conducted by choosing from the ground motions recorded during former events with the magnitude, source-to-site distance, fault type and the local site condition complying with the maximum earthquake considered at the site. The selection of the records in a specified magnitude range is of considerable importance since the magnitude is one of the main features of a ground motion and it affects the frequency content as well as the duration of the strong motion (Stewart et al., 2002). Fault distance is also one of the important parameters affecting the characteristics of ground motions especially for the case of near-fault earthquakes. Many researchers have shown that there is a relationship between the magnitude and pulse period (Alavi & Krawinkler, 2004; Baker, 2007; Fu & Menun, 2004; Somerville, 2002). Yet, within the design process, the choice of the required number of records and the selection of the ground motions are still more of an experience. This in turn necessitates the scaling in order to reduce the subjectivity with respect to the selected records. The ground motions chosen are often scaled to conform to the target demand levels traditionally defined by a response spectrum for the seismic hazard at the site. Different scaling techniques are employed to match the target spectrum (Abrahamson, 1992; American Society of Civil Engineers, 2010), keeping in mind that the specific characteristics of the earthquake reflected on the time history, such as the nature of the pulse, frequency content and the duration are not present on a response spectrum (Baker, 2010). Scaling of the earthquake records using a simple multiplier allows keeping the pulse information within the record. On the other hand, scaling with the spectral matching methods changes the frequency content of the record. A short summary of the scaling procedures utilized in this study is given below.

### 3.4 Ground Motion Scaling Methods

#### 3.4.1.1 Simple Scaling Approach

The simple scaling procedure for the ground motions based on the USACE-EM-1110-2-6051 (United States Army Corps of Engineers, 2003) is comprised of three distinct scaling steps over the period range of significant importance to the structural response. First, individual ground motions have to be scaled so as to satisfy the closeness requirements (Figure 3-2a). It is recommended that the sum of the differences of respective logarithms of the spectral accelerations of the scaled ground motion and the target spectrum to be equal to zero. The least number of ground motions that can be used for linear and nonlinear analyses are suggested as 3 and 5, respectively (United States Army Corps of Engineers, 2003).

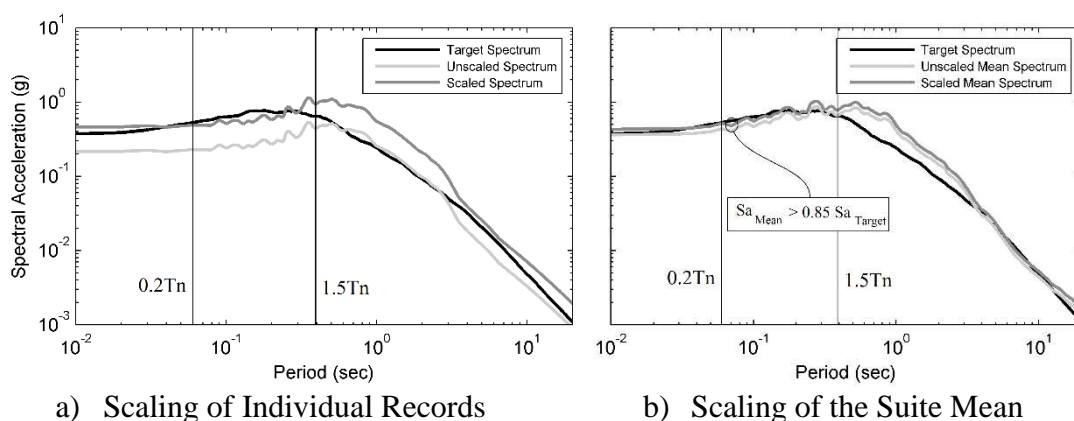


Figure 3-2 Simple Scaling Procedure (United States Army Corps of Engineers, 2003)

Subsequently, two additional scaling factors have to be applied to the suite of chosen records in order to guarantee the mean of the spectral accelerations of these motions to remain above a minimum spectral response threshold. Thus, a second scale factor is applied to the suite of motions in order to prevent the mean of the spectral accelerations from falling below 85 percent of the target spectrum. Finally, the average of the ratios of the mean response spectrum to target spectrum at each period in the range of interest is controlled and verified to be more than unity (Figure 3-2b). The period range of significant importance to the structural response is not explicitly

specified in (United States Army Corps of Engineers, 2003). Consequently, the suggestions of the ASCE/SEI-7-10 (American Society of Civil Engineers, 2010), i.e. a period range of  $0.2T_n \sim 1.5T_n$ , was used in this study.

#### **3.4.1.2 Non-Stationary Spectral Matching**

Time domain spectral matching approach tries to achieve an almost perfect fit between the individual ground motions' spectrum and the target spectrum. The method, implemented in the software RSPM, utilizes wavelet transforms to modify the motion while preserving the non-stationary nature of the originals (Abrahamson, 1992). Special considerations have to be taken using the spectral matching technique according to (United States Army Corps of Engineers, 2003). Similar to the procedure suggested for the simple scaling of records, first, the individual ground motions have to be scaled to lie at the approximate level of target spectrum in the period range of significant importance for the structural response (Figure 3-2a). Following the spectral matching of the suite, the minimum requirements regarding the mean of the scaled records have to be verified; that is, the mean of the spectrally matched ground motions should lie above 85 percent of the target spectrum. It is worth noting that the ground motions modified with this approach usually match to the target spectra with negligible difference, rendering the latter requirement redundant. For this procedure, the minimum number of selected ground motions in a suite is recommended as 1 and 5 for linear and nonlinear analyses, respectively (United States Army Corps of Engineers, 2003).

#### **3.4.1.3 Maximum Incremental Velocity**

Incremental velocity is an intensity measure for a ground motion defined as the area under the acceleration time history between two consecutive points of zero acceleration. Maximum incremental velocity is the maximum of these quantities in a given motion providing a metric on the nature of the pulses within the record. In this scaling method, the ground motions are scaled linearly by a factor to match their maximum incremental velocities (MIV) to that of the target MIV (Kurama & Farrow,

2003). The simplicity of application and the independence of the scaling factor from the natural frequency of the structure, which eliminates the effect of changes to the structural system on the scaling procedure, were suggested as the advantages of this scaling technique. A reduction in scatter in the EDPs compared to other scaling procedures was observed while using MIV approach for high ductility buildings subjected to near fault motions (Kurama & Farrow, 2003).

#### **3.4.1.4 Scaling Based on the Fundamental Period's Response Spectrum Amplitude**

Scaling of the ground motions for matching the spectrum amplitude at the fundamental frequency to a target demand quantity was commonly applied before the suggestion of the use of a frequency range of importance in the matching procedure. This scarcely used technique is utilized in this study with a slight modification: instead of the use of the conventional 5% damping ratio, the representative damping ratio for the SSI system at the first fundamental frequency was used for the scaling of the ground motions, henceforth referred to as  $T_n$  Scaling method. The large effect of the SSI on the frequency response of these large structures encased in the ground is generally quantified by a significant increase of the damping ratio in contrast to the typical building structures. This effect and the corresponding equivalent damping ratio is largely dependent on the moduli ratios of the foundation and the structure as well as the geometry of the system. Therefore, different damping ratios were used for scaling for each of the systems considered. These values were obtained applying the half power band width method on the crest acceleration frequency response function. Subsequently, the obtained equivalent damping ratios were used in computation of the response spectrums for the selected suite.

### 3.4.2 Ground Motion Scaling

### 3.4.3 Ground Motion Suite

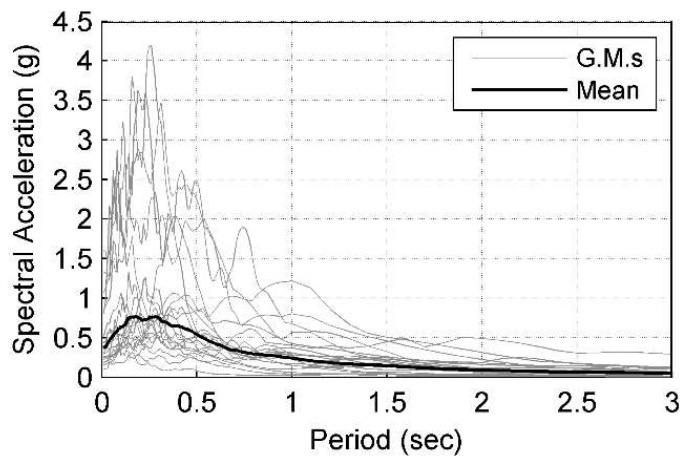
For the design or evaluation of a structural system for seismic hazard, the earthquake records shall be selected from the events whose magnitude, source-to-site distance, type of faulting comply with the maximum earthquake considered at the site (American Society of Civil Engineers, 2010; United States Army Corps of Engineers, 2003). Local site condition of the utilized records should also comply with the corresponding properties of the design site (Section 2.3.4).

Table 3-1 Selected Near Fault Ground Motions

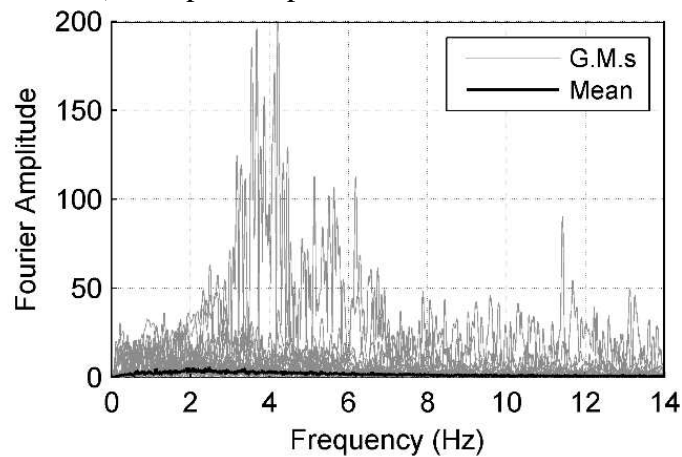
ID	Event	Date	PGA (g)	PGV (cm/sec)	M <sub>w</sub>	R <sub>jb</sub> (km)	V <sub>s30</sub> (m/sec)	Fault Mech.
1	San Fernando	1971	1.23	114.41	6.6	0.00	2016.1	Rev.
2	San Fernando	1971	0.20	12.83	6.6	21.5	969.1	Rev.
3	Tabas, Iran	1978	0.86	123.34	7.4	1.79	766.8	Rev.
4	Morgan Hill	1984	0.09	2.89	6.2	14.9	1428.1	Str. S.
5	Loma Prieta	1989	0.48	33.62	6.9	8.84	1428.1	Rev. O.
6	Uttarkashi, India	1991	0.25	29.8	6.8	21.7	Rock	Rev.
7	Landers	1992	0.78	133.33	7.3	2.19	1369.0	Rev.
8	Northridge-01	1994	0.15	14.63	6.7	15.1	1222.5	Rev.
9	Northridge-01	1994	0.43	44.26	6.7	4.92	2016.1	Rev.
10	Northridge-01	1994	1.58	103.33	6.7	4.92	2016.1	Rev.
11	Kobe, Japan	1995	0.31	55.27	6.9	0.90	1043.0	Str. S.
12	Kocaeli, Turkey	1999	0.26	44.60	7.5	7.57	792.0	Str. S.
13	Kocaeli, Turkey	1999	0.23	38.27	7.5	3.62	811.0	Str. S.
14	Chamoli, India	1999	0.36	45.31	6.8	17.3	Rock	Str. S.
15	Loma Prieta	1989	0.44	95.73	6.9	3.2	1070.3	Rev. O.
16	Tottori, Japan	2000	0.18	12.63	6.6	15.2	940.2	Str. S.
17	Tottori, Japan	2000	0.23	21.45	6.6	15.6	967.3	Str. S.
18	Parkfield-02	2004	0.24	14.60	6.0	4.66	907.0	Str. S.
19	Iwate, Japan	2008	0.29	26.24	6.9	16.3	825.8	Rev.
20	Duzce, Turkey	1999	1.03	40.20	7.1	4.21	760.0	Str. S.

Based on these suggestions, the suite, comprised of 20 pairs of time histories, was chosen so as to reflect the different characteristics of the ground motions on the

chosen demand parameters. The recordings from 14 different earthquakes in a magnitude range of 6 to 7.5 were selected from sites designated as rock/hard rock (NEHRP site conditions A and B) with hypo-central distances of 0 to 20 km (Table 2-5) focusing mainly on the effect of the source to site distance. The response spectra and the Fourier spectra of the motions are presented in Figure 3-3.



a) Response Spectra of the Ground Motions



a) Fourier Spectra of the Ground Motions

Figure 3-3 Ground Motion Definition

The geometric-mean spectrum of the suite was assumed as the design spectrum (that is, target spectrum (Reyes & Kalkan, 2012)) throughout this study (Figure 3-3a). The mean value of the design spectrum and the corresponding EDPs for time history analyses with unscaled ground motions from the suite were treated as the benchmark values. For the MIV scaling, the target MIV value was selected as the geometric mean of the unscaled ground motions.

## 3.5 Results

### 3.5.1 Statistical Investigation of the Scaling Techniques' Effectiveness

The scaling of the chosen ground motions presents an important challenge given the results should be accurate, consistent and efficiently retrieved. The accuracy of the results from the set are implied by the proximity of the mean of the EDP values to the expected response, defined as the benchmark value for the target demand level. Efficiency is measured with the relative ease with which the results are achieved, i.e. the dispersion within a given set should be lowered by the corresponding scaling methodology to facilitate the use of the scaling in the analyses.

The accuracy and dispersion for the scaled suite comprised of all motions are investigated in Figure 3-4 through Figure 3-7 for different EDPs often used in the design and evaluation of gravity dams. The accuracy of the scaling technique was studied by comparing the geometric mean of the EDP results from the scaled suite with the geometric mean obtained from the unscaled (i.e. the benchmark results). In order to facilitate an easy comparison between the estimates, the difference between the scaled suite and the original suite is presented by dividing the response from the scaled motions by the benchmark's corresponding mean value in each figure. Each symbol on Figure 3-4 through Figure 3-7 represents the ratio of the considered EDP with the unscaled benchmark for the particular scaling technique. The effect of the scaling technique on the dispersion was investigated by calculating the standard deviation for the whole scaled suite. The reduction in the dispersion, as expected to be provided by the scaling technique, is shown by presenting the ratio of the geometric standard deviation on the EDP for the scaled and unscaled ground motions, as before. Each bar on Figure 3-4 through Figure 3-7 represent the ratio of the standard deviations for the scaled and unscaled suites, calculated for the particular scaling technique. It should be noted that throughout this study the mean and standard deviation terms in case of displacement and stress EDPs refer to the above definitions, abbreviated for the sake of brevity.

The same procedure was employed in calculation of the accuracy and dispersion of the cumulative inelastic duration and stress-time area EDPs. However, due to the presence of zero quantities for such EDPs in case of models without overstressing, comparison of the results was conducted using the arithmetic mean and standard deviation. The overstressing is determined by the tensile strength of the material. For determining the CID, the tensile strength for each system was assumed to be set at one half of the benchmark quantity for maximum principal stress EDP obtained from the unscaled suite. Such a choice was merely to emulate the possible design variations for systems with different geometries and loading conditions, i.e. target concrete strength may be selected differently in practice for different systems depending on the assessment results.

The effectiveness of the scaling techniques for the maximum crest displacement and principal stress at the heel of the dam are presented in Figure 3-4 and Figure 3-5. Except for the spectral matching technique, the mean displacements and stresses for the scaled ground motions agree very well with the unscaled suite. The results from the spectrum matching technique were consistently lower compared to the benchmark quantities; however, the difference was not substantial. The standard deviations for the scaled suites were obtained substantially lower than unscaled showing these techniques are successful in reducing the inter-set variability for these EDPs. The scaling reduced the standard deviation of the EDPs considerably: except for MIV scaling, the standard deviation for the crest displacement and maximum principal stress for the scaled suite was one half of the unscaled suite. The standard deviation for MIV scaling was somewhat higher, approaching the original suite's value for the narrower canyons.

The comparison of the results of the scaled and unscaled suites for the cumulative inelastic demand ratio is presented in Figure 3-6 in the same form. The scaling of the ground motion led to the underestimation of the CID regardless of the implemented scaling technique for the majority of the cases considered. For the simple scaling, the scaled motion set appear to underestimate the mean CID by 40-50%. The results from  $T_n$  scaling was similar, although the mean appears to be predicted better. The mean

value for the sets scaled with the spectral matching and MIV scaling were closer to the target; however, MIV scaling also introduces significant dispersion compared to the other approaches. Overall, the mean CID value for the scaled sets was uncomfortably smaller compared to the benchmark counterpart for all the techniques.

The comparison of the scaled and unscaled suites for the cumulative time area above the tensile strength at the heel of the dam (Figure 3-7) follow the same pattern as the CID values reported in Figure 3-6. The mean results for the scaled suite were considerably less than the unscaled suite for this EDP. The scaling of the records introduced a significant bias for this quantity. In this respect, MIV scaling was the best performing scaling technique although the mean EDP for the scaled suite was still significantly smaller than the unscaled suite.

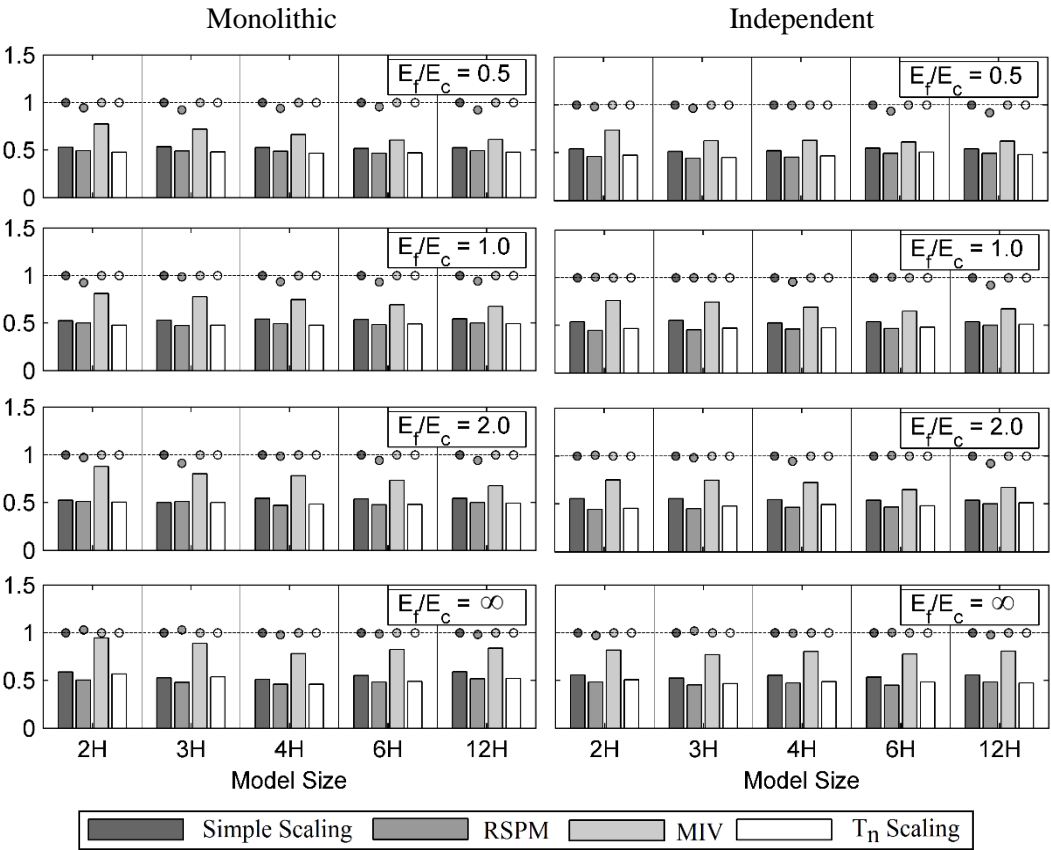


Figure 3-4 The Accuracy and Dispersion of the Scaled Suites, Max. Crest Disp.

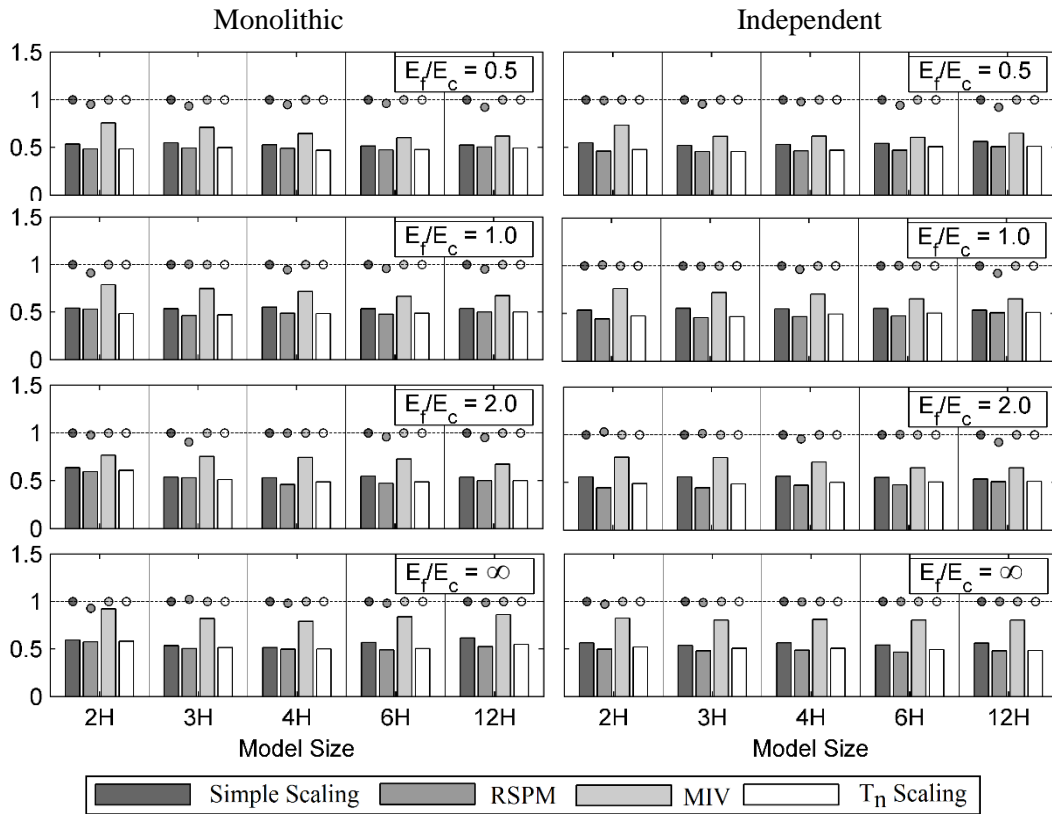


Figure 3-5 The Accuracy and Dispersion of the Scaled Suites for the Maximum Principal Stress

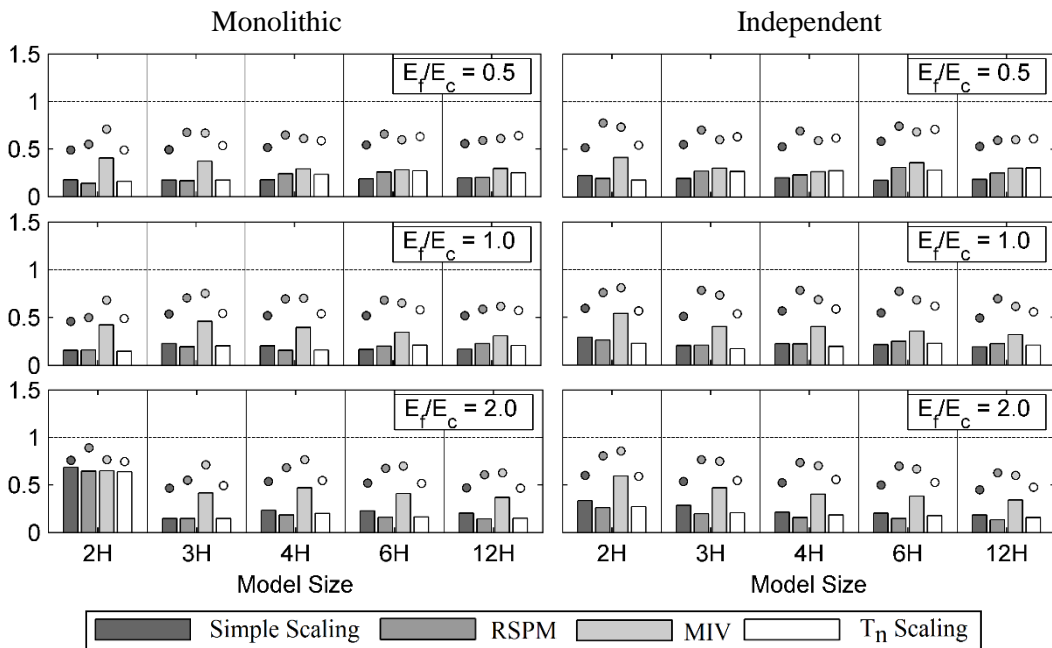


Figure 3-6 The Accuracy and Dispersion of the Scaled Suites for the Cumulative Inelastic Duration

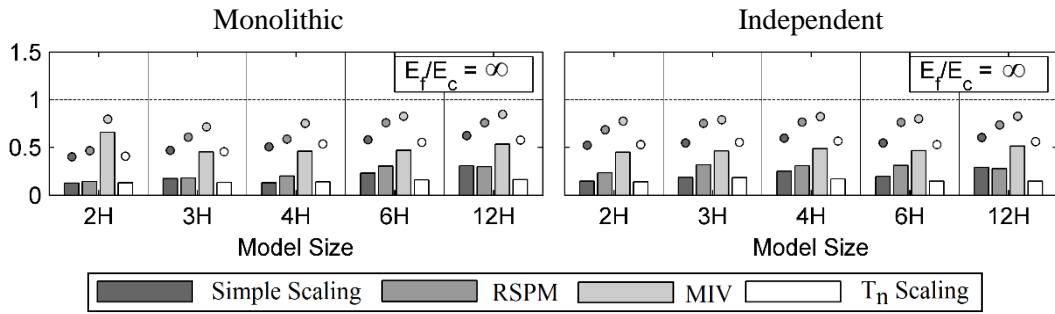


Figure 3-1 (Continued) The Accuracy and Dispersion of the Scaled Suites for the Cumulative Inelastic Duration

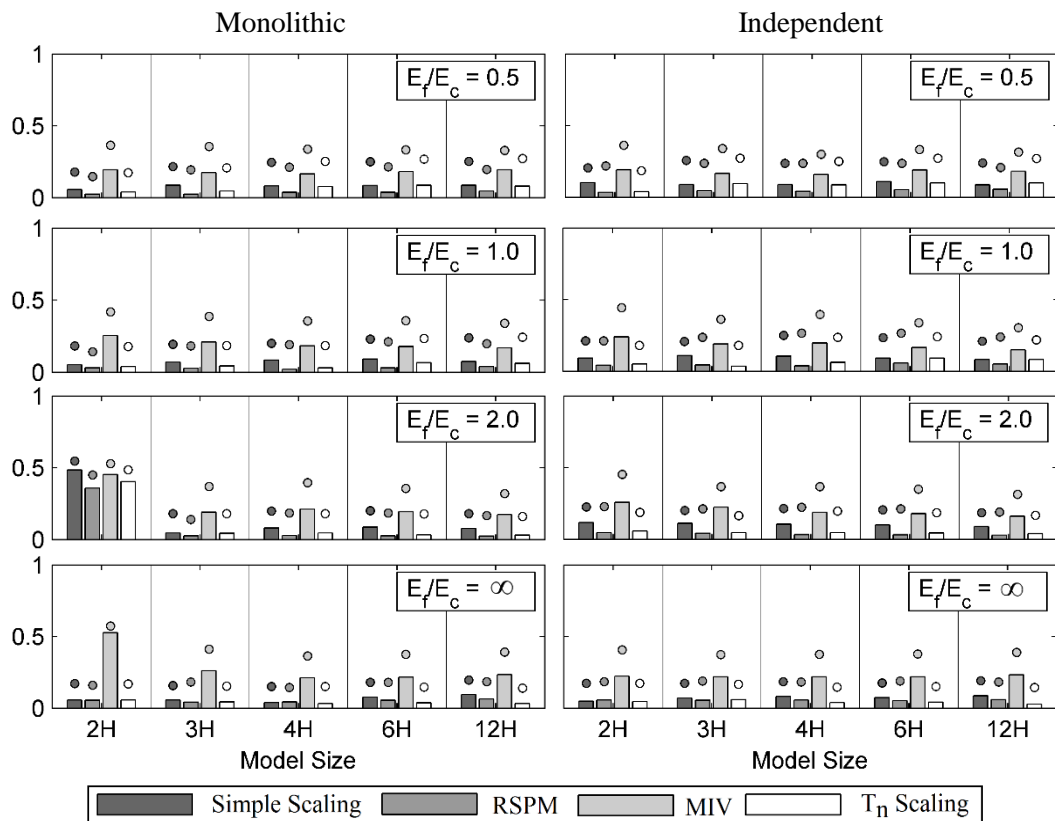


Figure 3-7 The Accuracy and Dispersion of the Scaled Suite for the Cumulative Stress-Time Area

### 3.5.2 Selection of the Records

The analysis sets are often produced from the available suite of motions which comply with the seismic hazard expected at the site. Within the pool of the available ground motions, there is usually a significant flexibility for selecting a set comprised of a limited number of motions. Given the wide variety of sets that can be produced,

the selection of the records becomes a challenging task. The dispersion observed in the EDPs for the scaled and unscaled suites shown above also verify that a large variability can be introduced to a set selected from a larger sample. In this respect, the results of the analysis for different EDPs and the scaling techniques presented in the previous section provide an opportunity to single out ground motions yielding lower dispersion in EDP predictions in order to help with the selection of motions to a smaller analysis set. Given a possible set for ground motions, which of the ground motions in this set can be avoided in order to obtain EDP results with a small degree of variance? The relationship between the variance introduced to the set and the ground motion properties are investigated. The ground motion properties considered were, 1) the physical properties such as the moment magnitude of the considered event and 2) the properties related to the chosen time history, the intensity measures such as the PGA, spectral acceleration, Arias intensity, etc.

The relation between the deviation from the benchmark stress values and the chosen ground motion properties are presented in Figure 3-8. The deviation from the benchmark was defined as the relative difference of the predicted values and benchmark results (Equation 3-1). Each point in the figures represent the % deviation of a particular motion's EDP from the unscaled suite's mean EDP for the chosen scaling technique. The deviation of the prediction of the maximum stress for each scaled motion is shown with the corresponding intensity measure for the motion, the moment magnitude, the peak ground acceleration (PGA), the pseudo-acceleration ( $S_a$ ) at the fundamental frequency, and the Arias intensity ( $I_A$ ). For the sake of brevity, the results are presented for a dam system with 4H canyon width and a moduli ratio of unity idealized using independent monoliths.

$$\text{Error}(\%) = \frac{\text{EDP}_{\text{scaled}} - \text{EDP}_{\text{unscaled}}}{\text{EDP}_{\text{unscaled}}} \times 100 \quad (3-1)$$

It is evident from the results that it is hard to predict the expected dispersion of scaled motion for any scaling technique from the moment magnitude. The simple scaling

was the only technique that showed a slight trend here: exclusion of motions with magnitudes higher than 7 would likely yield smaller dispersion in a set.

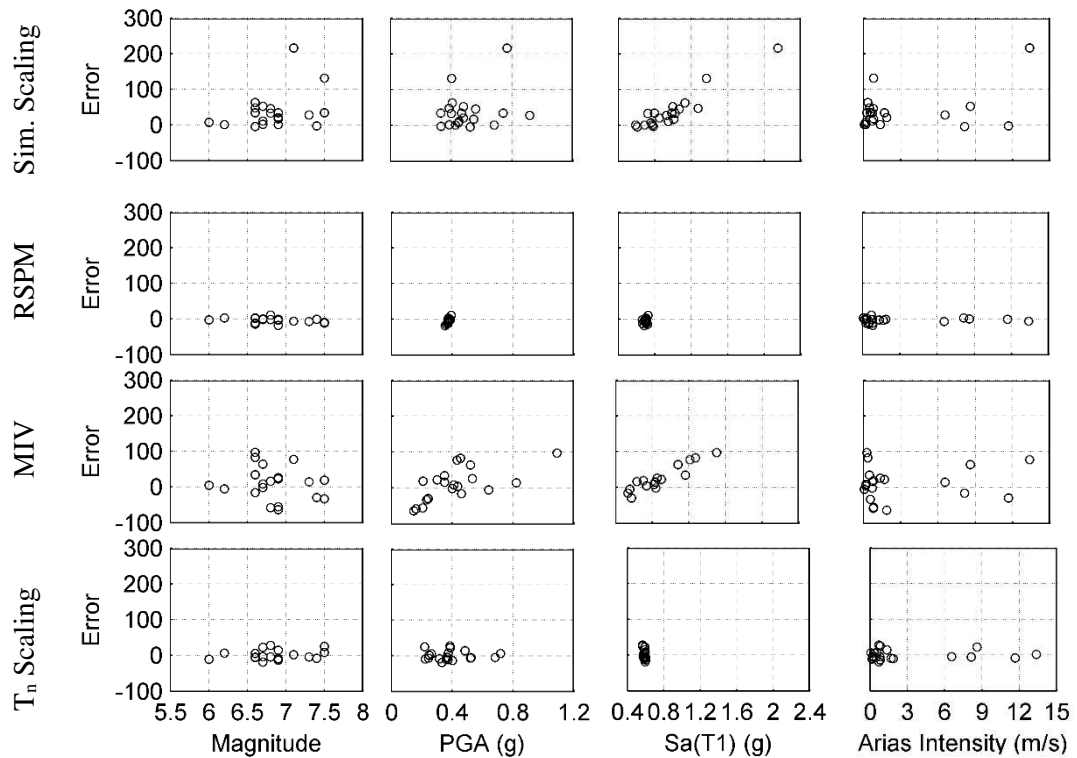


Figure 3-8 Error in the Stress Prediction vs. Ground Motion Intensity Measures

The same trend was valid for the PGA as well: i.e. selecting ground motion bins with PGA would not be a viable selection approach. On the other hand, there was a correlation among the prediction of the demand and the spectral intensity measure ( $S_a$ ). This correlation was expected given the stress quantities would be heavily affected by the response spectrum amplitude for the first mode. For both the simple scaling and the MIV technique, exclusion of motions with higher spectral accelerations compared to the target would reduce the dispersion in a given set. Figure 3-8 suggests that choosing ground motions with 0.8 (g) as the upper bound value for the response spectrum amplitude at the natural frequency would result in the least dispersion of the results which in turn could lower the required minimum number of ground motions in a given set. Given the RSPM and T<sub>n</sub> scaling imply a perfect fit to the spectral amplitude at the fundamental frequency, there is a

considerably low inter-set deviation in the stress predictions. Finally, any correlation between the prediction errors and the Arias intensity measure was not observed.

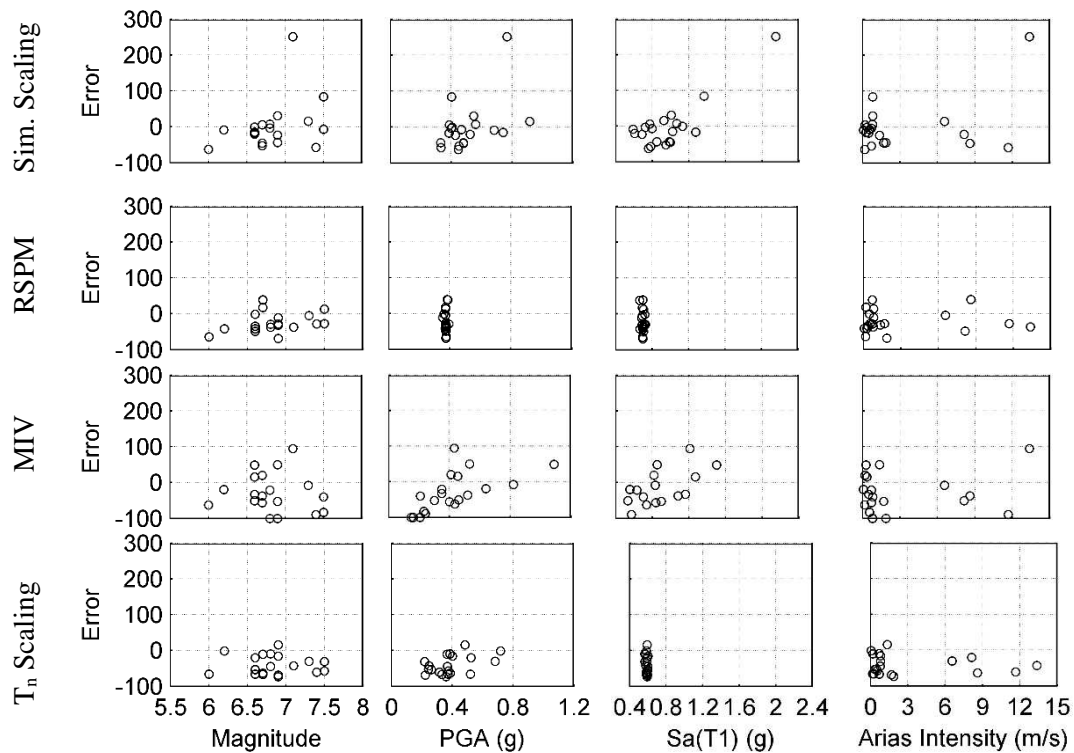


Figure 3-9 Error in the CID vs. Ground Motion Intensity Measures

The relation between the deviation from the benchmark CID values and the chosen ground motion properties are presented in Figure 3-9. As before, the magnitude was not observed to have a correlation with the dispersion from mean except perhaps the simple scaling technique. Spectral acceleration on the fundamental frequency was observed to be correlated to the dispersion from the mean CID for the simple scaling and the fundamental frequency scaling. The Arias intensity and the PGA for a ground motion did not appear to be correlated with the CID quantity observed. It is evident that modal quantities should be used as discriminating parameters for the duration related quantities as well.

### 3.6 Investigation of the Required Number of Ground Motions

While the use of a large number of motions is preferred, practical limitations would prevail most of the time during the selection of the ground motion set for the seismic assessment of structural systems. The common suggestion used in this respect is usually the recommendations of ASCE/SEI-7-10 of using 7 motions and using the average of the EDPs from these 7 motions as the design outcome (American Society of Civil Engineers, 2010). These recommendations appear to be based solely on the engineering judgment of the aforementioned committee (Reyes & Kalkan, 2012). One would expect even a higher number of motions should be used for the seismic assessment of dams given the associated risks with the system failure. However, even with the current computational resources, a detailed 3D time history analysis of a dam system is still very costly. With the requirement of parametric analyses, one can imagine the computational burden a large number of ground motions would impose on the designer for these systems. In this respect, the determination of the minimum number of motions that could be used for effective prediction of the demand quantities becomes an important issue.

For the purpose of determining the appropriate number of ground motions that should be used in transient seismic analyses, the suite of 20 motions as given in Section 2 was used as the selection pool. For each scaling method, sets comprised of 1 to 10 ground motions out of this pool were formed. The possibility of obtaining a different set from the 20 motion suite increases with the increasing number of motions in a given set, i.e. 167960 and 184756 different sets can be drawn from the suite for sets comprised of 9 and 10 different motions, respectively. In this fashion, the inter-set consistency between different ground motion sets can be evaluated forming a measure of the robustness (stability) of the analysis technique: i.e. different parties should obtain similar EDPs for the same target level for sets comprised of different motions. The ground motions within each set were scaled to the target levels in accordance with the scaling methodologies chosen.

The scatters of the mean values of the compiled sets are presented in Figure 3-10 for the maximum principal stress at the heel of the dam. For an increasing number of motions included in the set, as depicted by the horizontal axis of the curve, the results for the chosen EDP are presented, each point in the figure representing the mean of the selected EDP from a respective ground motion set. For the sake of brevity, the results are presented for only two idealizations, i.e. for monolithic as well as independent systems with a moduli  $E_f/E_c$  ratio of 0.5 built in canyon of 4H width. The results were obtained similarly for the other moduli ratios and canyon widths. In order to demonstrate the dependency of the inter-set variability to the scaling technique, the values presented in this figure are normalized by the benchmark mean quantity for each model (the mean EDP for the benchmark suite, calculated for the complete set of 20 motions).

The large inter-set variability for the simple scaling and MIV techniques is clearly demonstrated by the large scatter observed in Figure 3-10. The scattering of the results decreased as expected with the increase of the number of ground motions in the set for all the scaling procedures. In contrast to the results from the simple scaling and MIV techniques, the response spectrum matching technique as well as  $T_n$  scaling approach yielded considerably less inter-set variability as shown by the significantly reduced scatter. The bias introduced to the EDP estimate by scaling technique is also clearly seen for the simple scaling technique. The likelihood of choosing a ground motion set which overestimate the stress is significantly high if a small number of motions are chosen. A bias, on the opposite side was observed for the RSPM scaling, almost consistently, the ground motion sets scaled with the spectrum matching technique yield marginally smaller stress estimates compared to the benchmark case.

The downward bias introduced on the CID by the scaling techniques is clearly shown in Figure 3-11. While the CID values for some of the sets were above the benchmark in the simple scaling, especially for sets formed with a small number of ground motions, the statistics quickly converged to the trend when the number of ground motions in a set were increased. The mean result for the samples for the other scaling techniques directly showed the downward bias on the CID due to the scaling

technique regardless of the motion selection. On the other hand, the inter-set dispersion was substantially reduced for sets containing more than 5 motions.

A summary of the nature of the prediction for the different scaling procedures are presented in Figure 3-12 including the results for all the analysis cases considered in a box-plot format. The horizontal axis on this figure shows the number of ground motions in the selected set. The vertical axis in Figure 3-12a represents the ratio of the mean EDP of all possible suites to their benchmark counterparts: the results presented with symbols are the median values for all the 40 DFRI systems. In order to show the general trend regardless of the geometry or the moduli ratio, the first and third quartiles of the distribution of the results from the considered systems (i.e. 40 different DFRI cases) are presented as the limits in box plots for each scaling procedure. Comparison of the standard deviations in the sets for each scaling procedure is presented in the same fashion in Figure 3-12b in order to show the change of the dispersion for each EDP with respect to the scaling method regardless of the system. As shown in Figure 3-12a, the scaling of the motions led to a bias in the analysis results even though the variance on the EDPs were reduced compared to the analyses conducted for the ground motions from the original suite. The mean value statistics show that the simple scaling technique overestimated the mean stress significantly if the ground motion set was comprised of 4 or lesser number of motions.

The mean quantities for the MIV and the  $T_n$  scaling agreed well with the benchmark means regardless of the number of motions chosen. The conclusions for the maximum principal stress mean, as given above for all the moduli and V/H ratios for the considered systems, do not deviate from the conclusions presented before in Figure 3-10, showing the results are consistently obtained for all of the considered cases.

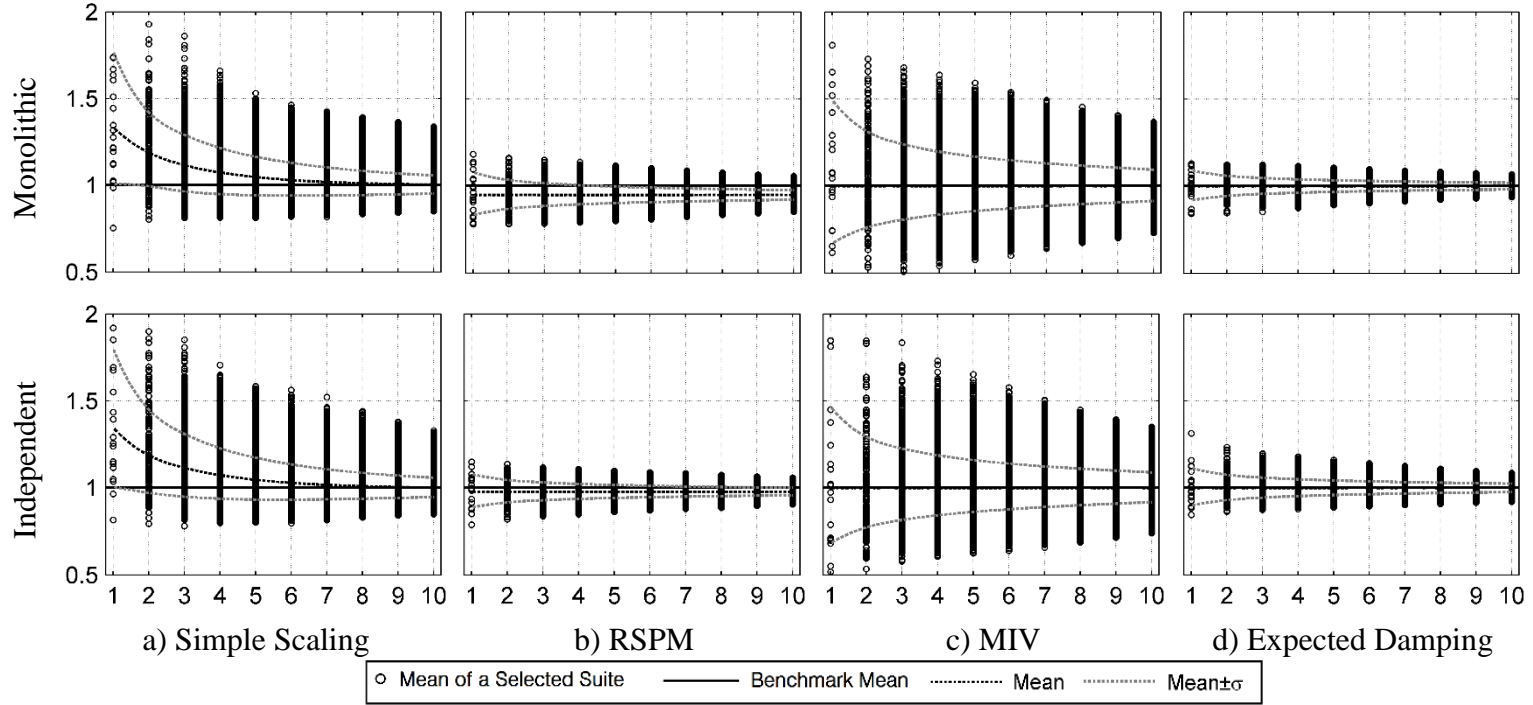


Figure 3-10 Maximum Principal Stress

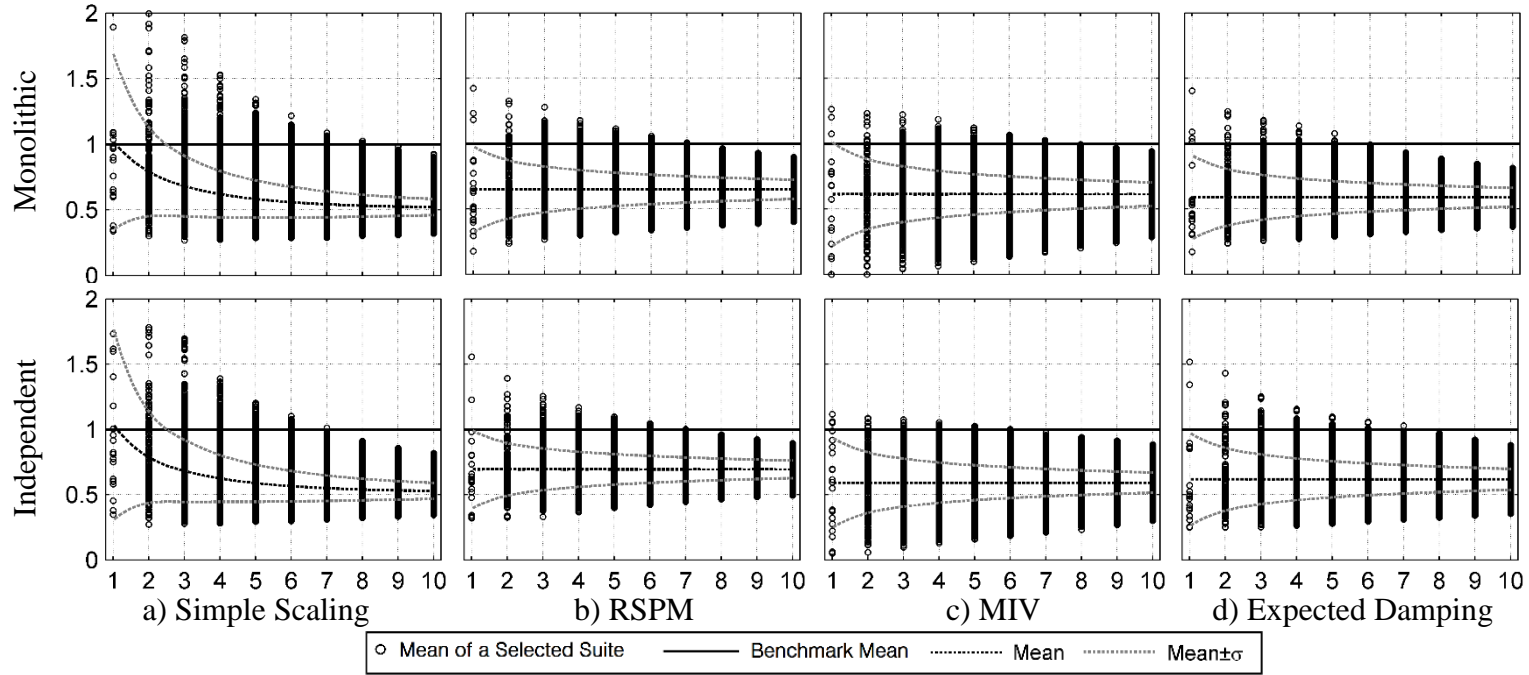


Figure 3-11 Cumulative Inelastic Duration

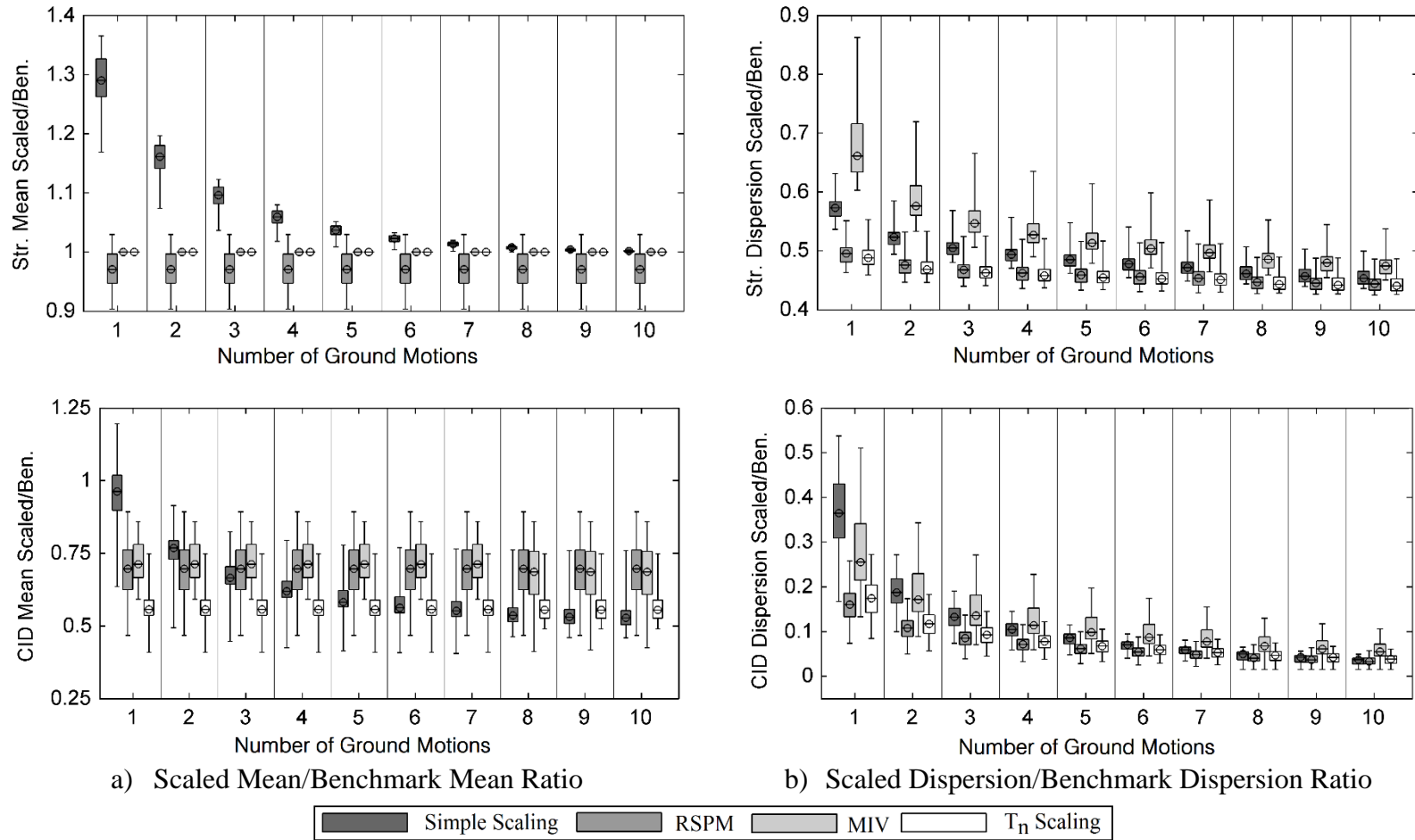


Figure 3-12 Comparison of the Accuracy and Efficiency for Different DFRI Systems

The decrease of the variance in the maximum principal stress by the inclusion of a higher number of ground motions in an analysis set is also clearly observed in Figure 3-12 for all scaling procedures. The use of 7 or more ground motions led to a 40-60% reduction on the unscaled suite's dispersion. However, the reduction in the variance did not necessarily indicate increased accuracy.

The mean results for the CID quantity obtained from all the cases underline the downward bias on the scaled sets' CID values regardless of the scaling procedure employed. The range of the mean values were much larger compared to the stress EDP and the bias was consistently to the downward side for the different geometries and moduli ratios considered. The decrease in the variance was similar to the former case; however, again, there appears to be significant differences in variances for the different analysis cases considered (with different geometry and moduli ratios). The variance was substantially lowered when a large number of motions (i.e. 7 or more) were included in the analysis set.

Considering the above mentioned results regarding the accuracy and the dispersion on the predicted EDP for different sets of ground motions, the number of motions to be included in a set for obtaining reasonably accurate results was investigated. For this purpose, first, an acceptable range on the EDPs that could be used for the design and evaluation of the dam systems was chosen. On the lower bound, the prediction of an EDP quantity by a motion set with at most 10% error was considered as acceptable practice. For the upper bound, the prediction of the mean larger than 50% of the benchmark estimate was considered to be poor practice that might lead to the overdesign of systems. The number of sets for each scaling procedure that did not satisfy these limits was calculated from the complete sampling of the analyses for the chosen number of ground motions. The sample statistics were calculated for sets formed with 1 to 10 ground motions. The statistics of the sets henceforth obtained are presented in Figure 3-13 for the 40 different DFRI cases considered showing the probability of obtaining unacceptable (inaccurate) results for each EDP for the different number of ground motions chosen. The quartile bounds on the samples are

provided with shaded zones in the same figure. A threshold level of 5% is outlined for each plot in order to show the number of ground motions required for a given scaling procedure to yield accurate results: i.e. Samples of sets providing the mean result outside of the acceptable range has fallen to less than 5% of the overall samples that can be formed from the suite.

Investigation of the results presented in Figure 3-13 shows the likelihood of obtaining more accurate results increased as expected by increasing the number of motions included in the analysis set. The investigation of the results obtained from the simple scaling procedure for the maximum principal stress reveals that using the mean of eight or more ground motions was generally required in order to reduce the probability of obtaining poor results to 5%. In other words, the use of 8 or more ground motions in a chosen set yielded 95% probability of being within -10 to +50% of the benchmark EDP obtained from a large number of ground motions. This conclusion was valid for almost 75% of the 40 DFRI analysis cases considered. Similarly, a considerably large number of motions was required to get close to the benchmark stress prediction for monolithic systems using the response spectrum matching technique. However, for the independent idealization, the use of 3 or 4 ground motions yielded acceptable results close to the benchmark quantities.

Among the considered scaling procedures, MIV-scaling yielded the largest variance on the prediction of the maximum stress EDP. This phenomenon was reflected on the means of the sets scaled with the MIV technique a large quantity of which fell out of the acceptable range for the EDP. For obtaining an acceptable EDP prediction, more than 10 records should be used in a given set as shown in Figure 3-13.

The number of motions required for accurate prediction of the maximum principal stress EDP is summarized in Figure 3-14 for the simple scaling and fundamental frequency scaling procedure. Finally, the investigation of the results for sets scaled to the fundamental period spectrum amplitude showed that the use of 5 or more

motions within a set leads to acceptable EDP predictions compared to the benchmark EDP. This conclusion was valid for 90% of the DFRI analysis cases considered.

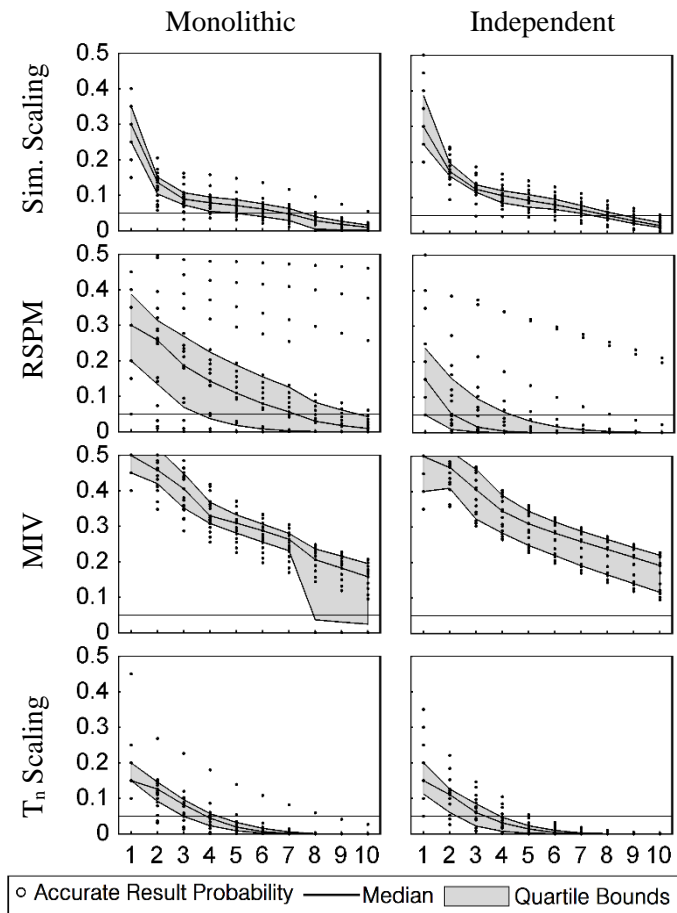


Figure 3-13 Probability of Obtaining Accurate Results

The number of motions required for accurate prediction of the maximum principal stress EDP is summarized in Figure 3-14 for the simple scaling and fundamental frequency scaling procedures. The results for the monolithic system show that for the majority of the cases, the use of 8 or more ground motions should properly address the inter-set variability and lead to acceptable EDP predictions.

For the systems comprised of independent monoliths, 9 or more ground motions appear to be a more reliable selection. There was no identifiable trend regarding the effect of foundation-structure moduli ratio on the number of motions that should be

selected. For scaling with the fundamental frequency, the use of 5 motions appears to be a good choice except perhaps for some of the systems in very narrow valleys.

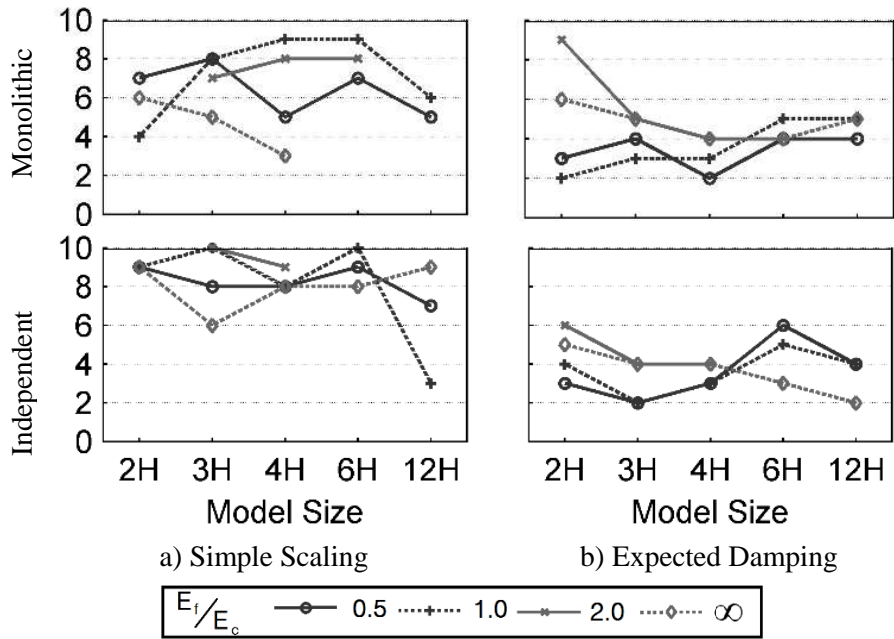


Figure 3-14 Required Number of Ground Motions to Obtain Accurate Results

## CHAPTER 4

### CONCLUSIONS AND FUTURE STUDIES

#### 4.1 Conclusions

In this study, two of the critical challenges regarding the transient analysis of concrete gravity dam structures in practice were addressed. In chapter 2, the common 2D analysis approach for determining the seismic demand on the concrete gravity dams were compared to the three dimensional counterpart using the rigorous DFRI formulations (Fenves & Chopra, 1984a; Wang & Chopra, 2008b). This study represents the first rigorous comparison of these analysis approaches for determining the seismic demands for gravity dams taking into account the full soil-structure-reservoir interaction effect. A range of foundation-structure moduli ( $E_f/E_c$ ) and height to width (V/H) ratios with empty as well as the full reservoir conditions were considered in order to determine the effects of the modeling choice on the design and evaluation of these systems. The following conclusions can be drawn based on the results of the analyses.

- There was a significant difference in the fundamental frequency estimates for the 2D and 3D systems which was only alleviated for V/H and  $E_f/E_c$  ratios in excess of 6 and 2, respectively, for monolithic dam systems. A similar difference in the frequency estimate was observed for systems comprised of independent monoliths. The difference was reduced for V/H and  $E_f/E_c$  ratios greater than 4 and 2, a threshold slightly smaller than the former.
- The 2D solution significantly underestimated the peak of the frequency response function even for systems in very wide canyons such as those with

width to height ratios of 6. Consequently, the damping ratios for all cases, excluding the models with  $V/H$  greater than 6 and models on rigid foundations, were overestimated in the 2D analyses. The differences in the damping ratios were highest for the lower of the  $V/H$  and  $E_f/E_c$  ratios.

- For both the monolithic and independent systems, the differences between the 2 and 3D analyses' displacement predictions were significantly reduced only when the canyon width approached 6 times the dam height. However, the trend was very different. For the monolithic systems, 2D systems significantly overestimated the displacements, while for the systems comprised of independent monoliths, the reverse was valid.
- For the monolithic systems, the principal stress at the toe of the dam was predicted significantly higher with a 2D analysis for canyon widths lower than  $6H$  regardless of the moduli ratio. The 2 and 3D analysis get consistent with increasing canyon width. On the other hand, for the system comprised of independent monoliths, the 2D model consistently underestimated the toe stress by as much as 40% in the mean sense. The difference between the 2 and 3D results reduced with increasing foundation rigidity. The 2D models yielded consistently conservative results compared to 3D models only for the fixed base condition.
- The use of 70 different ground motions for the comparison of time domain predictions showed that there was a significant dependency on the frequency content of the motion in obtaining the demand quantity. Coupled with the frequency response function (i.e. due to dam-reservoir-foundation interaction), this led to the large variance observed for the difference between the 2 and 3D results depending on the ground motion. This variance was substantially large for the monolithic systems and narrow canyons. For the systems comprised of independent monoliths, the variance was significantly lower. The relatively higher contribution of the higher frequency content for the monolithic systems, compared to the flat frequency response after the fundamental mode observed in the systems comprised of independent monoliths, is probably the cause of this behavior.

- The presence of the reservoir increased the aforementioned variance in the differences between the 2 and 3D results to some extent: but this effect was only visible for the systems comprised of independent monoliths.

The results of the analyses showed that except for the gravity dams constructed in very wide canyons, i.e. larger than 6 times the dam height, the predictions from the 2 and 3D analyses can be very different. This trend was valid for both the monolithic case and for systems built with independent monoliths with or without the reservoir. The 2D analyses yielded conservative results for the former, unconservative for the latter. The selection of ground motion is much more important for the former case. In conclusion, given the recent trend of RCC gravity dam construction for a wide range of canyon widths, the seismic effects need to be considered in a 3D configuration.

Investigation of the effectiveness of the ground motion scaling procedures for the dynamic analysis of concrete gravity dams considering the full dam-foundation-reservoir interaction was conducted in chapter 3. The scaling techniques were evaluated for a variety of canyon geometries and foundation-structure moduli ratios. The ground motion sets were chosen from a benchmark set comprised of 20 records and the efficiency, accuracy and the consistency of the results from the chosen sets were evaluated by comparing the results to the benchmark suites' EDP results. The following conclusions can be drawn based on the results of this study.

- When applied to the benchmark suite, all the scaling procedures led to suites with similar mean EDP values while reducing the variance considerably on the crest displacement and the maximum principal stress EDPs. The reduction in variance was limited only for the MIV scaling technique for these EDPs.
- The performance of the scaling procedures for the cumulative inelastic duration demand showed a different trend. When the benchmark suite was scaled, the CID was underestimated consistently for the majority of the models. The same trend was valid for the stress time-area demands.

- The minimum number of records to address the inter-set variability was investigated using the sample statistics of motions compiled from the benchmark suite for a given number of motions included in an analysis set. The considerable reduction in the inter-set variance among the mean values of EDPs for possible different set selections was shown.
- For the maximum principal stress EDP, the minimum number of required ground motions for obtaining acceptable predictions was determined to be 8 and 5 for the simple scaling procedure and  $T_n$  scaling, respectively. Scaling to the fundamental frequency spectral amplitude with the expected SSI damping was very effective in reducing the variances and predicting the means. The variability observed in the MIV scaling and the downward bias introduced in spectral matching techniques led to the requirement to use impractically large numbers of motions in a ground motion set for these scaling procedures.
- The different frequency response for the system geometry and foundation-structure moduli ratio affects the performance of the scaling procedures changing the mean predictions as well as variances. However, a definite trend regarding the effect of these variables on the scaling technique or a particular favoring of a procedure could not be observed. The abovementioned recommendations appear to hold in a general sense for all the DFRI systems considered.

The results showed that stress and displacement based EDPs were accurately predicted by means of the scaling techniques. Considering the dominance of the first mode in gravity dams, the use of scaling to the fundamental frequency spectral amplitude with expected damping appears superior compared to the other methods. However, for the duration based EDPs representative of the possible nonlinear behavior on these systems, the scaling procedures yielded considerable underestimation in the prediction of the mean EDPs.

## 4.2 Future Studies

The accurate modeling of the concrete gravity dam systems for the prediction of the nonlinear behavior including the soil-structure interaction still appears to be a major issue. Consequently, the analysis framework in which the performance based assessment of these structures can be made is still far from established. Summarized below are three important research questions in this respect:

- Widely used in nonlinear assessment of concrete dams is the massless formulation of the foundation media. As mentioned earlier, such a method is not capable of representing the considerable effects of radiation damping. Yet, for the nonlinear analysis of these structures, calibrations regarding the damping force and natural period of the structure is of significant importance given that frequency domain techniques are limited to linear analyses. Thus, based on the results of the rigorous DFRI solutions, equivalent damping ratio for a set of parameters such as height (in addition to width and foundation moduli) should be determined to be used in nonlinear 3D modeling of the DFRI systems using massless foundations.
- Required computational time and effort for the nonlinear analysis of DFRI systems can easily be impractical given the size and complexity of the structure, foundation and reservoir that have to be modeled. As a result, development of simple assessment tools capable of representing the nonlinear behavior of the system, at least for the low levels of damage is beneficial (Ghanaat, 2004). Yet, the proposed quantities as the threshold values determining the need for nonlinear analysis is merely based engineering experience and judgment. The aforementioned values for the proposed DCR range as well as the limitations on distribution of overstressed locations on the dam section have to be investigated using the available rigorous modeling techniques and comparison of the results with those of the nonlinear analyses. Given the importance of the 3D modeling for a wide range of gravity dams

(Chapter 2), the criteria addressing the distribution of the overstressed regions on a 2D section has to be reestablished for the 3D approach.

- As shown in chapter 3, all of the scaling procedures represented an unconservative bias in the damage (cumulative inelastic duration) prediction. Implementation of some modifications in the simple scaling approach might overcome the aforementioned issue. Results of the present study suggests that multiplying individual ground motions to be at the benchmark level can reduce the dispersion in displacement or stress demand prediction but at the same time decrease the accuracy in the unconservative side for damage prediction of the DFRI systems. While only the mean response spectrum of a suite of ground motions can be scaled over the period range of interest, the effects of the first scaling step in Simple scaling procedure and its possible biasing nature on the nonlinear damage prediction of these DFRI systems needs to be investigated.

## REFERENCES

- Abrahamson, N. A. (1992). Non-stationary spectral matching. *Seismological research letters*, 63, 30-40.
- Akpınar, U., Aldemir, A., & Binici, B. (2011). *Different Analysis Strategies for RCC Dam Design*. Paper presented at the 5th International Conference on Advanced Computational Engineering and Experimenting.
- Alavi, B., & Krawinkler, H. (2004). Behavior of moment-resisting frame structures subjected to near-fault ground motions. *Earthquake engineering & structural dynamics*, 33(6), 687-706.
- Aldemir, A., Akpınar, U., Arıcı, Y., & Binici, B. (2012). *Seismic Design and Performance of an High RCC Dam*. Paper presented at the 15th World Conference on Earthquake Engineering.
- Aldemir, A., Yilmazturk, S. M., Yucel, A. R., Binici, B., Arıcı, Y., & Akman, A. (2015). *Analysis Methods for the Investigation of the Seismic Response of Concrete Dams*. Paper presented at the Teknik Dergi.
- American Society of Civil Engineers. (2010). ASCE/SEI-7-10.
- Arıcı, Y., Binici, B., & Aldemir, A. (2014). Comparison of the expected damage patterns from two- and three-dimensional nonlinear dynamic analyses of a roller compacted concrete dam. *Structure and Infrastructure Engineering*, 10(3), 305-315.
- Baker, J. W. (2007). Quantitative classification of near-fault ground motions using wavelet analysis. *Bulletin of the Seismological Society of America*, 97, 1486–1501.

Baker, J. W. (2010). Conditional mean spectrum: Tool for ground-motion selection. *Journal of structural Engineering*, 137(3), 322-331.

Bertero, V. V., Mahin, S. A., & Herrera, R. A. (1978). Aseismic design implications of near- fault San Fernando earthquake records. *Earthquake engineering & structural dynamics*, 6(1), 31-42.

Bougacha, S., & Tassoulas, J. L. (1991). Seismic Analysis of Gravity Dams. I: Modeling of Sediments. *Journal of engineering mechanics*, 117(8), 1826-1837.

Bybordiani, M., & Arici, Y. (2015). *On Soil-Structure Interaction Analysis of Concrete Gravity Dams in Frequency Domain*. Paper presented at the 3. TDMSK, Izmir, Turkey.

Bybordiani, M., & Arici, Y. (2016). The Use of 3D Modeling for the Prediction of the Seismic Demands on the Gravity Dams. *earthquake engineering and structural dynamics*, (Under Review).

Chopra, A. K. (1970). Earthquake response of concrete gravity dams. Earthquake Engineering Research Center: University of Berkeley, California.

chopra, A. K. (2012). *Dynamics of Structures: Theory and Applications to Earthquake Engineering* (4th edition ed.). Englewood Cliffs, New Jersey: Prentice Hall.

Fenves, G., & Chavez, J. W. (1996). *Evaluation of earthquake induced sliding in gravity dams*. Paper presented at the 11th World Conference on Earthquake Engineering, Acapulco, Mexico.

Fenves, G., & Chopra, A. K. (1984a). EAGD-84: A computer program for earthquake response analysis of concrete gravity dams. Earthquake Engineering Research Center: University of Berkeley, California.

Fenves, G., & Chopra, A. K. (1984b). Earthquake analysis of concrete gravity dams including reservoir bottom absorption and dam- water- foundation rock interaction. *Earthquake engineering & structural dynamics*, 12(5), 663-680.

Fenves, G., & Chopra, A. K. (1987). Simplified Earthquake Analysis of Concrete Gravity Dams. *Journal of structural Engineering*, 113(8), 1688-1708.

Fok, K.-L., & Chopra, A. K. (1986). Frequency response functions for arch dams: Hydrodynamic and foundation flexibility effects. *Earthquake engineering & structural dynamics*, 14(5), 769-795.

Fok, K., Hall, J. F., & Chopra, A. K. (1986). EACD-3D: A computer program for three-dimensional earthquake analysis of concrete dams. Earthquake Engineering Research Center: University of Berkeley, California.

Fu, Q., & Menun, C. (2004). *Seismic-environment-based simulation of near-fault ground motions*. Paper presented at the Proceedings of the 13th World Conference on Earthquake Engineering.

Ghanaat, Y. (2004). *Failure modes approach to safety evaluation of dams*. Paper presented at the Proceedings of the 13th World Conference on earthquake engineering.

Hall, J. F., & Chopra, A. K. (1980). Dynamic response of embankment, concrete-gravity and arch dams including hydrodynamic interaction. Earthquake Engineering Research Center: University of Berkeley, California.

Hall, J. F., Heaton, T. H., Halling, M. W., & Wald, D. J. (1995). Near-source ground motion and its effects on flexible buildings. *Earthquake Spectra*, 11(4), 569-605.

Kurama, Y. C., & Farrow, K. T. (2003). Ground motion scaling methods for different site conditions and structure characteristics. *Earthquake engineering & structural dynamics*, 32(15), 2425-2450.

Lilhanand, K., & Tseng, W. S. (1988). *Development and application of realistic earthquake time histories compatible with multiple-damping design spectra*. Paper presented at the 9th World Conference on Earthquake Engineering.

Lotfi, V., & Espandar, R. (2004). Seismic analysis of concrete arch dams by combined discrete crack and non-orthogonal smeared crack technique. *Engineering Structures*, 26(1), 27-37.

Lotfi, V., Roesset, J. M., & Tassoulas, J. L. (1987). A technique for the analysis of the response of dams to earthquakes. *Earthquake engineering & structural dynamics*, 15(4), 463-489.

Medina, F., Dominguez, J., & Tassoulas, J. L. (1990). Response of dams to earthquakes including effects of sediments. *Journal of structural Engineering*, 116(11), 3108-3121.

O'Donnell, A. P., Kurama, Y. C., Kalkan, E., & Taflanidis, A. A. (2013). *Experimental Evaluation of Ground Motion Scaling Methods for Nonlinear Analysis of Structural Systems*. Paper presented at the Structures Congress 2013.

PEER. (2015). Strong Motion Database.

Rashed, A. A., & Iwan, W. D. (1984). Hydrodynamic Pressure on Short- Length Gravity Dams. *Journal of engineering mechanics*, 110(9), 1264-1283.

Reyes, J. C., & Kalkan, E. (2012). How many records should be used in an ASCE/SEI-7 ground motion scaling procedure? *Earthquake Spectra*, 28(3), 1223-1242.

Somerville, P. G. (2002). *Characterizing near fault ground motion for the design and evaluation of bridges*. Paper presented at the Third National Conference and Workshop on Bridges and Highways. Portland, Oregon.

Soysal, B. F. (2014). Performance of Concrete Gravity Dams Under Earthquake Effects *M.Sc. Dissertation*.

Stewart, J. P., Chiou, S.-J., Bray, J. D., Graves, R. W., Somerville, P. G., & Abrahamson, N. A. (2002). Ground motion evaluation procedures for performance-based design. *Soil dynamics and earthquake engineering*, 22(9), 765-772.

Tan, H., & Chopra, A. K. (1995). Earthquake analysis and response of concrete arch dams. Earthquake Engineering Research Center: University of Berkeley, California.

Tan, H., & Chopra, A. K. (1996). EACD-3D-96: A computer program for three-dimensional earthquake analysis of concrete dams. Structural Engineering, Mechanics, and Materials: University of Berkeley, California.

U.S. Bureau of Reclamation. (1976). Design of gravity dams: U.S. Government Printing Office, Denver, Colorado.

United States Army Corps of Engineers. (1995). Seismic design provisions for roller compacted concrete dams: Washington, DC.

United States Army Corps of Engineers. (2003). Time-history dynamic analysis of hydraulic concrete structures: Washington, DC.

Wang, H., & Chopra, A. K. (2008a). Analysis and response of concrete arch dams including dam–water–foundation rock interaction to spatially-varying ground motion. Earthquake Engineering Research Center: University of Berkeley, California.

Wang, H., & Chopra, A. K. (2008b). EACD-3D-2008: A computer program for three dimensional earthquake analysis of concrete dams considering spatially-varying ground motion. Earthquake Engineering Research Center: University of Berkeley, California.

Westergaard, H. M. (1933). Water Pressures on Dams during Earthquakes. *American Society of Civil Engineers*, 98(2), 418-433.

Yilmazturk, S. M. (2013). Three Dimensional Dynamic Response of a Concrete Gravity Dam *M.Sc. Dissertation: MIDDLE EAST TECHNICAL UNIVERSITY*

Yilmazturk, S. M., Arici, Y., & Binici, B. (2015). Seismic assessment of a monolithic RCC gravity dam including three dimensional dam–foundation–reservoir interaction. *Engineering Structures*, 100, 137-148.

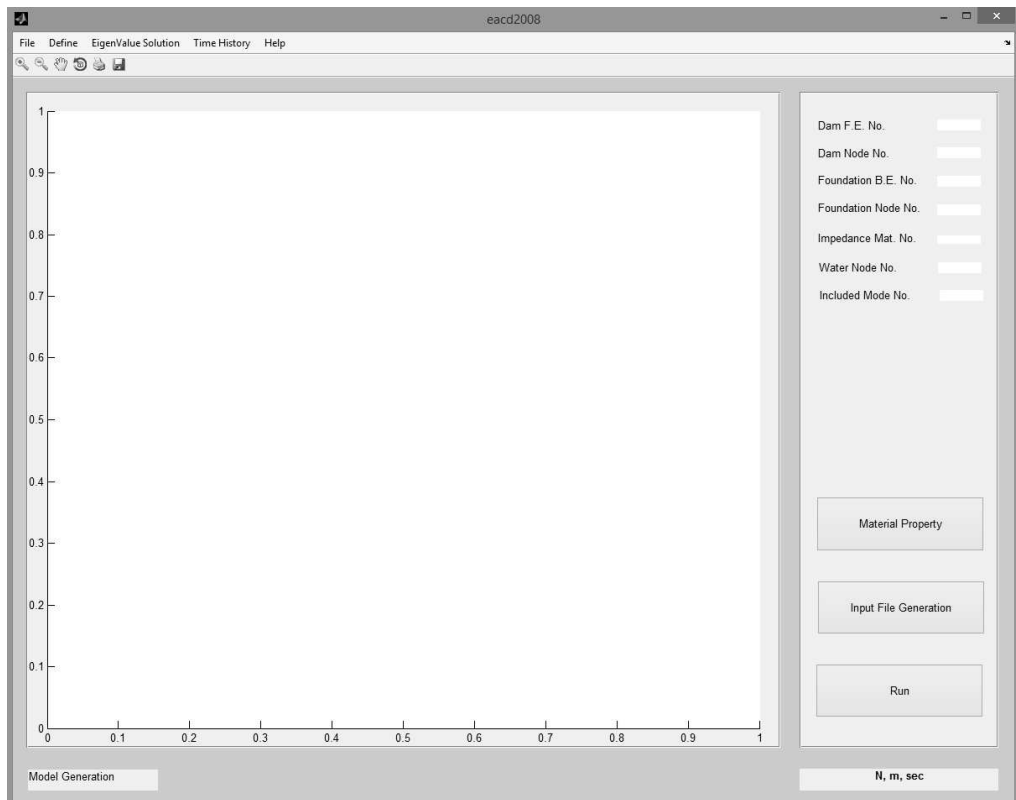
Yucel, A. R. (2013). Seismic Analysis of Concrete Gravity Dams Including Dam-Foundation-Reservoir Interaction *M.Sc. Dissertation: Middle East Technical University, Ankara, Turkey.*

Zhang, L., & Chopra, A. K. (1991). Computation of spatially varying ground motion and foundation-rock impedance matrices for seismic analysis of arch dams. Earthquake Engineering Research Center: University of Berkeley, California.

## APPENDIX A

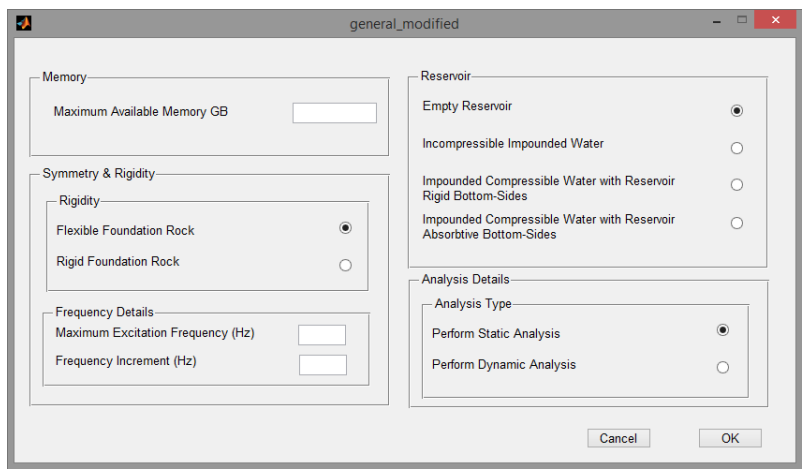
Modeling and post-processing of DFRI systems were conducted with the development of a Graphical User Interface (GUI) for EACD08 named as EACD08-ModPro. Presented in this appendix is an overview of the required steps to be taken in using the aforementioned software for conducting structural analysis of concrete gravity dams. As shown in Figure A-1, the background of the software consists of three major sections:

1. Menu bar, comprised of pre- and post-processing windows.
2. Main window for the visualization of the dam finite element model.
3. Indicators for the number of finite and boundary elements on right side.

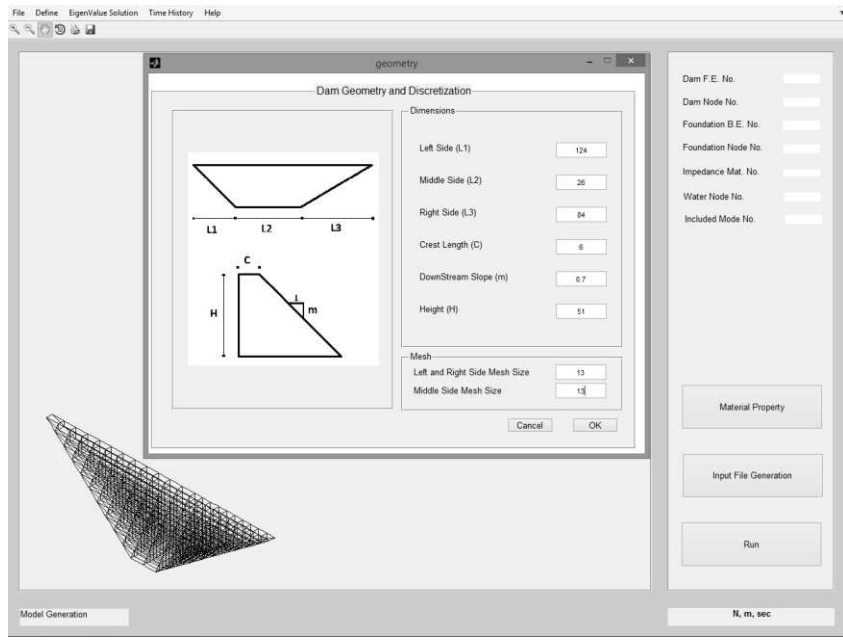


A-1 Software Background

The basic assumptions regarding the model are entered using the general window. The amount of available memory, foundation type, reservoir characteristics, etc. are defined in this part. The number of discrete frequency points to be used in the frequency domain analysis of the DFRI model is also set in this window (Figure A-2). Following the definition of the general parameters, the geometry of the canyon and dam is defined as presented in Figure A-3. The mesh size can be different for the middle part and the shoulders. Yet, the same number of elements are used in the both shoulder to satisfy the requirements of a structured finite element mesh.



A-2 General Definition of the Model



A-3 Geometrical Definition of the Dam

Finally, the material properties of the foundation as well as the dam body are defined. The constant hysteretic damping ratio is assumed to be at a default value of 0.1. It should be noted that Young's modulus and mass density should be input in G.Pa. and  $\text{kg/m}^3$ .

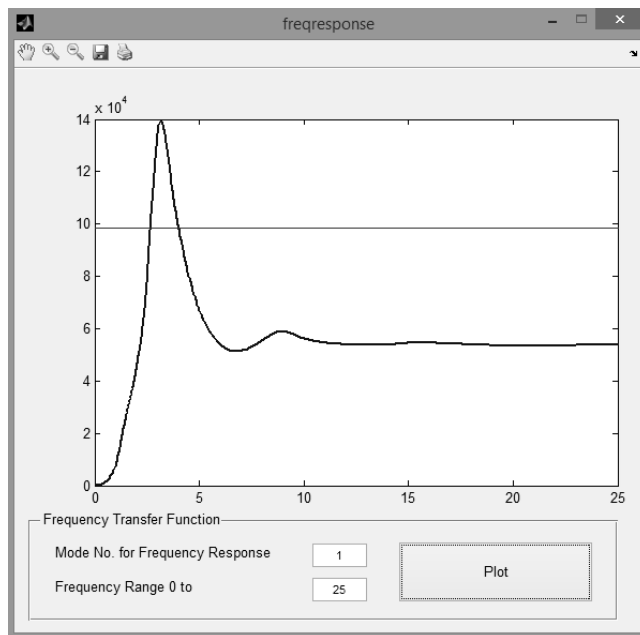
The image shows a software dialog box titled "material" with three sections for defining material properties. Each section contains four input fields with numerical values.

Property	Value
<b>Foundation Material Property</b>	
Young's Modulus G.Pa.	10
Poisson's Ratio	0.25
Unit Mass	2500
Constant Hyteretic Damping Factor	0.1
<b>Dam Material Property</b>	
Young's Modulus G.Pa.	24
Poisson's Ratio	0.2
Unit Mass	2400
Constant Hyteretic Damping Factor	0.1
<b>Reservoir Material Property</b>	
Unit Mass	1000
Wave Reflection Coefficient	

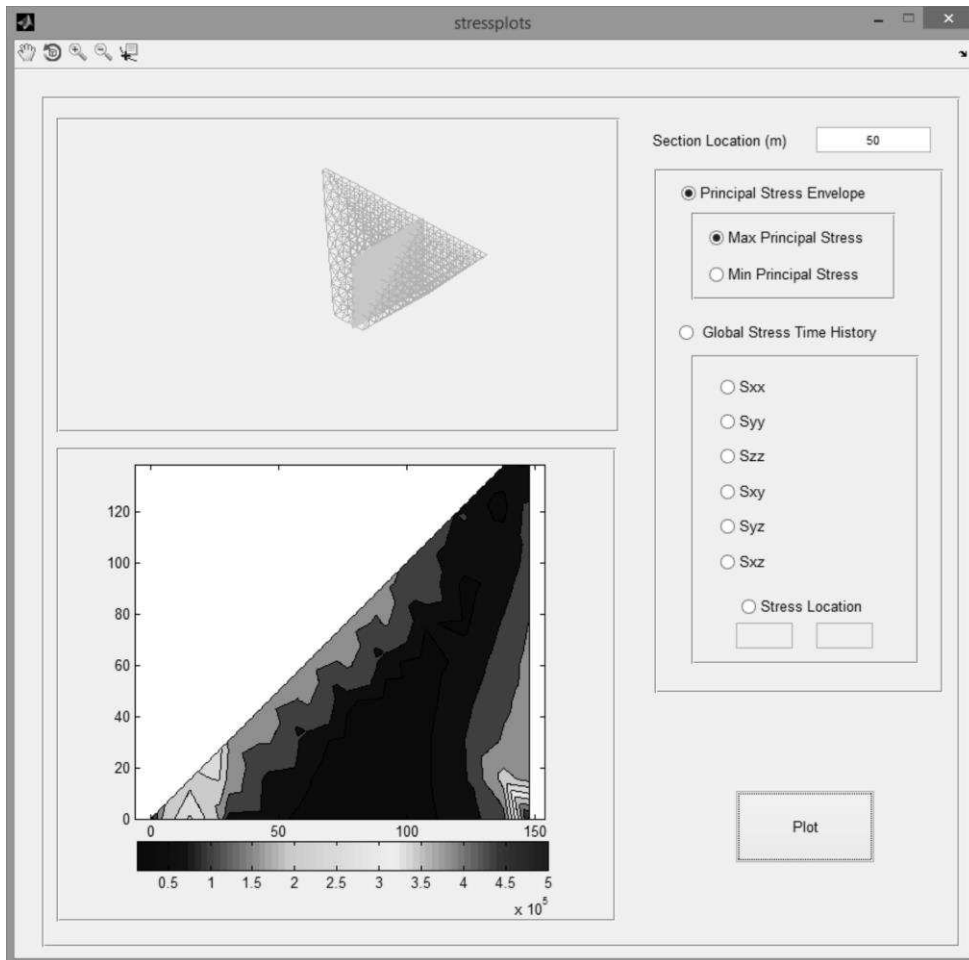
At the bottom of the dialog box are two buttons: "Cancel" and "OK".

A-4 Material Properties for the Dam and Foundation

After the generation of the input file, analysis can be conducted. Depending on the model size, analysis procedure can last from a couple of minutes up to (possibly) many days. Thus, as described in the documentation of this software (EACD08-ModPro), the use of the parallelized version of EACD is strongly recommended for the models with boundary elements' number exceeding 500. Once the frequency domain analysis is completed, the frequency response functions as well as mode shapes can be obtained. Figure A-5 shows the above mentioned response for the first mode of a system for a frequency range of 0 to 25 Hz. The frequency response functions of the system are used along with the ground motion records frequency content to obtain the analysis results using inverse Fourier transform. The displacement and stress results can be obtained using the relevant GUI components. Figure A-6 shows the wide range of tools provided in the post-processing unit for obtaining the stress results. The time histories of the stress components, principal stresses as well as their envelopes at any dam section in the upstream direction can be obtained.



A-5 Frequency Response Functions



A-6 Stress Contours



## APPENDIX B

The following is the source code of a bash file written to manage the multi-core impedance matrices computation of the EACD-3D-08 engine. Number of frequency points and available cores are assumed to be input in a text file named "FreqNoCoreNo.txt".

```
#!/bin/bash
read -r nf1 nc <FreqNoCoreNo.txt
declare -i add
#creating input files needed for each frequency value
dir=$(pwd)
for (( i=1; i <= $nf1; i++ ))
do
    a='input_'
    b='.dat'
    c="$a$i$b"
    cp input.dat $(pwd)/$c
done
if [ "$nc" -ge "$nf1" ]
#if the number of core exceeds the number of frequency points
then
    for (( i=1; i <= $nf1; i++ ))
    do
        a='Freq'
        b='.out'
        c="$a$i$b"
        ./$c &
```

```

        done
    wait
else
#if the number of frequency points exceeds the number of cores
    for ((j=1; j <= $((nf1/nc)); j++ ))
        do
            for (( i=1; i <= $nc; i++ ))
                do
                    a='Freq'
                    b='.out'
                    c="$a$((nc*(j-1)+i))$b"
                    ./$c &
                done
            wait
        done
#running the remaining frequency points which are less than number of cores
    if [ "$((nf1%nc))" -ne "0" ]
    then
        for (( i=$((j-1)*nc+1)); i <= $nf1; i++ ))
            do
                a='Freq'
                b='.out'
                c="$a$i$b"
                ./$c &
            done
        wait
    fi
fi
#running the maineacd to continue subprogram 1 and the remaining
#a=maineacd.out
./maineacd.out

```